Accessing and Repairing DNA Damage in the Nucleosome Core Particle

By Paul J. Caffrey

B.S. Northeastern University 2013

A Dissertation Submitted in Partial Fulfillment of the Requirements for the Degree of

Doctor of Philosophy in the Department of Chemistry at Brown University

Providence, Rhode Island March 2021

This dissertation by Paul J. Caffrey is accepted in its present form by the Department of Chemistry as satisfying the dissertation requirement for the degree of Doctor of Philosophy

Recommended to the Graduate Council

Date_____ _____

Dr. Sarah Delaney, Advisor

Date_____ _____

Dr. Amit Basu, Reader

Date_____ _____

Dr. Eunsuk Kim, Reader

Approved by the Graduate Council

Date_____ _____

Dr. Andrew Campbell, Dean of the Graduate School

Curriculum Vitae

Paul Caffrey

(508) 685 7570

paul_caffrey@brown.edu

EDUCATION

Brown University **May 2021 (expected)**
Doctor of Philosophy in Chemistry
Advisor: Prof. Sarah Delaney

Northeastern University **May 2013**
Bachelor of Science in Chemistry
Advisors: Dr. Graham Jones and Dr. Sune Nielsen (Woods Hole Oceanographic Institute)

RESEARCH EXPERIENCE

Brown University **July 2016-present**

Graduate Research Assistant

- Designed and conducted research for several projects focused on the relationships between DNA repair enzymes and packaged DNA using enzymatic assays.

Curadel LLC **September 2014-May 2016**

Chemist

- Oversaw R&D development of synthetic and analytical protocols novel fluorophores a startup environment for translation into cGMP environment

Smithers-Viscient **August 2013-April 2014**

Chemistry Technician II

- Worked with biological samples to track metabolite fate of commercial products in accordance with EPA, FDA, and OECD GLP guidelines

Woods Hole Oceanographic Institute **July 2012-January 2013**

Undergraduate Research Assistant

- Worked in a clean lab environment studying seawater and sediment core samples to evaluate thallium isotope ratios in the study of fluid fluxes through oceanic crusts

Sigma-Aldrich **July 2010-December 2010**

Undergraduate Co-op Chemist **July 2011-December 2011**

- Synthesized, optimized, and characterized bioactive small molecules for commercial production

PUBLICATIONS

1. **Caffrey P.J.**, and Delaney S. Nucleosome Core Particles Lacking H2B or H3 Tails are Altered Structurally and have Differential Base Excision Repair Fingerprints. *Biochemistry*. (2021) **60** (3): 210-218. doi: 10.1021/acs.biochem.0c00877

2. **Caffrey P.J.**, Kher R., Bian K., Li D., Delaney S. Comparison of the Base Excision and Direct Reversal Repair Pathways for Correcting 1,N6-Ethenoadenine in Strongly Positioned Nucleosomes. *Chem. Res. Toxicol.* (2020) **33** (7): 1888-1896. doi: 10.1021/acs.chemrestox.0c00089

***Honored as ACS Editors' Choice for May 1, 2020*

3. **Caffrey, P. J.** and Delaney S. Chromatin and Other Obstacles to Base Excision Repair: Potential Roles in Carcinogenesis. *Mutagenesis* (2020) **35** (1): 39-50. doi: 10.1093/mutage/gez029

4. Kennedy E.E., **Caffrey P.J.**, Delaney S. Initiating Base Excision Repair in Nucleosome Core Particles. *DNA Repair* (2018) **71**: 97-92. doi: 10.1016/j.dnarep.2018.08.011

PATENTS

1. Caffrey, Paul. 2017. METHOD OF PREPARING DIAMINOPHENOTHIAZINIUM. WO 2017/116903 Al

TEACHING EXPERIENCE

Brown University **July-August 2018**

Teaching Assistant for Summer at Brown

- Taught both in class and laboratory course for high school summer students
- Aided in the creation and execution of laboratory experiments that demonstrated in-class concepts

Brown University **January 2018-May 2018**

Teaching Assistant Organic Chemistry I

- Taught laboratory courses for novice undergraduate students
- Proctored exams and graded exams and laboratory reports

Brown University **September 2017-December 2017**

Teaching Assistant General Chemistry

- Taught laboratory course for novice undergraduate students
- Proctored exams and graded exams and laboratory reports

Brown University **September 2017-December 2017**

Teaching Assistant Chemical Biology

- In class TA for advanced undergraduate and graduate students
- Proctored exams, aided exam preparation, graded exams, and held office hours to aid students

Brown University **July 2017-August 2017**

Teaching Assistant for Organic Chemistry I

- Taught novice students in a flipped classroom environment with an accelerated curriculum
- Aided in exam preparation and ran problem sessions outside of normal class time

Brown University **January 2017-May 2017**

Teaching Assistant Organic Chemistry I

- Taught laboratory courses for novice undergraduate students
- Proctored exams and graded exams and laboratory reports

Brown University **September 2016-December 2016**

Teaching Assistant Organic Chemistry II

- Taught laboratory courses for intermediate undergraduate students
- Proctored exams and graded exams and laboratory reports

INVITED SEMINARS

Brown University Structural Biology Community Meeting
November 2019
Accessing and Repairing DNA Damage in the Nucleosome Core Particle for the Base Excision and Direct Repair Pathways

Graduate Student Ambassador to Northeastern University
March 2020 (postponed due to COVID-19)
Accessing and Repairing DNA Damage in the Nucleosome Core Particle

CONFERENCES AND POSTER PRESENTATIONS

Gordon Research Conference on Nucleosides, Nucleotides and Oligonucleotides
Salve Regina University, June 2019
Poster presentation: *The Effect of Histone Tail Clipping on the Initiation of Base Excision Repair*

12th New Enzymology Kinetic Workshop
University of Texas at Austin, January 2018

SERVICE AND LEADERSHIP

Geochemistry Research Response Committee **2020**

- One of only three graduate students selected to help coordinate a safe re-opening of research in response to the COVID-19 pandemic through the development and implementation of new policies

Graduate Student Coordinator for Prospective Student Visitation **2017-2020**

- Oversaw the coordination of panels and activities involving current graduate students and prospective students for the visitation weekend

Laboratory and Radiation Safety Officer **2017-2021**

- Train new lab members on laboratory safety and radiation safety concerns including hazards, waste disposal, and proper PPE
- A liaison between the laboratory and Environmental Health and Safety Office at Brown

Coordinator Stand Up for Graduate Student Employees **2017-2020**

- Worked alongside other graduate students and the American Federation of Teachers to organize and win a vote for a graduate student union
- Helped organize specific union actions to highlight issues that were of concern to graduate students with a particular focus on highlighting the needs of international students

Vote Captain for Stand Up for Graduate Student Employees **2018**

- Gathered signature on union authorization cards to trigger a vote in accordance with NLRB guidelines
- Ensured that all eligible graduate student voters were informed of the date and polling locations for union voting

Preface and Acknowledgements

To my advisor, Dr. Sarah Delaney, who through example and teaching helped form me into a better scientist.

To my fellow lab members who are also my friends. Thank you for always being there when times were tough and making those days feel short even when the hours were long.

To my friends who have known me from before my graduate school journey. Thank you for always being there for support and as a reminder of life outside a graduate program.

To my family for having been there for my entire life and encouraging me in whatever endeavors I chose to pursue. You have always been a constant source of strength and motivation. None of this would have been possible without you.

To Alex, the one who made bad days disappear the moment I got home and always made sure to celebrate the good ones. You got me through all the things life threw at me during my graduate journey. I cannot wait to see what journeys lay ahead of us and I know with you by my side we can conquer any challenges yet to come.

I dedicate this thesis to my father, Declan. Unfortunately, you only were able to see the beginning of this journey but without you I never would have traveled down this path, yet alone seen it to the end. You were the rock of our family and your support, determination, and ingenuity were an inspiration for my entire life.

Table of Contents

List of Tables

List of Figures

Chapter 1: Introduction to DNA Structure, Damage, Mutagenesis, and Repair†

†Adapted from:

Caffrey, P. J. and Delaney S.

Chromatin and Other Obstacles to Base Excision Repair: Potential Roles in Carcinogenesis. *Mutagenesis* (**2020**) 35 (1): 39-50. doi: 10.1093/mutage/gez029

1.1 Introduction to DNA

Deoxyribonucleic acid (DNA) is the biomolecule responsible for the storage of genetic information. It is comprised of three main components: the phosphate backbone, the sugar, and the nucleobase (**Figure 1.1**). Nucleic acids were first isolated by Swiss physician Friedrich Miescher from white blood cell nuclei, from which the name nucleic acid is derived.[1] Despite this discovery it would take decades to determine the underlying structure and function of DNA. The pioneering work of Albrecht Kossel between 1885 and 1901 led to the discovery and isolation of the five main nucleobases: adenine, cytosine, guanine, thymine, and uracil.[2] It was then the contributions of Phoebus Levene that identified the separate phosphate, sugar, and base components that comprised DNA.[3]

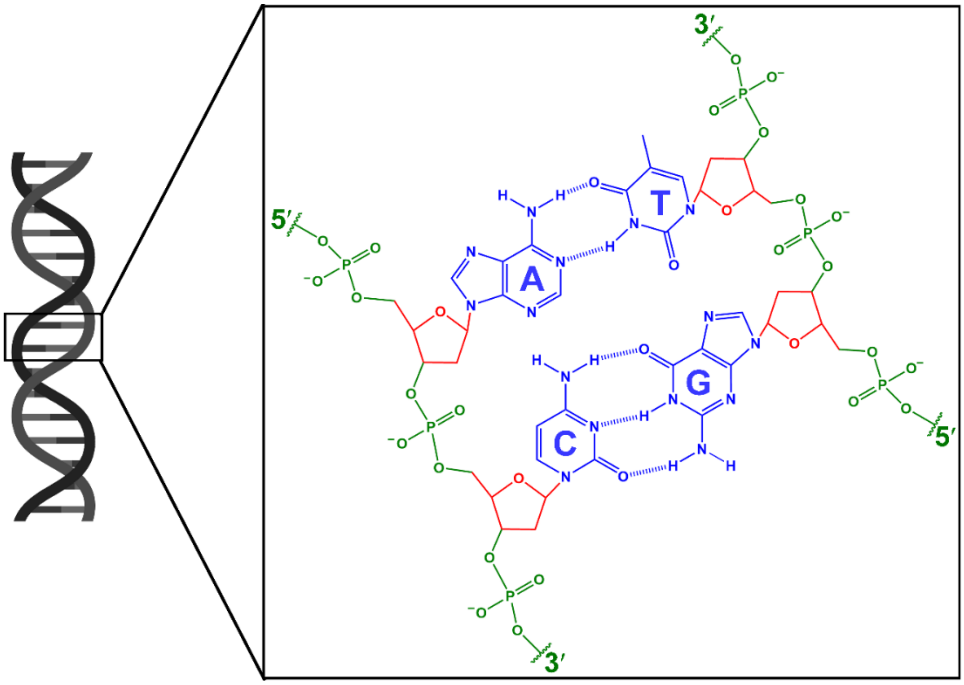

Figure 1.1 Structure of DNA. DNA is assembled into a double helix via hydrogen bond interactions (dashed lines) between two complementary strands of DNA. Each strand of DNA is comprised of a nucleobase (blue), deoxyribose sugar (red), and phosphate backbone (green). Adenine (A) pairs with thymine (T) while guanine (G) pairs with cytosine (C).

After the discovery of the individual components of DNA, the scientific community next turned to understanding its function and elucidating its assembled structure. In 1927, Nikolai Koltsov proposed the nature of inherited traits as arising from a large biomolecule whereby "two mirror strands that would replicate in a semi-conservative fashion using each strand as a template."[4] Despite the identification of the individual components of DNA and a proposal on how genetic information may be passed down via complementary strands, the exact structure of DNA was not yet ascertained. In 1953, James Watson and Francis Crick elucidated the double helical structure of DNA, in large part thanks to X-ray diffraction data obtained by Rosalind Franklin.[5] Franklin's contributions included the determination that the backbone had to be on the outside of the helix and that the two strands of DNA had to be antiparallel. This insight would lead to the discovery of hydrogen bonding between complementary bases as the driving force behind the double helical structure (**Figure 1.1**). These vital pieces of data allowed Watson and Crick to propose the double helical structure of DNA as opposed to the triple helical model with bases orientated outwards proposed by Linus Pauling.[6]

The structure of DNA was the final component that allowed for the proposal by Crick in 1957 of the central dogma of biology: DNA is transcribed into RNA which is then translated to protein.[7] The culmination of all these works revolutionized the modern fields of biology and biochemistry and the broader scientific understanding of genetics. However, as with many new scientific breakthroughs, they opened new avenues of

inquiry. One of these questions that arose was one that, in theory, seemed simple enough: how do organisms maintain the integrity of their genomes?

1.2 DNA Chemical Reactivity

While DNA serves as an optimal biomolecule for the storage of genetic information, it is also chemically reactive and susceptible to modification and degradation.[8, 9] DNA is constantly inundated by damaging agents from both endogenous and exogenous sources.[10, 11] Endogenous sources of damaging agents include normal byproducts of metabolism including reactive oxygen species (ROS), reactive nitrogen species (RNS), and reactive byproducts of lipid peroxidation.[12] Exogenous sources include pollutants and UV light, but also intentional intervention as in the case of certain chemotherapeutic agents.[13] Regardless of the exact source, all these agents may react with DNA and result in alteration to the chemical structure of DNA.

The damage resultant from reaction with these agents includes single- and double-strand breaks, inter- and intra-strand crosslinks, abasic sites, and modification of the nucleobases.[14] All of these forms of damage can compromise the integrity of an organism's genome. While damage like crosslinks and strand breaks result in substantial alteration to the canonical DNA double helix, damage to the nucleobases may not dramatically alter the overall structure of DNA. There is a wide array of chemical modifications to nucleobases that can occur including: alkylation, deamination, and hydrolysis. These subtle alterations to nucleobases can therefore result in difficult detection and repair by cellular mechanisms that subsequently result in accumulation of modified nucleobases. The basis of this thesis will be the investigation of the repair mechanisms of these modified nucleobases and developing an underlying biochemical

understanding of the origin of observed mutational hotspots arising from unsuccessful repair.

1.3 Implications of DNA Damage

The wide array of DNA damage our bodies experience can, if left unrepaired, result in mutagenesis and cellular death. While the damage itself cannot be replicated, it can cause a mutation in our genome that can. Accumulation of mutations throughout the genome, particularly in key genes like p53 or RAS, has been linked to carcinogenesis.[15] Other more cytotoxic lesions, such as crosslinks or strand breaks, can result in polymerase stalling and halt DNA replication inducing apoptosis.

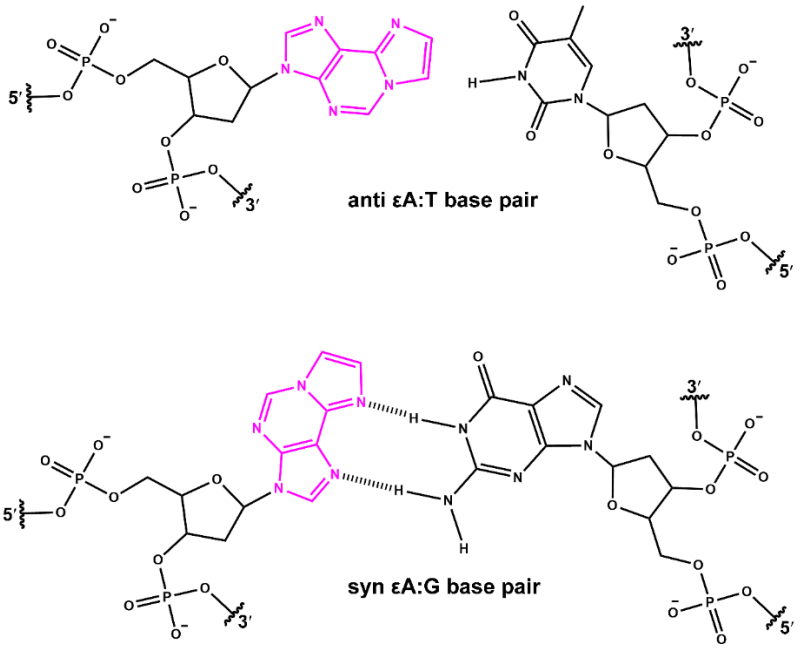

Figure 1.2 Example of mutagenic potential of nucleobase lesion. The top shows how the mutagenic εA lesion loses the ability to correctly bond T due to Watson-Crick binding face alterations. The bottom shows how rotation about the glycosidic bond can expose the Hoogsteen pairing face that stabilizes the syn conformation of εA and allows mispairing with G.

The focus of this thesis will be the repair of alkylated nucleobases. The DNA lesion 1,N^6-ethenoadenine (εA, **Figure 1.2** in pink) is a mutagenic adduct[16] generated by exposure of A to various DNA damaging agents such as vinyl chloride and aldehyde byproducts of lipid peroxidation.[17, 18] The alteration of the Watson-Crick binding face to form the etheno ring results in a loss of hydrogen bonding capability (**Figure 1.2**, top). Instead of forming hydrogen bonds with T, εA adopts a nonplanar arrangement that promotes π stacking with flanking bases to stabilize the DNA helix.[19] However, further studies demonstrated that εA can adopt a *syn* conformation that allows hydrogen bonding with *anti* G (**Figure 1.2**, bottom).[20] Furthermore, εA is an unstable lesion and can undergo further reactions to produce highly mutagenic derivatives that produces a wide variety of mutations (**Figure 1.3**).[22] These results demonstrate the molecular mechanism that underlies the mutagenic potential of εA.

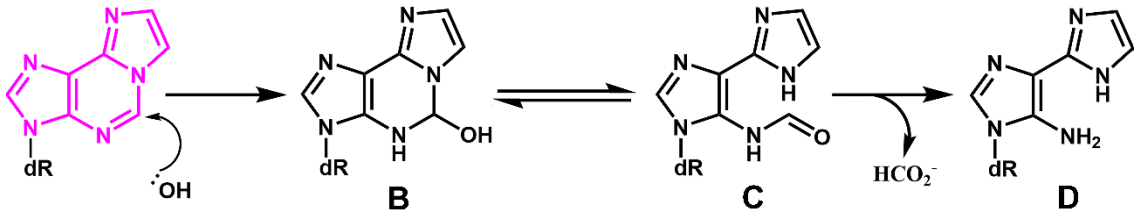

Figure 1.3 Further reactions of εA. εA (pink) undergoes an addition of a hydroxyl group to produce product B. Product B undergoes rearrangement to C that then undergoes deformylation to product the highly mutagenic D.

Elevated εA levels have been detected in numerous cancerous tissues and in tissues of chronic inflammatory diseases that are associated with future cancer development.[21] The A→T transversion, possibly induced by εA and its degradation products,[22] is a common mutation observed in the *P53* and *RAS* genes and is associated

with carcinogenesis.[23] This carcinogenic effect of εA necessitates a thorough understanding of how cells efficiently repair and remove such damage.

1.4 Repair of Modified Nucleobases by the Base Excision Repair Pathway

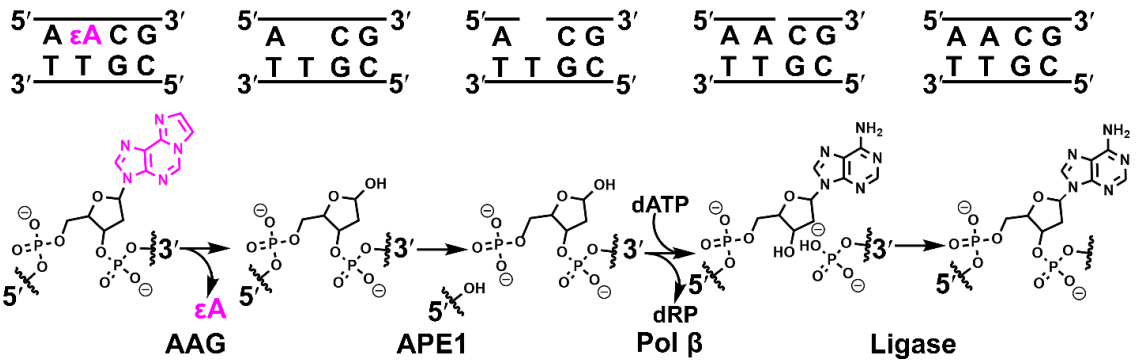

Figure 1.4 Example of base excision repair. Base excision repair of 1,N6 -ethenoadenine (εA). The εA lesion is colored pink along with the four steps of the repair catalyzed by AAG, APE1, pol β, and DNA ligase

There are a variety of cellular mechanisms that allow for the repair of DNA damage.[24] The base excision repair (BER) pathway is responsible for the repair of modified nucleobases, hereafter termed lesions (**Figure 1.4**). This pathway is initiated by a glycosylase, which is responsible for the recognition and excision of the lesion by cleavage of the glycosidic bond. Each of the 11 known human glycosylases recognizes specific lesions that together span a variety of modifications (**Table 1.1** includes major, but not all, lesions). Glycosylases may be classified as either bifunctional or monofunctional. Bifunctional glycosylases first remove the lesion and then catalyze a strand break 3′ to the abasic site. Monofunctional glycosylases only excise the lesion, resulting in an apurinic/apyrimidinic (AP) site that is further processed by AP endonuclease 1 (APE1), which incises the backbone to create a nick with 3'-OH and 5'-deoxyribose phosphate (5′-dRP) termini. Polymerase β (pol β) removes the 5'-dRP and

catalyzes nucleotide incorporation at the 3'-OH. Finally, the repair is completed by a DNA ligase that seals the nick in the backbone.[14]

Table 1.1 Human Glycosylases and Major Substrates. Bold indicates the lesion removed from a mispaired substrate. Abbreviations: 8-oxo-7,8-dihydroguanine (8-oxoG); thymine glycol (Tg); 5,6-dihydrouracil (5,6-DHU); hydroxymethyluracil (hmU); 5-hydroxycytosine (5-hC); 5-formylcytosine (5-fC); 5-carboxycytosine (5-caC); 5-fluorouracil (5-FU); 2,6-diamino-4-hydroxy-5-formamidopyrimidine G (FapyG); 4,6-diamino-5-formamidopyrimidine A (FapyA); guanidinohydantoin (Gh); spiroiminodihydantoin (Sp); 3-methyladenine (3-meA); 7-methylguanine (7-meG); 7-methyladenine (7-meA); 3-methylguanine (3-meG); 1,N^6-ethenoadenine (εA); uracil (U); xanthine (X); hypoxanthine (Hx); 5-hydroxyuracil (5-hU).

Glycosylase	Substrate
AAG (alkyladenine glycosylase)	3-meA, 7-meA, εA, Hx, X
UNG (Uracil DNA Glycosylase)	U; 5-FU
SMUG1 (Single Strand Selective Monofunctional Uracil Glycosylase 1)	U; hmU; 5-FU
TDG (Thymine DNA Glycosylase)	**T**:G; **U**:G; 5-caC; 5-fC; 5-FU
MBD4 (Methyl-CpG-Binding Domain 4)	**T**:G; **U**:G; **hmU**:G
MUTYH (MutY DNA Glycosylase)	**A**:8-oxoG
OGG1 (8-Oxoguanine DNA Glycosylase)	**8-oxoG**:C; FapyG
NTH1 (Endonuclease III-like Protein 1)	FapyA; FapyG; Tg; 5,6-DHU; 5-hC; 5-hU
NEIL1 (Endonuclease VIII-like Protein 1)	Sp; Gh; FapyG; FapyA; Tg; 5,6-DHT; 5,6-DHU
NEIL2 (Endonuclease VIII-like Protein 2)	Sp; Gh; 5-hU; 5,6-DHT; 5,6-DHU; 5-hC
NEIL3 (Endonuclease VIII-like Protein 3)	Sp; Gh; FapyG; FapyA; 5,6-DHT; 5,6-DHU

The eleven identified human glycosylases and are categorized based on their structural architecture which falls into one of six superfamilies.[25] Each glycosylase has

specificity for the removal of a small number of lesions. Notably, given the average formation of 10^4 lesions per cell per day, a given glycosylase may have to search tens of thousands of base pairs (bp) to identify its target.[9, 26] Certain lifestyle factors, such as smoking, increase the rates of lesion formation and the need efficient DNA repair. For εA, it has been observed that εA urinary levels in smokers are significantly higher than in non-smokers, specifically 56±12 pg/mL in smokers compared to 18±5 pg/mL in non-smokers.[27] Notably, this detection method requires excision of εA to be detected so any non-excised lesions or lesions repaired by another pathway would not be detected by this methodology. Therefore, it is reasonable to assume that these values represent the lower end of εA levels in these populations.

Despite different glycosylases having different target lesions, a majority of glycosylases have a conserved mechanism.[25] This mechanism utilizes a base flipping process to extrude the lesion from the helix, plug the resulting space left by the extrahelical lesion with an amino acid residue, and catalyze glycosidic bond cleavage via an S_N1-like mechanism.[28] For AAG, the loss of hydrogen bonding in εA promotes base flipping into the active site of the enzyme where His136 can form a hydrogen bond with the extruded lesion.[29, 30] The resulting hole is plugged by Tyr162 to stabilize the DNA helix. The stabilized complex then undergoes the S_N1-like cleavage of the glycosidic bond (**Figure 1.5**) at a rate of 0.04 min^{-1}.[31] The cleavage of the glycosidic bond is the rate-limiting step of the reaction. Notably, it was with the advent of synthetic organic chemistry methods to produce DNA oligomers with a single and site-specifically incorporated lesions that allowed for both these mechanistic studies and substrate specificity of glycosylases to be identified.

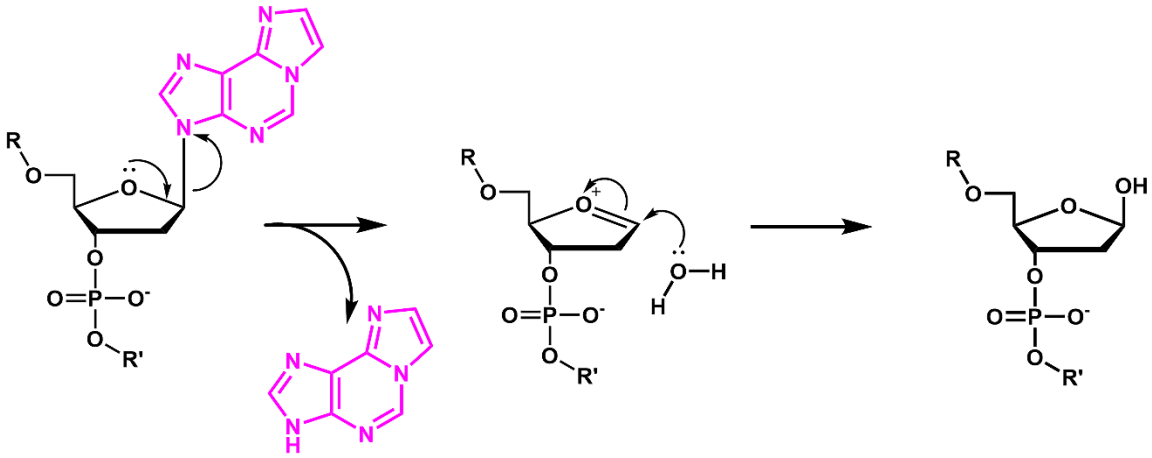

Figure 1.5 Mechanism of glycosidic bond cleavage. After identification of εA (pink), AAG triggers the S_N1-like cleavage of the glycosidic bond. The oxocarbenium intermediate is then subjected to nucleophilic attack by water leaving behind an abasic site.

1.5 Clinical implications of BER Gone Awry

Due to the essential role of BER in maintaining genomic integrity, a multitude of ramifications for human health result when any part of the pathway is deficient or aberrant. These errors in BER can occur at any step in the pathway, from the initiation of the repair event by a glycosylase to the final sealing of the nick by DNA ligase. The relationship between errors in the BER pathway and the development and prognosis of cancer have been investigated extensively. Here we will focus on how aberrations in the initiation of BER by glycosylases can be manifested in clinical outcomes for human patients.

Mutations to human glycosylases has been observed in various cancers. Mutations in glycosylases responsible for the repair of oxidative damage have been observed such as MUTYH in colorectal cancer[32-34] and cholangiocarcinoma,[35] NTH1 in colorectal cancer, [36, 37] NEIL1 in cholangiocarcinoma,[35] and NEIL2 in lung cancer.[38] These observations are not just unique to glycosylases that repair oxidative damage as mutations

in the uracil superfamily DNA glycosylases UNG and TDG have been implicated in familial colorectal cancer.[39] These mutations in BER enzymes demonstrate the health implications of any defect in the BER pathway.

Dysregulated expression of glycosylases can be as deleterious as mutations. Abnormally low expression of OGG1 has been linked to gastric cancer,[40] aggressive breast cancer,[41] ovarian cancer,[42] and lung cancer.[43] Abnormal NTH1 expression has been implicated in the development of cancer by promoting genetic instability. [44] Combinatorial deletion of NTH1 and NEIL1 leads to the development of pulmonary and hepatocellular tumors in mice. [45] Similarly, combined knockout of SMUG1 and UNG leads to increased risk of cancer in mice. [46] Furthermore, deficiency in SMUG1 expression has also been identified in highly aggressive breast cancers. [47] The overexpression of AAG has been associated with development of breast cancer. [48] Surprisingly, while AAG-deficient mice exhibit greater sensitivity to alkylation damage, they do not show overt phenotypic abnormalities or an increased propensity for developing cancer. [49, 50] Taken together these results highlight the how abnormalities in the complex regulation of DNA damage and repair can lead to severe consequences. Fortunately, our bodies have also evolved other pathways to repair certain modified nucleobases.

1.6 Direct Reversal Repair (DRR) of DNA

In contrast to BER repair of modified nucleobases which utilize a series of enzymes, the direct reversal (DRR) pathway utilizes a single enzyme to repair convert a modified nucleobase into the correct canonical one. DRR is observed in the repair of alkylated nucleobases and the repair of UV induced photoproducts. The DRR pathway

can be characterized by three approaches to repair: methyltransferases, oxygenases, and photolyases. Each of these approaches utilize unique chemistry to accomplish the repair of their substrates.

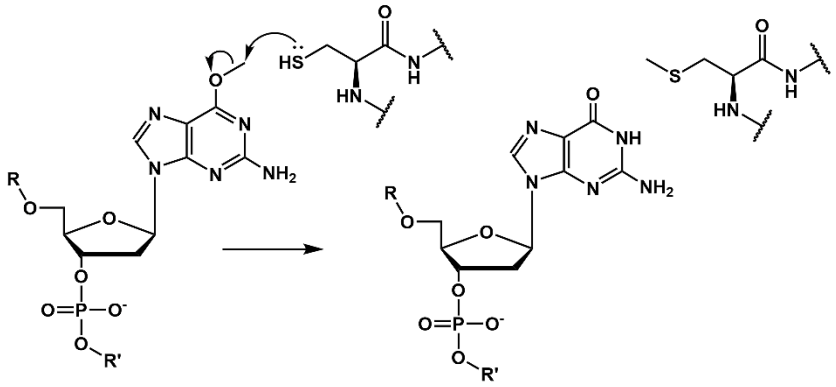

Figure 1.6 Mechanism of direct reversal repair of O^6-methylguanine. The alkyl group from the O^6 position is transferred via an S_N2 mechanism to the internal Cys 145 of the MGMT protein that is then deactivated.

O^6-alkylguanine DNA alkyltransferase (MGMT) is the protein responsible for the direct repair of O^6-methylguanine to guanine. MGMT utilizes an S_N2 mechanism to transfer the methyl from position 6 on O^6-methylguanine to its active site to convert MGMT into its inactive form (**Figure 1.6**). MGMT does not regenerate its active site after it has performed this chemistry and is referred to as a "suicide" enzyme. Unlike the other DRR pathways, MGMT repair is stoichiometric and thus MGMT is not a true enzyme.

The AlkB family of dioxygenases performs chemistry to directly transform several alkylated nucleobases. These enzymes utilize Fe (II), α-ketoglutarate, and molecular oxygen to perform DRR (**Figure 1.7**).[51] Based on sequence homology, up to nine human homologs have been identified as being structurally similar to *E. coli* AlkB.[52] ALKBH2 and ALKBH3 are the enzymes responsible for DRR of DNA in humans.[53, 54] In

particular, ALKBH2 is considered the "housekeeping homolog" responsible for repairing lesions in double-stranded DNA.[55] Within the cell, ALKBH2 is distributed throughout the nucleoplasm with some accumulation within the nucleoli. ALKBH2 possesses a proliferating cell nuclear antigen (PCNA) interacting motif that relocates ALKBH2 to replication foci during S phase.[56] In a manner similar to glycosylases, ALKBH2 flips its target lesion into its active site prior to chemistry.[57] In contrast to other AAG, ALKBH2 does not possess any damage-check step as the nature of its chemistry does not require it; only its substrates will present the correct conformation to undergo reaction in the active site.[57, 58] AlkB homologs are ubiquitous,[51] being observed in RNA viruses,[59] aerobic bacteria,[60] and metazoans.[61]

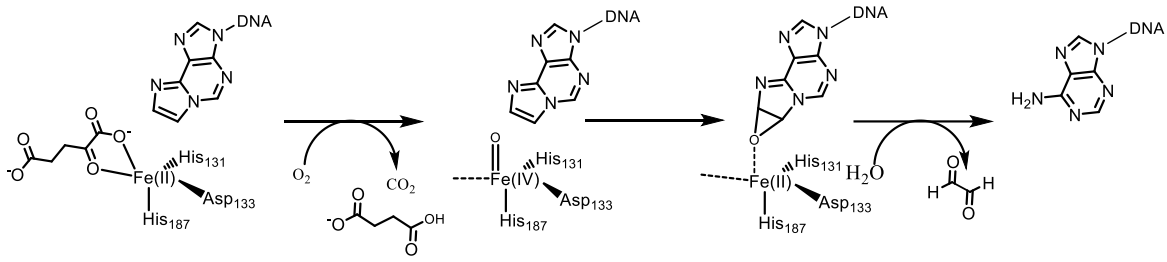

Figure 1.7 Direct reversal repair of εA. The Fe(II) center of the AlkB enzymes utilize molecular oxygen and α-ketoglutarate to generate a highly reactive Fe(IV)-oxo species and release succinate. This reactive species reacts with εA to generate an epoxide intermediate that is then hydrolyzed to release glyoxal and A. The active site returns to its resting Fe(II) state and can undergo additional catalysis.

The final class of DRR is the repair of UV induced photoproducts by a class of enzymes known as photolyases. These enzymes repair the 6-4 and cyclobutane photoproducts that result in pyrimidine dimers between cytosine or thymine on the same strand of DNA.[62] These enzymes are expressed in living organisms exposed to sunlight, with the notable exceptions of placental mammals including humans.[63] These enzymes require UV light for both their activation and chemistry as well as FADH to promote

electron transfer that allow for direct DNA repair.[64] As photolyases repair damage which causes helical distortions and have not been observed in humans[65] they are unique in our discussion of DRR enzymes.

1.7 Clinical Manifestations of DRR Abnormalities

MGMT has been well studied for a strong correlation between its expression levels and various cancers. The first report of a preventative role of MGMT in carcinogenesis was reported in 1993, when it was observed that overexpression of MGMT in mice prevented thymic lymphomas after treatment with the known carcinogen methyl-N-nitrosourea.[66] This protective effect was also later observed in tissue specific expression for liver,[67] skin,[68] and lung[69] tumors. The direct role of MGMT can be further elucidated in knockout mice that demonstrate enhanced sensitivity to alkylating agents.[70] Furthermore, hypermethylation of the MGMT promoter and subsequently lower expression levels have been associated with G→A transitions in KRAS[71] and p53[72] genes. Taken together these results indicate a strong association between DRR of alkylation damage and carcinogenesis.

MGMT is not the only DRR enzyme that has been investigated for potential roles in carcinogenesis. ALKBH2 knockdown in bladder cancer tissues has been demonstrated to limit tumor development.[73] Altered expression and mutations to ALKBH2 have been observed in pediatric brain tumors[74] and gastric cancers.[75] ALKBH3 expression has been shown to be shown to indicate poorer post-operative outcomes for patients with pancreatic cancer[76] and promote the survival and invasiveness of urothelial carcinoma cells.[77] Understanding the DRR pathway and its role in carcinogenesis can help identify potential genotypes that are susceptible to future cancer development. Elucidating the

exact cellular mechanisms under which DRR works may also aid in understanding the inconsistent relationship between altered DRR enzymes and disease. The understanding of these repair pathways can also inform the creation of customized treatment options based on how these pathways function in a specific cancer.

1.8 DNA repair and Chemotherapy

While it is often tempting to think of DNA damage solely as a negative, there are instances where it can be harnessed for beneficial outcomes. Chemotherapeutic approaches generally target DNA replication due to the high levels of synthesis in cancerous cells. However, patients receiving chemotherapy can develop resistance to previously effective drugs.[78] One mechanism of resistance involves DNA repair and several chemotherapeutic agents directly alter nucleobases and produce lesions that can be excised by glycosylases or repaired by DRR. Many review articles have addressed the connections between BER and cancer therapy.[79-83] Understanding the molecular mechanisms of how these drugs work and their interactions with DNA repair enzymes could offer powerful understanding to inform future chemotherapeutic approaches.

The chemotherapeutic agent 5-fluorouracil (5-FU) works via several mechanisms. It inhibits thymidylate synthase (TS) and, as a result, dUMP levels increase 100-fold within 3 h of treatment in cancer cells.[84] This high level of dUMP may contribute to lethality via misincorporation of uracil (U) into DNA. Despite these high levels of U, UNG knockout does not confer any altered responsiveness to 5-FU.[85] However, 5-FU can be incorporated into DNA [86] and its excision by SMUG1 confers resistance to cells.[87] Furthermore, 5-FU is a substrate for UNG, TDG, and SMUG1 in an overlapping system that may create a complex response to 5-FU treatment. Taken

together, these results demonstrate that 5-FU efficacy could be affected by the UDG superfamily of glycosylases, either through removal of 5-FU directly or U incorporated following TS inhibition.

The chemotherapeutic temozolomide (TMZ) is an alkylating agent that produces lesions that are recognized by AAG. Decreased sensitivity to a variety of chemotherapeutic agents was observed in mouse embryonic stem cells overexpressing AAG, which was postulated to be derived from an enhanced ability to repair damaged bases.[88-90] Other work has shown that overexpression of AAG in breast cancer cells increases sensitivity to chemotherapeutics, including TMZ, which was attributed to increased strand breaks via generation of AP sites.[91] Furthermore, overexpression of AAG has been demonstrated to result in microsatellite instability, frameshift mutagenesis, and increased strand breaks upon exposure to alkylating agents.[92] Knockdown of AAG in human carcinoma cells showed enhanced sensitivity to chemotherapeutics, including TMZ in direct contradiction to the results seen in breast cancer cells.[93] AAG-deficient mice showed enhanced resistance to some alkylating therapeutics but demonstrated susceptibility to others.[94, 95] It is apparent from these studies that the relationship between AAG and chemotherapeutic response remains to be fully elucidated.

AAG is not the only repair enzyme implicated in modulating the response to alkylating chemotherapeutic agents. Intriguingly, despite the associations between lower MGMT expression and carcinogenesis mentioned above there is often higher MGMT expression in malignant tumors.[96] It is important to note that xenografts show expression levels of MGMT are quite heterogeneous[97] so a nuanced approach should be utilized in

applying these conclusions. Nonetheless, MGMT expressing tumors have demonstrated almost complete resistance to alkylating chemotherapeutics at maximum tolerated dosages while MGMT deficient cells demonstrate enhanced sensitivity.[98, 99] ALKBH2 has also shown to modulate responses to chemotherapeutics as downregulation led to increased sensitivity to alkylating agents.[73] The potential for AlkB homolog inhibitors to serve as anticancer agents has also been investigated.[100]

The overlapping nature of these various repair pathways should also be investigated when trying to elucidate the role of DNA repair on chemotherapeutic resistance. The overlap of substrates between BER and DRR may help establish a robust, complementary cellular response to alkylation damage than either pathway alone. Indeed, a study investigating the effects of combined knockouts found evidence of epistasis between the three enzymes whereby while single or double knockouts of AAG, ALKBH2/AAG, ALKBH3/AAG were more susceptible to alkylation damage, cells were able to survive multiple rounds of alkylating damage but triple knockouts were not.[101] The relationships between these pathways should also consider the cellular environments in which they may be working, such as during different phases of cell cycle. The potential obstacles to the activity of these enzymes in these different cellular environments, such as the packaging of DNA, need to be better understood to inform future therapies.

1.9 DNA in Eukaryotic Organisms

DNA in eukaryotes is packaged extensively into chromatin. The nucleosome core particle (NCP) is the basic unit of packaging in eukaryotic chromatin. The NCP is comprised of 145-147 base pairs of DNA wrapped approximately 1.7 times around an

octamer core of histone proteins[102] and contains a 2-fold axis of pseudosymmetry known as the dyad axis (**Figure 1.8**). The octamer core is comprised of two copies of each histone protein: H2A, H2B, H3, and H4,[103] each containing a globular core region and a disordered tail.[102]

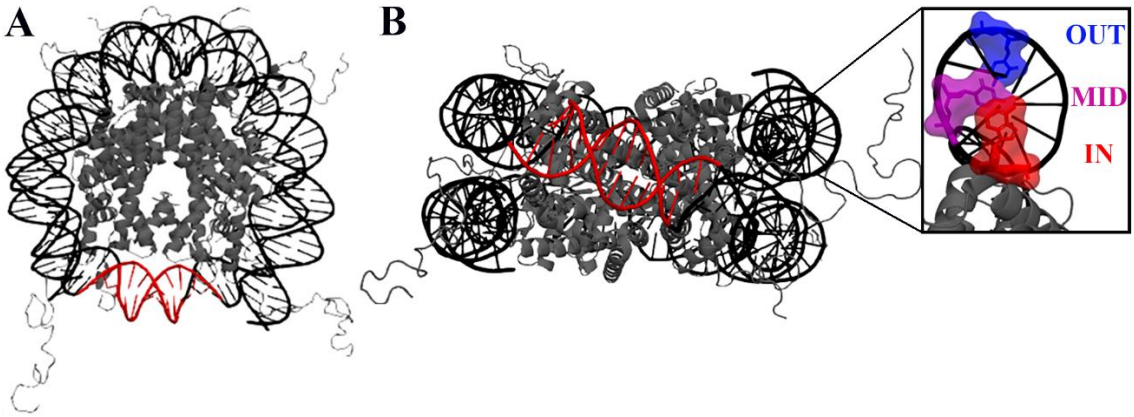

Figure 1.8 Positions of nucleobases in the NCP. Representation of the NCP with the dyad region indicated in red. This representation was created by merging crystal structures of an NCP with a histone octamer containing N-terminal tail regions (PDB entries 3lz0 and 1kx5, respectively). (A) Top view and (B) side view of the NCP with the rotational positions of nucleobases relative to the histone core indicated. Outward (blue), midway (purple), and inward (red) facing nucleobases are highlighted (only

Within an NCP, any given nucleobase is present within a unique local structural architecture that governs how it may be accessed by enzymes. When considering the activity of a glycosylase in an NCP, a variety of factors must be considered. First and foremost, the nature of the lesion's unique location and environment within the NCP must be considered. The location of any position can be defined by two parameters: (1) its rotational positioning, i.e. orientation in the DNA helix facing inwards towards the histones (IN), outwards towards solution (OUT), or somewhere in between (MID) and (2) its translational position defined as its distance from the dyad axis, i.e. located more internally in the NCP or closer to the DNA ends. Another consideration with regards to translational positioning is the observed phenomenon of DNA ends near the exit/entry

region spontaneously and transiently dissociating from the histone core (**Figure 1.9**). This dynamic unwrapping of the DNA ends has been observed by FRET experiments[104-107] and by increased accessibility of these sites to restriction enzymes.[108] Furthermore, the periodicity of the DNA within the NCP varies depending on its translational position.[109] Additional factors, such as the presence of superhelices and the histone tails also create further nuances in local NCP microenvironments.

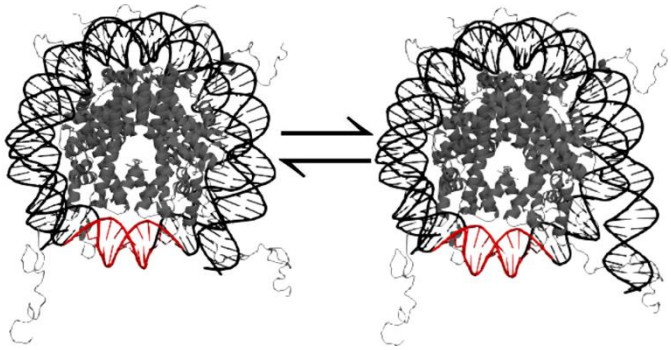

Figure 1.9 Dynamic unwrapping of DNA in the NCP. Representation of the wrapped (left) and partially unwrapped (right) states of the DNA ends in the NCP. The dyad is highlighted in red to act as a reference point of the least dynamic region in the NCP.

Foundational studies have demonstrated that damage formation in the NCP occurs differentially depending on rotational position[110] and strength of association of the DNA to the octamer core.[111] When considered as a whole, these factors illustrate that damage located within the NCP is a complex substrate for DNA repair. Early studies demonstrated that the NCP inhibits the activity of UNG and SMUG1 compared to unpackaged DNA at certain locations in the NCP.[112] Further the repair of alkylation damage in regions occupied by nucleosomes exhibited slower rates of repair when compared to regions between nucleosomes.[113, 114] Understanding the effects of DNA packaging on initiation of BER by glycosylases can contribute to our understanding of the links between DNA damage repair and carcinogenesis.

1.10 Packaged DNA as an Obstacle to BER

DNA repair within the NCP has been most extensively studied in the dyad region, a location where there is minimal transient unwrapping of the DNA. The dyad region also lacks adjacent DNA superhelices. To characterize initiation of BER in the dyad region, our laboratory investigated the activity of several glycosylases working under identical reaction conditions.[115] Specifically, we investigated the activity of the OGG1 glycosylase excising 8-oxoG, UNG excising U, and AAG excising εA. The rotational orientation for each target lesion was varied to face OUT, MID, or IN. Both AAG and UNG exhibited activity that correlated with rotational orientation, with the OUT lesion being most readily excised, and the IN lesion the least, a result that was observed by others studying UNG.[116] Significantly, two kinetic phases can be resolved for UDG acting on MID and IN sites, and it has been proposed by us[117] and others[118] that these biphasic kinetics reflect conformational changes within the NCP that expose occluded sites. In contrast to AAG and UNG, OGG1 had limited excision activity, regardless of rotational orientation of the lesion. Significantly, we have shown that the OGG1 activity is inhibited in the dyad region regardless of rotational positioning.[117] Furthermore, others have shown that activity of NTH1 removing Tg is lower in the dyad region compared to an area located towards the DNA entry/exit area for an IN lesion.[119] Decreased NCP dynamics and the unique periodicity of DNA near the dyad may explain the inhibition of certain glycosylases in this region of the NCP.

With its own unique architecture that lacks the dynamics observed at sites closer to the entry/exit region, the dyad region is not representative of the DNA throughout the entire NCP. We therefore expanded our investigations of rotational positioning to a

region close to the DNA entry/exit region with a focus on the excision activity of OGG1 and UDG.[120] The target lesions, 8-oxoG and U, were located approximately 20 bp from the end of the DNA. In contrast to the dyad region, glycosylase activity was observed at all rotational positions, albeit to varying degrees. Additionally, biphasic kinetics were observed for all rotational positions, reflecting that conformational changes in the NCP may modulate access to lesions toward the DNA ends of the NCP due to transient unwrapping. SMUG1 and UNG have been reported to experience fewer translational effects when comparing the entry/exit region and the dyad.[112] However, reduction of unwrapping via crosslinking of the DNA to the histone octamer reduces repair by UNG.[121, 122] Furthermore, enhanced repair activity closer to the DNA ends was previously observed with UNG,[123] consistent with our results showing greater repair of the DNA closer to the entry/exit region. Additionally, both NTH1 and NEIL1 have shown enhanced excision activity on Tg lesions in the DNA entry/exit region.[124] Lesion exposure rates have also been shown to be rate limiting for NTH1, further solidifying the importance of transient unwrapping in facilitating BER initiation.[125] Experiments in yeast provide *in vivo* evidence that BER enzymes may exploit DNA unwrapping. Treatment with MMS reveals all nucleobase positions throughout the NCP are susceptible to damage. However, after a period of recovery time there is persistent damage in the dyad region, indicative of hindered repair, which subsequently leads to mutations.[126] Further evidence demonstrates somatic and germline mutations follow the periodicity in the NCP.[127] Specifically, mutations are observed in areas of the genome packaged IN towards the histones. These observed mutational hotspots are hypothesized to be a result of hindered repair at these sites.[127] Taken together, these results show that DNA lesions

that are rotationally IN as well as those located in the dyad region are less likely to be repaired, perpetuating mutagenic and cytotoxic effects.

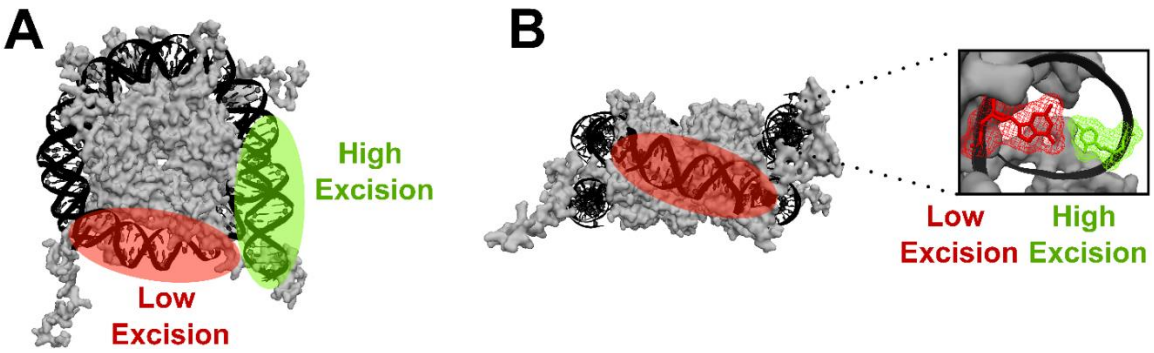

Figure 1.10 General trends of glycosylase activity in the NCP. (A) Investigation of glycosylase activity on lesions in different translational locations reveal how increased dynamics toward the DNA entry/exit region (green) show higher excision than less dynamic areas like the dyad axis (red). (B) Investigation of glycosylase activity on lesions in different rotational locations reveal that lesions oriented OUT (green) are excised better than IN sites (red). The red highlighted dyad remains a general exception to the correlation between rotational position and excision activity.

Inhibition of BER in certain NCP locations may further explain how obstacles to glycosylase activity lead to carcinogenesis. The general trends observed for glycosylases show lesion in areas of increased dynamics or oriented OUT are generally repaired better than those in less dynamic areas or oriented IN **(Figure 1.10)**. DNA packaging in NCPs leads to differential repair based on the unique NCP architecture location of the lesion, with some sites being easier to access for repair than others. Therefore, certain types of damage in certain locations within the NCP are far less likely to be removed than others. However, even for damage that is recognized and removed by a glycosylase, the downstream BER processes still need to be completed. The multiple enzymes needed for complete BER repair represent a distinct disadvantage in the difficult architecture of the NCP when compared to DRR.

1.11 Overcoming DNA packaging

Chromatin remodeling is the dynamic alteration of chromatin architecture that allows for greater access to DNA enzymes. The main mechanisms of remodeling are post translational modifications to the histones and ATP dependent remodeling complexes. Reversible modifications are known to alter chromatin structure, such as the formation of more accessible euchromatin by acetylation that helps promote gene transcription.[128] Besides reversible PTMs such as methylation, phosphorylation, and acetylation, proteolytic clipping of the histone tails has been identified as an irreversible modification.[129, 130] Remodeling complexes catalyze more vigorous alterations to nucleosome structure including octamer sliding,[131] octamer disassembly,[132] and histone variant exchanges.[133]

Remodeling complexes allow for broader changes to nucleosomes than those caused by PTMs, including histone eviction and histone exchange. Complexes like SWI/SNF[134] and Chd1[135] dock onto the histone tails and use ATP hydrolysis to drive octamer sliding and ejection of some or all histone proteins within the octamer. Some remodeling complexes such as SWR1[133] and INO80[136] also promote the exchange of canonical histones for variants. Variant histones are histone proteins that can be substituted for the canonical proteins in the NCP and can confer unique function and structure. The histones that possess the most variants are H2A and H3. H2A variants include H2A.X, H2A.Z, macroH2A, and H2A.Bbd which have specific localization that implicates their role(s) in defined biological processes including DNA repair. For example, H2A.X is distributed throughout the genome and is associated with double-strand break repair [137] and H2A.Z mediates an essential chromatin remodeling step for

the repair of DSBs. [138] The macro domain of macroH2A reduces the recruitment of DNA repair machinery while also compacting chromatin following poly(ADP-ribose) polymerase 1 (PARP1) activation.[139] Similarly, the H3 variant CENP-A interacts with PARP2[140] and CENP-A is found in nuclear foci and depletion of CENP-A results in increased apoptosis following irradiation.[141] CENP-A recruitment is also observed upon induction of DSBs in both human and mouse cells.[142] The unique architecture imparted by variants to the NCP via alterations in DNA-histone contacts and changes in histone size (**Figure 1.11**) may allow for altered access to DNA enzymes. Indeed, chromatin remodeling is one of the first parts of the cellular response to DNA damage[143] and we have seen enhanced BER in NCPs containing H2A variants.[144] The occurrence of remodeling in response to DNA damage highlights the need to overcome DNA packaging for DNA repair to occur efficiently.

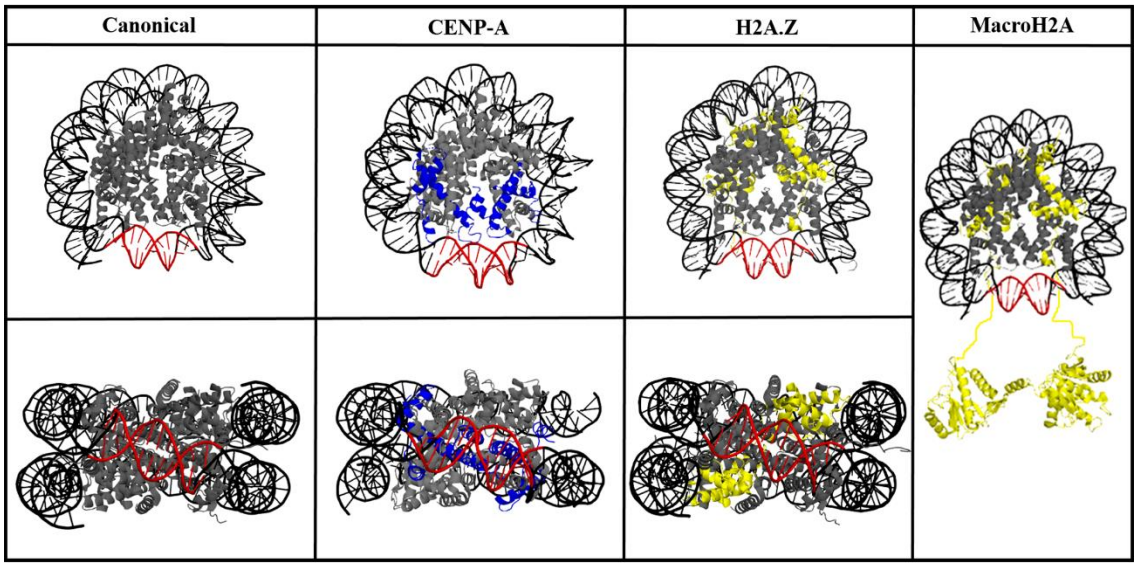

Figure 1.11 Differential structures of variant containing NCPs. The dyad region is highlighted in red, H3 variants in blue, and H2A variants in yellow. The canonical NCP (PDB 3lz0), CENP-A (PDB 3AN2), and H2A.Z (PDB 1F66) are shown. The macroH2A structure consists of an NCP with the histone domain (PDB 1U35), the macro domain (PDB 6FY5), and a cartoon representation of the unstructured linker. Top panels represent top views and bottom panels represent side views.

Newer investigations of nucleotide excision repair (NER) proteins have revealed their roles in BER and overcoming the problems of DNA packaging. It has been demonstrated that NER lesions packaged into chromatin result in differential repair by the NER pathway.[145] UV-DNA damage binding protein (UV-DDB) is a heterodimeric protein consisting of DDB1 and DDB2 that has been shown to act as a damage sensor for lesions in the context of chromatin.[146] Intriguingly, more recent work has shown the involvement of UV-DDB with the BER pathway. In short duplexes, UV-DDB has been shown the stimulate the activity of OGG1 on 8-oxoG, APE1 incision of abasic sites, and pol β nucleotide incorporation.[147] Furthermore, UV-DDB binding to abasic sites has been observed in cryo-EM structures to induce a register shift of occluded IN lesions independent of ATP.[148] This may explain earlier work which had identified a "factor" from human cellular extracts that promoted ATP independent BER activity in

nucleosomes.[149] These exciting results implicate UV-DDB as another potential mechanism of promoting BER in chromatin.

1.12 Concluding Remarks and Gap in Knowledge

DNA repair is essential to the protection of an organism's genetic code as well as its survival. While there is a vast array of DNA damage that can occur, there are also numerous pathways to repair this damage. The BER and DRR pathways are the major pathways involved in the repair of damage to DNA nucleobases. However, the packaging of DNA into chromatin presents these cells with a paradox. While sequestration of DNA can help protect the genome, it can also exclude DNA repair enzymes from accessing and repairing damage. The work of this thesis elucidates how BER and DRR enzymes are affected by DNA packaging.

The proceeding work will investigate BER and DRR in packaged DNA and how it can be modulated by the alteration of the histone proteins or addition of other proteins. Chapter 2 focuses on a comparison of the BER and DRR pathways in the repair of alkylated DNA distributed throughout various geometric positions within the base unit of DNA packaging, the NCP. A comparison of AAG and ALKBH2 reveals the effects of DNA packaging on each repair pathway. Chapter 3 investigates the effects of histone tail removal on NCP structure and AAG excision activity. Finally, chapter 4 explores the role of UV-DDB in conjunction with AAG to initiate BER in the NCP. Together these studies aim to elucidate how the repair of damaged nucleobases occurs in chromatin and the various potential cellular strategies to overcome inhibition by this packaging.

1.13 References

1. Dahm, R., Discovering DNA: Friedrich Miescher and the early years of nucleic acid research. *Human Genetics* **2008,** *122* (6), 565-581.

2. Jones, M. E., Albrecht Kossel, a biographical sketch. *Yale J Biol Med* **1953,** *26* (1), 80-97.

3. Levene, P. A., On the biochemistry of Nucleic Acids 2. *J. Am. Chem. Soc.***1910,** *32* (2), 231-240.

4. Koltsov, N., Physical–chemical fundamentals of morphology. *Prog. Exp. Biol. B* **1927,** *7*, 3-31.

5. Watson, J. D.; Crick, F. H. C., Molecular Structure of Nucleic Acids: A Structure for Deoxyribose Nucleic Acid. *Nature* **1953,** *171* (4356), 737-738.

6. Pauling, L.; Corey, R. B., A Proposed Structure For The Nucleic Acids. *Proc. Natl. Acad. Sci. U.S.A* **1953,** *39* (2), 84-97.

7. Crick, F. H., On protein synthesis. *Symp Soc Exp Biol* **1958,** *12*, 138-63.

8. Gates, K. S., An overview of chemical processes that damage cellular DNA: spontaneous hydrolysis, alkylation, and reactions with radicals. *Chem. Res. Toxicol.* **2009,** *22* (11), 1747-60.

9. Lindahl, T., Instability and decay of the primary structure of DNA. *Nature* **1993,** *362*, 709.

10. Swenberg, J. A.; Lu, K.; Moeller, B. C.; Gao, L.; Upton, P. B.; Nakamura, J.; Starr, T. B., Endogenous versus exogenous DNA adducts: their role in carcinogenesis, epidemiology, and risk assessment. *Toxicol. Sci.* **2011,** *120 Suppl*, S130-45.

11. Hoeijmakers, J. H., Genome maintenance mechanisms for preventing cancer. *Nature* **2001,** *411* (6835), 366-74.

12. De Bont, R.; van Larebeke, N., Endogenous DNA damage in humans: a review of quantitative data. *Mutagenesis* **2004,** *19* (3), 169-185.

13. Cheung-Ong, K.; Giaever, G.; Nislow, C., DNA-Damaging Agents in Cancer Chemotherapy: Serendipity and Chemical Biology. *Chemistry & Biology* **2013,** *20* (5), 648-659.

14. Schermerhorn, K. M.; Delaney, S. A kinetic perspective on base excision repair of DNA. *Acc. Chem. Res.* **2014**, *47* (4) 1238–1246

15. Harris, C. C., Chemical and Physical Carcinogenesis: Advances and Perspectives for the 1990s. *Cancer Res.* **1991,** *51* (18 Supplement), 5023s-5044s.

16. Levine, R. L.; Yang, I.-Y.; Hossain, M.; Pandya, G. A.; Grollman, A. P.; Moriya, M., Mutagenesis Induced by a Single 1,*N6*,-Ethenodeoxyadenosine Adduct in Human Cells. *Cancer Res.* **2000,** *60* (15), 4098-4104.

17. El Ghissassi, F.; Barbin, A.; Nair, J.; Bartsch, H., Formation of 1,N6-Ethenoadenine and 3,N4-Ethenocytosine by Lipid Peroxidation Products and Nucleic Acid Bases. *Chem. Res. Toxicol.* **1995,** *8* (2), 278-283.

18. Guengerich, F. P.; Crawford, W. M.; Watanabe, P. G., Activation of vinyl chloride to covalently bound metabolites: roles of 2-chloroethylene oxide and 2-chloroacetaldehyde. *Biochemistry* **1979,** *18* (23), 5177-5182.

19. Kouchakdjian, M.; Eisenberg, M.; Yarema, K.; Basu, A.; Essigmann, J.; Patel, D. J., NMR studies of the exocyclic 1,N6-ethenodeoxyadenosine adduct (epsilon dA) opposite thymidine in a DNA duplex. Nonplanar alignment of epsilon dA(anti) and dT(anti) at the lesion site. *Biochemistry* **1991,** *30* (7), 1820-8.

20. De los Santos, C.; Kouchakdjian, M.; Yarema, K.; Basu, A.; Essigmann, J.; Patel, D. J., NMR studies of the exocyclic 1,N6-ethenodeoxyadenosine adduct (.epsilon.dA) opposite deoxyguanosine in a DNA duplex. .epsilon.dA(syn).cntdot.dG(anti) pairing at the lesion site. *Biochemistry* **1991,** *30* (7), 1828-1835.

21. Nair, U.; Bartsch, H.; Nair, J., Lipid peroxidation-induced DNA damage in cancer-prone inflammatory diseases: A review of published adduct types and levels in humans. *Free Radic. Biol. Med.* **2007,** *43* (8), 1109-1120.

22. Basu, A. K., et al. (1993). "Mutagenic and genotoxic effects of three vinyl chloride-induced DNA lesions: 1,N6-ethenoadenine, 3,N4-ethenocytosine, and 4-amino-5-(imidazol-2-yl)imidazole." *Biochemistry* 32(47): 12793-12801.

23. Barbin, A., Etheno-adduct-forming chemicals: from mutagenicity testing to tumor mutation spectra. *Mutat. Res. Rev. Mutat. Res.* **2000,** *462* (2), 55-69.

24. Sancar, A.; Lindsey-Boltz, L. A.; Unsal-Kaçmaz, K.; Linn, S., Molecular mechanisms of mammalian DNA repair and the DNA damage checkpoints. *Annu. Rev. Biochem.* **2004,** *73*, 39-85.

25. Brooks, S. C.; Adhikary, S.; Rubinson, E. H.; Eichman, B. F., Recent advances in the structural mechanisms of DNA glycosylases. *Biochim. Biophys. Acta.* **2013,** *1834* (1), 247-71.

26. Friedman, J. I.; Stivers, J. T., Detection of damaged DNA bases by DNA glycosylase enzymes. *Biochemistry* **2010,** *49* (24), 4957-67.

27. Chen, H.-J. C.; Chiu, W.-L., Detection and Quantification of 1,N6-Ethenoadenine in Human Urine by Stable Isotope Dilution Capillary Gas Chromatography/Negative Ion Chemical Ionization/Mass Spectrometry. *Chem. Res. Toxicol* **2003,** *16* (9), 1099-1106.

28. Stivers, J. T.; Jiang, Y. L., A Mechanistic Perspective on the Chemistry of DNA Repair Glycosylases. *Chem. Rev.* **2003,** *103* (7), 2729-2760.

29. Lau, A. Y.; Schärer, O. D.; Samson, L.; Verdine, G. L.; Ellenberger, T., Crystal structure of a human alkylbase-DNA repair enzyme complexed to DNA: mechanisms for nucleotide flipping and base excision. *Cell* **1998,** *95* (2), 249-58.

30. Lau, A. Y.; Wyatt, M. D.; Glassner, B. J.; Samson, L. D.; Ellenberger, T., Molecular basis for discriminating between normal and damaged bases by the human alkyladenine glycosylase, AAG. *Proc. Natl. Acad. Sci. U.S.A* **2000,** *97* (25), 13573-13578.

31. Wolfe, A. E.; O'Brien, P. J., Kinetic mechanism for the flipping and excision of 1,N(6)-ethenoadenine by human alkyladenine DNA glycosylase. *Biochemistry* **2009,** *48* (48), 11357-11369.

32. Cleary, S. P.; Cotterchio, M.; Jenkins, M. A.; Kim, H.; Bristow, R.; Green, R.; Haile, R.; Hopper, J. L.; LeMarchand, L.; Lindor, N.; Parfrey, P.; Potter, J.; Younghusband, B.; Gallinger, S., Germline MutY Human Homologue Mutations and Colorectal Cancer: A Multisite Case-Control Study. *Gastroenterology* **2009,** *136* (4), 1251-1260.

33. Ali, M.; Kim, H.; Cleary, S.; Cupples, C.; Gallinger, S.; Bristow, R., Characterization of Mutant MUTYH Proteins Associated With Familial Colorectal Cancer. *Gastroenterology* **2008,** *135* (2), 499-507.e1.

34. Parker, A. R.; Eshleman, J. R., Human MutY: gene structure, protein functions and interactions, and role in carcinogenesis. *Cell. Mol. Life Sci.* **2003,** *60* (10), 2064-2083.

35. Forsbring, M.; Vik, E. S.; Dalhus, B.; Karlsen, T. H.; Bergquist, A.; Schrumpf, E.; Bjoras, M.; Boberg, K. M.; Alseth, I., Catalytically impaired hMYH and NEIL1 mutant proteins identified in patients with primary sclerosing cholangitis and cholangiocarcinoma. *Carcinogenesis* **2009,** *30* (7), 1147-54.

36. Rivera, B.; Castellsagué, E.; Bah, I.; van Kempen, L. C.; Foulkes, W. D., Biallelic NTHL1 Mutations in a Woman with Multiple Primary Tumors. *N. Engl. J. Med.* **2015,** *373* (20), 1985-1986.

37. Weren, R. D. A.; Ligtenberg, M. J. L.; Kets, C. M.; de Voer, R. M.; Verwiel, E. T. P.; Spruijt, L.; van Zelst-Stams, W. A. G.; Jongmans, M. C.; Gilissen, C.; Hehir-Kwa, J. Y.; Hoischen, A.; Shendure, J.; Boyle, E. A.; Kamping, E. J.; Nagtegaal, I. D.; Tops, B. B. J.; Nagengast, F. M.; Geurts van Kessel, A.; van Krieken, J. H. J. M.; Kuiper, R. P.; Hoogerbrugge, N., A germline homozygous mutation in the base-excision repair gene NTHL1 causes adenomatous polyposis and colorectal cancer. *Nature Genetics* **2015,** *47*, 668.

38. Dey, S.; Maiti, A. K.; Hegde, M. L.; Hegde, P. M.; Boldogh, I.; Sarkar, P. S.; Abdel-Rahman, S. Z.; Sarker, A. H.; Hang, B.; Xie, J.; Tomkinson, A. E.; Zhou, M.; Shen, B.; Wang, G.; Wu, C.; Yu, D.; Lin, D.; Cardenas, V.; Hazra, T. K., Increased risk of lung cancer associated with a functionally impaired polymorphic variant of the human DNA glycosylase NEIL2. *DNA Repair* **2012,** *11* (6), 570-578.

39. Broderick, P.; Bagratuni, T.; Vijayakrishnan, J.; Lubbe, S.; Chandler, I.; Houlston, R. S., Evaluation of NTHL1, NEIL1, NEIL2, MPG, TDG, UNG and SMUG1genes in familial colorectal cancer predisposition. *BMC Cancer* **2006,** *6* (1), 243.

40. Ni, J.; Mei, M.; Sun, L., Oxidative DNA damage and repair in chronic atrophic gastritis and gastric cancer. *Hepato-gastroenterology* **2012,** *59* (115), 671-5.

41. Karihtala, P.; Kauppila, S.; Puistola, U.; Jukkola-Vuorinen, A., Absence of the DNA repair enzyme human 8-oxoguanine glycosylase is associated with an aggressive breast cancer phenotype. *Br. J. Cancer* **2012,** *106* (2), 344-347.

42. Xu, X.; Wang, Y.; Guo, W.; Zhou, Y.; Lv, C.; Chen, X.; Liu, K., The significance of the alteration of 8-OHdG in serous ovarian carcinoma. *J. Ovarian Res.* **2013,** *6* (1), 74-74.

43. Mambo, E.; Chatterjee, A.; de Souza-Pinto, N. C.; Mayard, S.; Hogue, B. A.; Hoque, M. O.; Dizdaroglu, M.; Bohr, V. A.; Sidransky, D., Oxidized guanine lesions and hOgg1 activity in lung cancer. *Oncogene* **2005,** *24*, 4496.

44. Werner, E. M.; Shah, J. A.; Limpose, K. L.; Li, Z.; Dynan, W. S.; Doetsch, P. W.; Sarker, A. H.; Trego, K. S.; Cooper, P. K.; Leung, S. W.; Corbett, A. H.; Ramalingam, S. S., Overexpression of the base excision repair NTHL1 glycosylase causes genomic instability and early cellular hallmarks of cancer. *Nucleic Acids Res.* **2018,** *46* (9), 4515-4532.

45. Chan, M. K.; Ocampo-Hafalla, M. T.; Vartanian, V.; Jaruga, P.; Kirkali, G.; Koenig, K. L.; Brown, S.; Lloyd, R. S.; Dizdaroglu, M.; Teebor, G. W., Targeted deletion of the genes encoding NTH1 and NEIL1 DNA N-glycosylases reveals the

existence of novel carcinogenic oxidative damage to DNA. *DNA Repair* **2009,** *8* (7), 786-794.

46. Dingler, F. A.; Kemmerich, K.; Rada, C.; Neuberger, M. S., Germline ablation of SMUG1 DNA glycosylase causes loss of 5-hydroxymethyluracil- and UNG-backup uracil-excision activities and increases cancer predisposition of Ung−/−Msh2−/− mice. *Nucleic Acids Res.* **2012,** *40* (13), 6016-6025.

47. Abdel-Fatah, T. M. A.; Albarakati, N.; Bowell, L.; Agarwal, D.; Moseley, P.; Hawkes, C.; Ball, G.; Chan, S.; Ellis, I. O.; Madhusudan, S., Single-strand selective monofunctional uracil-DNA glycosylase (SMUG1) deficiency is linked to aggressive breast cancer and predicts response to adjuvant therapy. *Breast Cancer Res. Treat.* **2013,** *142* (3), 515-527.

48. Cerda, S. R.; Turk, P. W.; Thor, A. D.; Weitzman, S. A., Altered expression of the DNA repair protein, N-methylpurine-DNA glycosylase (MPG), in breast cancer. *FEBS Lett.* **1998,** *431* (1), 12-18.

49. Engelward, B. P.; Weeda, G.; Wyatt, M. D.; Broekhof, J. L. M.; de Wit, J.; Donker, I.; Allan, J. M.; Gold, B.; Hoeijmakers, J. H. J.; Samson, L. D., Base excision repair deficient mice lacking the Aag alkyladenine DNA glycosylase. *Proc. Natl. Acad. Sci. U.S.A* **1997,** *94* (24), 13087-13092.

50. Elder, R. H.; Jansen, J. G.; Weeks, R. J.; Willington, M. A.; Deans, B.; Watson, A. J.; Mynett, K. J.; Bailey, J. A.; Cooper, D. P.; Rafferty, J. A.; Heeran, M. C.; Wijnhoven, S. W. P.; van Zeeland, A. A.; Margison, G. P., Alkylpurine–DNA–N-Glycosylase Knockout Mice Show Increased Susceptibility to Induction of Mutations by Methyl Methanesulfonate. *Mol. Cell. Biol.* **1998,** *18* (10), 5828-5837.

51. Fedeles, B. I.; Singh, V.; Delaney, J. C.; Li, D.; Essigmann, J. M., The AlkB Family of Fe(II)/alpha-Ketoglutarate-dependent Dioxygenases: Repairing Nucleic Acid Alkylation Damage and Beyond. *J. Biol. Chem.* **2015,** *290* (34), 20734-42.

52. Ougland, R.; Rognes, T.; Klungland, A.; Larsen, E., Non-homologous functions of the AlkB homologs. *J. Mol. Cell Biol.* **2015,** *7* (6), 494-504.

53. Aas, P. A.; Otterlei, M.; Falnes, P. Ø.; Vågbø, C. B.; Skorpen, F.; Akbari, M.; Sundheim, O.; Bjørås, M.; Slupphaug, G.; Seeberg, E.; Krokan, H. E., Human and bacterial oxidative demethylases repair alkylation damage in both RNA and DNA. *Nature* **2003,** *421* (6925), 859-863.

54. Duncan, T.; Trewick, S. C.; Koivisto, P.; Bates, P. A.; Lindahl, T.; Sedgwick, B., Reversal of DNA alkylation damage by two human dioxygenases. *Proc. Natl. Acad. Sci. U.S.A* **2002,** *99* (26), 16660-16665.

55. Ringvoll, J.; Nordstrand, L. M.; Vågbø, C. B.; Talstad, V.; Reite, K.; Aas, P. A.; Lauritzen, K. H.; Liabakk, N. B.; Bjørk, A.; Doughty, R. W.; Falnes, P. Ø.; Krokan, H. E.; Klungland, A., Repair deficient mice reveal mABH2 as the primary oxidative demethylase for repairing 1meA and 3meC lesions in DNA. *EMBO J* **2006,** *25* (10), 2189-2198.

56. Gilljam, K. M.; Feyzi, E.; Aas, P. A.; Sousa, M. M. L.; Müller, R.; Vågbø, C. B.; Catterall, T. C.; Liabakk, N. B.; Slupphaug, G.; Drabløs, F.; Krokan, H. E.; Otterlei, M., Identification of a novel, widespread, and functionally important PCNA-binding motif. *J. Cell Biol.* **2009,** *186* (5), 645-654.

57. Yang, C.-G.; Yi, C.; Duguid, E. M.; Sullivan, C. T.; Jian, X.; Rice, P. A.; He, C., Crystal structures of DNA/RNA repair enzymes AlkB and ABH2 bound to dsDNA. *Nature* **2008,** *452* (7190), 961-965.

58. Yi, C.; Chen, B.; Qi, B.; Zhang, W.; Jia, G.; Zhang, L.; Li, C. J.; Dinner, A. R.; Yang, C. G.; He, C., Duplex interrogation by a direct DNA repair protein in search of base damage. *Nat. Struct. Mol. Biol.* **2012,** *19* (7), 671-6.

59. van den Born, E.; Omelchenko, M. V.; Bekkelund, A.; Leihne, V.; Koonin, E. V.; Dolja, V. V.; Falnes, P. Ø., Viral AlkB proteins repair RNA damage by oxidative demethylation. *Nucleic Acids Res.* **2008,** *36* (17), 5451-5461.

60. Sedgwick, B.; Bates, P. A.; Paik, J.; Jacobs, S. C.; Lindahl, T., Repair of alkylated DNA: Recent advances. *DNA repair* **2007,** *6* (4), 429-442.

61. Drabløs, F.; Feyzi, E.; Aas, P. A.; Vaagbø, C. B.; Kavli, B.; Bratlie, M. S.; Peña-Diaz, J.; Otterlei, M.; Slupphaug, G.; Krokan, H. E., Alkylation damage in DNA and RNA—repair mechanisms and medical significance. *DNA repair* **2004,** *3* (11), 1389-1407.

62. Sancar, A., Structure and function of DNA photolyase. *Biochemistry* **1994,** *33* (1), 2-9.

63. Essen, L. O.; Klar, T., Light-driven DNA repair by photolyases. *Cell Mol. Life. Sci.* **2006,** *63* (11), 1266-77.

64. Liu, Z.; Wang, L.; Zhong, D., Dynamics and mechanisms of DNA repair by photolyase. *Phys. Chem. Chem. Phys.* **2015,** *17* (18), 11933-11949.

65. Li, Y. F.; Kim, S. T.; Sancar, A., Evidence for lack of DNA photoreactivating enzyme in humans. *Proc. Natl. Acad. Sci. U.S.A* **1993,** *90* (10), 4389-4393.

66. Dumenco, L. L.; Allay, E.; Norton, K.; Gerson, S. L., The prevention of thymic lymphomas in transgenic mice by human O6-alkylguanine-DNA alkyltransferase. *Science* **1993,** *259* (5092), 219.

67. Nakatsuru, Y.; Matsukuma, S.; Nemoto, N.; Sugano, H.; Sekiguchi, M.; Ishikawa, T., O6-methylguanine-DNA methyltransferase protects against nitrosamine-induced hepatocarcinogenesis. *Proc. Natl. Acad. Sci. U.S.A* **1993,** *90* (14), 6468.

68. Becker, K.; Dosch, J.; Gregel, C. M.; Martin, B. A.; Kaina, B., Targeted Expression of Human O⁶-Methylguanine-DNA Methyltransferase (MGMT) in Transgenic Mice Protects against Tumor Initiation in Two-Stage Skin Carcinogenesis. *Cancer Res.* **1996,** *56* (14), 3244.

69. Liu, L.; Qin, X.; Gerson, S. L., Reduced lung tumorigenesis in human methylguanine DNA—methyltransferase transgenic mice achieved by expression of transgene within the target cell. *Carcinogenesis* **1999,** *20* (2), 279-284.

70. Shiraishi, A.; Sakumi, K.; Sekiguchi, M., Increased susceptibility to chemotherapeutic alkylating agents of mice deficient in DNA repair methyltransferase. *Carcinogenesis* **2000,** *21* (10), 1879-1883.

71. Esteller, M.; Toyota, M.; Sanchez-Cespedes, M.; Capella, G.; Peinado, M. A.; Watkins, D. N.; Issa, J.-P. J.; Sidransky, D.; Baylin, S. B.; Herman, J. G., Inactivation of the DNA Repair Gene *O6*- Methylguanine-DNA Methyltransferaseby Promoter Hypermethylation Is Associated with G to A Mutations in *KRAS* in Colorectal Tumorigenesis. *Cancer Res.* **2000,** *60* (9), 2368-2371.

72. Nakamura, M.; Watanabe, T.; Yonekawa, Y.; Kleihues, P.; Ohgaki, H., Promoter methylation of the DNA repair gene MGMT in astrocytomas is frequently

associated with G:C → A:T mutations of the TP53 tumor suppressor gene. *Carcinogenesis* **2001,** *22* (10), 1715-1719.

73. Pilžys, T.; Marcinkowski, M.; Kukwa, W.; Garbicz, D.; Dylewska, M.; Ferenc, K.; Mieczkowski, A.; Kukwa, A.; Migacz, E.; Wołosz, D.; Mielecki, D.; Klungland, A.; Piwowarski, J.; Poznański, J.; Grzesiuk, E., ALKBH overexpression in head and neck cancer: potential target for novel anticancer therapy. *Sci. Rep.* **2019,** *9* (1), 13249.

74. Cetica, V.; Genitori, L.; Giunti, L.; Sanzo, M.; Bernini, G.; Massimino, M.; Sardi, I., Pediatric brain tumors: mutations of two dioxygenases (hABH2 and hABH3) that directly repair alkylation damage. *J. Neuro-Oncol.* **2009,** *94* (2), 195-201.

75. Gao, W.; Li, L.; Xu, P.; Fang, J.; Xiao, S.; Chen, S., Frequent down-regulation of hABH2 in gastric cancer and its involvement in growth of cancer cells. *J. Gastroenterol. Hepatol.* **2011,** *26* (3), 577-84.

76. Yamato, I.; Sho, M.; SHIMADA, K.; Hotta, K.; Ueda, Y.; Yasuda, S.; Shigi, N.; Konishi, N.; Tsujikawa, K.; Nakajima, Y., PCA-1/ALKBH3 contributes to pancreatic cancer by supporting apoptotic resistance and angiogenesis. *Cancer Res.* **2012**, canres.0328.2012.

77. Shimada, K.; Fujii, T.; Tsujikawa, K.; Anai, S.; Fujimoto, K.; Konishi, N., ALKBH3 Contributes to Survival and Angiogenesis of Human Urothelial Carcinoma Cells through NADPH Oxidase and Tweak/Fn14/VEGF Signals. *Clin. Cancer Res.* **2012,** *18* (19), 5247-5255.

78. Galluzzi, L.; Senovilla, L.; Vitale, I.; Michels, J.; Martins, I.; Kepp, O.; Castedo, M.; Kroemer, G., Molecular mechanisms of cisplatin resistance. *Oncogene* **2012,** *31* (15), 1869-83.

79. Tell, G.; Wilson, D. M., 3rd, Targeting DNA repair proteins for cancer treatment. *Cell Mol. Life Sci* **2010,** *67* (21), 3569-3572.

80. Tell, G.; Fantini, D.; Quadrifoglio, F., Understanding different functions of mammalian AP endonuclease (APE1) as a promising tool for cancer treatment. *Cell Mol. Life Sci*. **2010,** *67* (21), 3589-608.

81. Wilson, D. M., 3rd; Simeonov, A., Small molecule inhibitors of DNA repair nuclease activities of APE1. *Cell Mol. Life Sci.* **2010,** *67* (21), 3621-31.

82. Wallace, S. S.; Murphy, D. L.; Sweasy, J. B., Base excision repair and cancer. *Cancer Lett.* **2012,** *327* (1), 73-89.

83. Wallace, S. S., Base excision repair: A critical player in many games. *DNA Repair* **2014,** *19*, 14-26.

84. Berger, S. H.; Hakala, M. T., Relationship of dUMP and free FdUMP pools to inhibition of thymidylate synthase by 5-fluorouracil. *Mol. Pharmacol.* **1984,** *25* (2), 303-309.

85. Epe, B.; Krokan, H. E.; Nilsen, H.; König, I.; Sneve, R.; Andersen, S.; Heine, T., Incorporation of dUMP into DNA is a major source of spontaneous DNA damage, while excision of uracil is not required for cytotoxicity of fluoropyrimidines in mouse embryonic fibroblasts. *Carcinogenesis* **2005,** *26* (3), 547-555.

86. Noordhuis, P.; Holwerda, U.; Van der Wilt, C. L.; Van Groeningen, C. J.; Smid, K.; Meijer, S.; Pinedo, H. M.; Peters, G. J., 5-Fluorouracil incorporation into RNA and DNA in relation to thymidylate synthase inhibition of human colorectal cancers. *Ann. Oncol.* **2004,** *15* (7), 1025-32.

87. An, Q.; Robins, P.; Lindahl, T.; Barnes, D. E., 5-Fluorouracil incorporated into DNA is excised by the Smug1 DNA glycosylase to reduce drug cytotoxicity. *Cancer Res.* **2007,** *67* (3), 940-5.

88. Allan, J. M.; Engelward, B. P.; Dreslin, A. J.; Wyatt, M. D.; Tomasz, M.; Samson, L. D., Mammalian 3-methyladenine DNA glycosylase protects against the toxicity and clastogenicity of certain chemotherapeutic DNA cross-linking agents. *Cancer Res.* **1998,** *58* (17), 3965-73.

89. Paik, J.; Duncan, T.; Lindahl, T.; Sedgwick, B., Sensitization of human carcinoma cells to alkylating agents by small interfering RNA suppression of 3-alkyladenine-DNA glycosylase. *Cancer Res.* **2005,** *65* (22), 10472-7.

90. Fu, D.; Calvo, J. A.; Samson, L. D., Balancing repair and tolerance of DNA damage caused by alkylating agents. *Nat. Rev. Cancer* **2012,** *12* (2), 104-120.

91. Rinne, M.; Caldwell, D.; Kelley, M. R., Transient adenoviral N-methylpurine DNA glycosylase overexpression imparts chemotherapeutic sensitivity to human breast cancer cells. *Mol. Cancer Ther.* **2004,** *3* (8), 955-67.

92. Klapacz, J.; Lingaraju, G. M.; Guo, H. H.; Shah, D.; Moar-Shoshani, A.; Loeb, L. A.; Samson, L. D., Frameshift mutagenesis and microsatellite instability induced by human alkyladenine DNA glycosylase. *Mol. Cell* **2010,** *37* (6), 843-853.

93. Paik, J.; Duncan, T.; Lindahl, T.; Sedgwick, B., Sensitization of Human Carcinoma Cells to Alkylating Agents by Small Interfering RNA Suppression of 3-Alkyladenine-DNA Glycosylase. *Cancer Res.* **2005,** *65* (22), 10472-10477.

94. Roth, R. B.; Samson, L. D., 3-Methyladenine DNA glycosylase-deficient Aag null mice display unexpected bone marrow alkylation resistance. *Cancer Res.* **2002,** *62* (3), 656-60.

95. Kisby, G. E.; Olivas, A.; Park, T.; Churchwell, M.; Doerge, D.; Samson, L. D.; Gerson, S. L.; Turker, M. S., DNA repair modulates the vulnerability of the developing brain to alkylating agents. *DNA Repair* **2009,** *8* (3), 400-412.

96. Citron, M.; Decker, R.; Chen, S.; Schneider, S.; Graver, M.; Kleynerman, L.; Kahn, L. B.; White, A.; Schoenhaus, M.; Yarosh, D., *O6*-Methylguanine-DNA Methyltransferase in Human Normal and Tumor Tissue from Brain, Lung, and Ovary. *Cancer Res.* **1991,** *51* (16), 4131-4134.

97. Belanich, M.; Randall, T.; Pastor, M. A.; Kibitel, J. T.; Alas, L. G.; Dolan, M. E.; Schold, S. C., Jr.; Gander, M.; Lejeune, F. J.; Li, B. F.; White, A. B.; Wasserman, P.; Citron, M. L.; Yarosh, D. B., Intracellular Localization and intercellular heterogeneity of the human DNA repair protein O(6)-methylguanine-DNA methyltransferase. *Cancer Chemother. Pharmacol.* **1996,** *37* (6), 547-55.

98. Schold, S. C.; Brent, T. P.; Hofe, E. v.; Friedman, H. S.; Mitra, S.; Bigner, D. D.; Swenberg, J. A.; Kleihues, P., O6-Alkylguanine-DNA alkyltransferase and sensitivity to procarbazine in human brain-tumor xenografts. *J. Neurosurg.* **1989,** *70* (4), 573.

99. Brent, T. P.; Houghton, P. J.; Houghton, J. A., O6-Alkylguanine-DNA alkyltransferase activity correlates with the therapeutic response of human rhabdomyosarcoma xenografts to 1-(2-chloroethyl)-3-(trans-4-methylcyclohexyl)-1-nitrosourea. *Proc. Natl. Acad. Sci. U.S.A* **1985,** *82* (9), 2985-2989.

100. Chen, F.; Bian, K.; Tang, Q.; Fedeles, B. I.; Singh, V.; Humulock, Z. T.; Essigmann, J. M.; Li, D., Oncometabolites d- and l-2-Hydroxyglutarate Inhibit the AlkB Family DNA Repair Enzymes under Physiological Conditions. *Chem, Res.Toxicol.* **2017,** *30* (4), 1102-1110.

101. Calvo, J. A.; Meira, L. B.; Lee, C.-Y. I.; Moroski-Erkul, C. A.; Abolhassani, N.; Taghizadeh, K.; Eichinger, L. W.; Muthupalani, S.; Nordstrand, L. M.; Klungland, A.; Samson, L. D., DNA repair is indispensable for survival after acute inflammation. *J. Clin. Investig.* **2012,** *122* (7), 2680-2689.

102. Luger, K.; Mader, A. W.; Richmond, R. K.; Sargent, D. F.; Richmond, T. J., Crystal structure of the nucleosome core particle at 2.8 A resolution. *Nature* **1997,** *389* (6648), 251-60.

103. Eickbush, T. H.; Moudrianakis, E. N., The histone core complex: an octamer assembled by two sets of protein-protein interactions. *Biochemistry* **1978,** *17* (23), 4955-64.

104. Yang, J. G.; Narlikar, G. J., FRET-based methods to study ATP-dependent changes in chromatin structure. *Methods* **2007,** *41* (3), 291-295.

105. Buning, R.; van Noort, J., Single-pair FRET experiments on nucleosome conformational dynamics. *Biochimie* **2010,** *92* (12), 1729-1740.

106. Lee, J. Y.; Lee, J.; Yue, H.; Lee, T.-H., Dynamics of Nucleosome Assembly and Effects of DNA Methylation. *J. Biol.Chem.* **2014**.

107. Kim, J.; Wei, S.; Lee, J.; Yue, H.; Lee, T.-H., Single-Molecule Observation Reveals Spontaneous Protein Dynamics in the Nucleosome. *J. Phys. Chem. B* **2016,** *120* (34), 8925-8931.

108. Polach, K. J.; Widom, J., Restriction enzymes as probes of nucleosome stability and dynamics. In *Methods Enzymol.*, Academic Press: 1999; Vol. 304, pp 278-298.

109. Hayes, J. J.; Tullius, T. D.; Wolffe, a. P., The structure of DNA in a nucleosome. *Proc. Natl. Acad. Sci. U.S.A* **1990,** *87* (19), 7405-9.

110. Suquet, C.; Smerdon, M. J., UV damage to DNA strongly influences its rotational setting on the histone surface of reconstituted nucleosomes. *J. Biol.Chem.***1993,** *268* (32), 23755-7.

111. Brown, D. W.; Libertini, L. J.; Suquet, C.; Small, E. W.; Smerdon, M. J., Unfolding of nucleosome cores dramatically changes the distribution of ultraviolet photoproducts in DNA. *Biochemistry* **1993,** *32* (40), 10527-31.

112. Nilsen, H.; Lindahl, T.; Verreault, A., DNA base excision repair of uracil residues in reconstituted nucleosome core particles. *EMBO J.* **2002,** *21* (21), 5943-52.

113. Li, S.; Smerdon, M. J., Base Excision Repair of N-Methylpurines in a Yeast Minichromosome: effects of transcription, DNA sequence, and Nucleosome Positioning. *J. Biol.Chem.* **1999,** *274* (18), 12201-12204.

114. Li, S.; Smerdon, M. J., Nucleosome Structure and Repair of N-Methylpurines in the GAL1-10 Genes of Saccharomyces cerevisiae. *J. Biol.Chem.* **2002,** *277* (47), 44651-44659.

115. Olmon, E. D.; Delaney, S., Differential Ability of Five DNA Glycosylases to Recognize and Repair Damage on Nucleosomal DNA. *ACS Chem. Biol.* **2017,** *12* (3), 692-701.

116. Beard, B. C.; Wilson, S. H.; Smerdon, M. J., Suppressed catalytic activity of base excision repair enzymes on rotationally positioned uracil in nucleosomes. *Proc. Natl. Acad. Sci. U.S.A* **2003,** *100* (13), 7465-7470.

117. Bilotti, K.; Tarantino, M. E.; Delaney, S., hOGG1 removes solution-accessible 8-oxoG lesions from globally-substituted nucleosomes except at the dyad region. *Biochemistry* **2018**.

118. Ye, Y.; Stahley, M. R.; Xu, J.; Friedman, J. I.; Sun, Y.; McKnight, J. N.; Gray, J. J.; Bowman, G. D.; Stivers, J. T., Enzymatic excision of uracil residues in nucleosomes depends on the local DNA structure and dynamics. *Biochemistry* **2012,** *51* (30), 6028-38.

119. Prasad, A.; Wallace, S. S.; Pederson, D. S., Initiation of base excision repair of oxidative lesions in nucleosomes by the human, bifunctional DNA glycosylase NTH1. *Mol. Cell. Biol.***2007,** *27* (24), 8442-53.

120. Bilotti, K.; Kennedy, E. E.; Li, C.; Delaney, S., Human OGG1 activity in nucleosomes is facilitated by transient unwrapping of DNA and is influenced by the local histone environment. *DNA Repair* **2017,** *59*, 1-8.

121. Hinz, J. M.; Rodriguez, Y.; Smerdon, M. J., Rotational dynamics of DNA on the nucleosome surface markedly impact accessibility to a DNA repair enzyme. *Proc. Natl. Acad. Sci. U.S.A* **2010,** *107* (10), 4646-51.

122. Rodriguez, Y.; Smerdon, M. J., The structural location of DNA lesions in nucleosome core particles determines accessibility by base excision repair enzymes. *J. Biol.Chem.* **2013,** *288* (19), 13863-13875.

123. Cole, H. A.; Tabor-Godwin, J. M.; Hayes, J. J., Uracil DNA Glycosylase Activity on Nucleosomal DNA Depends on Rotational Orientation of Targets. *J. Biol.Chem.* **2010,** *285* (4), 2876-2885.

124. Odell, I. D.; Newick, K.; Heintz, N. H.; Wallace, S. S.; Pederson, D. S., Non-specific DNA binding interferes with the efficient excision of oxidative lesions from chromatin by the human DNA glycosylase, NEIL1. *DNA Repair* **2010,** *9* (2), 134-43.

125. Maher, R. L.; Prasad, A.; Rizvanova, O.; Wallace, S. S.; Pederson, D. S., Contribution of DNA unwrapping from histone octamers to the repair of oxidatively damaged DNA in nucleosomes. *DNA Repair* **2013,** *12* (11), 964-971.

126. Mao, P.; Brown, A. J.; Malc, E. P.; Mieczkowski, P. A.; Smerdon, M. J.; Roberts, S. A.; Wyrick, J. J., Genome-wide maps of alkylation damage, repair, and mutagenesis in yeast reveal mechanisms of mutational heterogeneity. *Genome res.* **2017,** *27* (10), 1674-1684.

127. Pich, O.; Muiños, F.; Sabarinathan, R.; Reyes-Salazar, I.; Gonzalez-Perez, A.; Lopez-Bigas, N., Somatic and Germline Mutation Periodicity Follow the Orientation of the DNA Minor Groove around Nucleosomes. *Cell* **2018,** *175* (4), 1074-1087.e18.

128. Lee, D. Y.; Hayes, J. J.; Pruss, D.; Wolffe, A. P., A positive role for histone acetylation in transcription factor access to nucleosomal DNA. *Cell* **1993,** *72* (1), 73-84.

129. Campos, E. I.; Reinberg, D., Histones: Annotating Chromatin. *Annu. Rev. Genet.* **2009,** *43* (1), 559-599.

130. Azad, G. K.; Swagatika, S.; Kumawat, M.; Kumawat, R.; Tomar, R. S., Modifying Chromatin by Histone Tail Clipping. *J. Mol. Biol.* **2018,** *430* (18, Part B), 3051-3067.

131. Hamiche, A.; Sandaltzopoulos, R.; Gdula, D. A.; Wu, C., ATP-Dependent Histone Octamer Sliding Mediated by the Chromatin Remodeling Complex NURF. *Cell* **1999,** *97* (7), 833-842.

132. Lorch, Y.; Maier-Davis, B.; Kornberg, R. D., Chromatin remodeling by nucleosome disassembly *in vitro*. *Proc. Natl. Acad. Sci. U.S.A* **2006,** *103* (9), 3090-3093.

133. Mizuguchi, G.; Shen, X.; Landry, J.; Wu, W.-H.; Sen, S.; Wu, C., ATP-Driven Exchange of Histone H2AZ Variant Catalyzed by SWR1 Chromatin Remodeling Complex. *Science* **2004,** *303* (5656), 343-348.

134. Dechassa, M. L.; Sabri, A.; Pondugula, S.; Kassabov, S. R.; Chatterjee, N.; Kladde, M. P.; Bartholomew, B., SWI/SNF Has Intrinsic Nucleosome Disassembly Activity that Is Dependent on Adjacent Nucleosomes. *Mol. Cell* **2010,** *38* (4), 590-602.

135. Qiu, Y.; Levendosky, R. F.; Chakravarthy, S.; Patel, A.; Bowman, G. D.; Myong, S., The Chd1 Chromatin Remodeler Shifts Nucleosomal DNA Bidirectionally as a Monomer. *Mol. Cell* **2017,** *68* (1), 76-88.e6.

136. Papamichos-Chronakis, M.; Watanabe, S.; Rando, O. J.; Peterson, C. L., Global Regulation of H2A.Z Localization by the INO80 Chromatin-Remodeling Enzyme Is Essential for Genome Integrity. *Cell* **2011,** *144* (2), 200-213.

137. Dickey, J. S.; Redon, C. E.; Nakamura, A. J.; Baird, B. J.; Sedelnikova, O. A.; Bonner, W. M., H2AX: functional roles and potential applications. *Chromosoma* **2009,** *118* (6), 683-692.

138. Xu, Y.; Ayrapetov, M. K.; Xu, C.; Gursoy-Yuzugullu, O.; Hu, Y.; Price, B. D., Histone H2A.Z controls a critical chromatin remodeling step required for DNA double-strand break repair. *Mol. cell* **2012,** *48* (5), 723-733.

139. Timinszky, G.; Till, S.; Hassa, P. O.; Hothorn, M.; Kustatscher, G.; Nijmeijer, B.; Colombelli, J.; Altmeyer, M.; Stelzer, E. H. K.; Scheffzek, K.; Hottiger, M. O.; Ladurner, A. G., A macrodomain-containing histone rearranges chromatin upon sensing PARP1 activation. *Nat. Struct.l Mol. Biol.* **2009,** *16*, 923.

140. Saxena, A.; Wong, L. H.; Kalitsis, P.; Earle, E.; Shaffer, L. G.; Choo, K. H. A., Poly(ADP-ribose) polymerase 2 localizes to mammalian active centromeres and interacts with PARP-1, Cenpa, Cenpb and Bub3, but not Cenpc. *Hum. Mol. Genet.* **2002,** *11* (19), 2319-2329.

141. Ambartsumyan, G.; Gill, R. K.; Perez, S. D.; Conway, D.; Vincent, J.; Dalal, Y.; Clark, A. T., Centromere protein A dynamics in human pluripotent stem cell self-renewal, differentiation and DNA damage. *Hum. Mol. Genet.* **2010,** *19* (20), 3970-3982.

142. Zeitlin, S. G.; Baker, N. M.; Chapados, B. R.; Soutoglou, E.; Wang, J. Y. J.; Berns, M. W.; Cleveland, D. W., Double-strand DNA breaks recruit the centromeric histone CENP-A. *Proc. Natl. Acad. Sci. U.S.A* **2009,** *106* (37), 15762-15767.

143. Sellou, H.; Lebeaupin, T.; Chapuis, C.; Smith, R.; Hegele, A.; Singh, H. R.; Kozlowski, M.; Bultmann, S.; Ladurner, A. G.; Timinszky, G.; Huet, S., The poly(ADP-ribose)-dependent chromatin remodeler Alc1 induces local chromatin relaxation upon DNA damage. *Mol. Biol. Cell* **2016,** *27* (24), 3791-3799.

144. Li, C.; Delaney, S., Histone H2A Variants Enhance the Initiation of Base Excision Repair in Nucleosomes. *ACS Chem. Biol.* **2019,** *14* (5), 1041-1050.

145. Erik Wellinger, R.; Thoma, F., Nucleosome structure and positioning modulate nucleotide excision repair in the non-transcribed strand of an active gene. *EMBO J.* **1997,** *16* (16), 5046-5056.

146. Sugasawa, K., UV-DDB: A molecular machine linking DNA repair with ubiquitination. *DNA Repair* **2009,** *8* (8), 969-972.

147. Jang, S.; Kumar, N.; Beckwitt, E. C.; Kong, M.; Fouquerel, E.; Rapić-Otrin, V.; Prasad, R.; Watkins, S. C.; Khuu, C.; Majumdar, C.; David, S. S.; Wilson, S. H.; Bruchez, M. P.; Opresko, P. L.; Van Houten, B., Damage sensor role of UV-DDB during base excision repair. *Nat. Struct. Mol. Biol.* **2019,** *26* (8), 695-703.

148. Matsumoto, S.; Cavadini, S.; Bunker, R. D.; Grand, R. S.; Potenza, A.; Rabl, J.; Yamamoto, J.; Schenk, A. D.; Schübeler, D.; Iwai, S.; Sugasawa, K.; Kurumizaka, H.; Thomä, N. H., DNA damage detection in nucleosomes involves DNA register shifting. *Nature* **2019,** *571* (7763), 79-84.

149. Maher, R. L.; Marsden, C. G.; Averill, A. M.; Wallace, S. S.; Sweasy, J. B.; Pederson, D. S., Human cells contain a factor that facilitates the DNA glycosylase-mediated excision of oxidized bases from occluded sites in nucleosomes. *DNA Repair* **2017,** *57*, 91-97.

Chapter 2: Comparison of the Base Excision and Direct Reversal Repair Pathways for Repair of Alkylation Damage in Nucleosome Core Particles†

†Adapted from:

Paul J. Caffrey, Raadhika Kher, Ke Bian, Deyu Li, Sarah Delaney

Comparison of the Base Excision and Direct Reversal Repair Pathways for Correcting *1*,*N6*-Ethenoadenine in Strongly Positioned Nucleosome Core Particles

Chem. Res. Toxicol. (**2020**) 33 (7): 1888-1896. doi: 10.1021/acs.chemrestoc.0c00089

2.1 Abstract

1,N^6-ethenoadenine (εA) is a mutagenic lesion and biomarker observed in numerous cancerous tissues. Two pathways are responsible for its repair: base excision repair (BER) and direct reversal repair (DRR). Alkyladenine DNA glycosylase (AAG) is the primary enzyme that excises εA in BER, generating stable intermediates that are processed by downstream enzymes. For DRR, the Fe(II)/α-ketoglutarate-dependent ALKBH2 enzyme repairs εA by direct conversion of εA to A. While the molecular mechanism of each enzyme is well understood on unpackaged duplex DNA, less is known about their actions on packaged DNA. The nucleosome core particle (NCP) forms the minimal packaging unit of DNA in eukaryotic organisms and is comprised of 145-147 base pairs wrapped around a core of eight histone proteins. In this work, we investigated the activity of AAG and ALKBH2 on εA lesions globally distributed at positions throughout a strongly positioned NCP. Overall, we examined repair of εA at 23 unique locations in packaged DNA. We observed a strong correlation between rotational positioning of εA and AAG activity, but not ALKBH2 activity. ALKBH2 was more effective than AAG at repairing occluded εA lesions but only AAG was capable of full repair of any εA in the NCP. However, notable exceptions to these trends were observed, highlighting the complexity of the NCP as a substrate for DNA repair. Modeling of binding of the repair enzymes to NCPs revealed that some of these observations can be explained by steric interference caused by DNA packaging. Specifically, interactions between ALKBH2 and the histone proteins obstruct binding to DNA and leads to diminished activity. Taken together, these results support *in vivo* observations of alkylation damage profiles and contribute to our understanding of mutational hotspots.

2.2 Introduction

The DNA lesion 1,N^6-ethenoadenine (εA, **Figure 2.1**) is a mutagenic adduct[1] generated by exposure of A to various DNA damaging agents such as vinyl chloride and aldehyde byproducts of lipid peroxidation.[2, 3] Elevated εA levels have been detected in a number of cancerous tissues and in tissues of chronic inflammatory diseases.[4] The A•T to T•A transversion, possibly induced by εA, is a common mutation observed in the *P53* and *RAS* genes and is associated with carcinogenesis.[5] This carcinogenic effect of εA necessitates a thorough understanding of how cells efficiently repair and remove such damage.

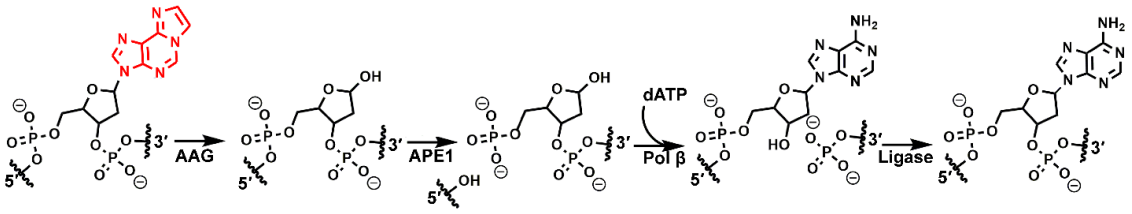

Figure 2.1 Base excision repair of εA (red) initiated by AAG

Two repair pathways recognize and repair the εA lesion: base excision repair (BER) and direct reversal repair (DRR). BER of εA is initiated by alkyladenine glycosylase (AAG) removing the lesion (**Figure 2.1**), generating an apurinic/apyrimidinic (AP) site.[6-7] Downstream BER enzymes process this AP site and complete the repair. AAG repairs alkylated nucleobases in bacteria,[8] yeast,[9] and mammalian cells.[10] A key component of recognition and removal of εA is the base-flipping mechanism.[11] Furthermore, while AAG only removes εA from double-stranded

substrates, it only requires contact with the lesion-containing strand for substrate recognition.[12]

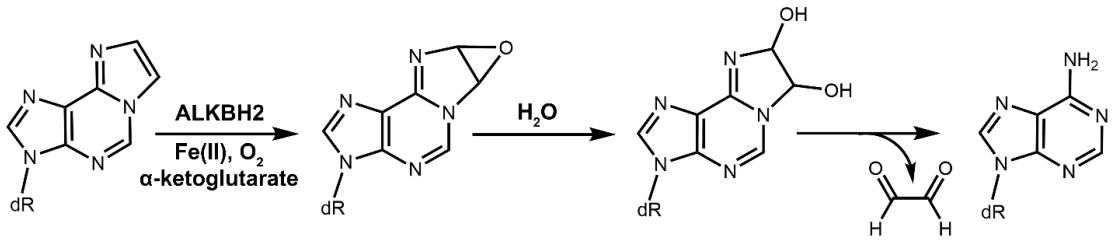

Figure 2.2 Mechanism of direct repair of εA by the AlkB family of dioxygenases

The repair of εA lesions by DRR is carried out by the AlkB family of dioxygenases, which performs chemistry to directly transform εA to canonical A with a single enzyme (**Figure 2.2**).[13-16] Based on sequence homology, up to nine human homologs have been identified as being structurally similar to *E. coli* AlkB.[17] ALKBH2 and ALKBH3 are the enzymes responsible for DRR of εA to A in humans[18, 19] with ALKBH2 primarily responsible for repairing lesions in double-stranded DNA.[20] AlkB homologs are ubiquitous,[21] being observed in RNA viruses,[22] aerobic bacteria,[23] and metazoans.[24] In a manner similar to AAG, ALKBH2 flips its target lesion into its active site prior to chemistry.[25] Unlike AAG, ALKBH2 requires contact with both strands of DNA to ensure its substrate specificity.[25]

While BER and DRR have been studied extensively in unpackaged DNA, they are not as well understood in the context of chromatin. The nucleosome core particle (NCP) is the basic packaging unit in eukaryotic chromatin and is comprised of 145-147 base pairs of DNA wrapped approximately 1.7 times around a histone protein core.[26] The

histone core is formed by two copies of each of the histone proteins H2A, H2B, H3, and H4.[27] Each histone contains a highly structured globular core and a disordered tail.[26] The location of any nucleobase within the NCP can be characterized according to two parameters: rotational positioning and translational positioning. The rotational can be defined as outwards towards the solution (OUT), inwards towards the histone core (IN), or a position somewhere in between (MID). The translational position of a nucleobase is based on its distance from the dyad axis. It is known that DNA located further from the dyad axis and closer to the entry-exit points is subject to spontaneous and transient dissociation from the histone core.[28, 29] Furthermore, lesions with different rotational and translational positions exist in varied microenvironments within an NCP which can influence DNA repair.

Most literature reports have investigated how AAG and ALKBH2 function on unpackaged DNA substrates. To the best of our knowledge, no work has been reported on DRR in the context of an NCP. The BER and DRR pathways may differ in their ability to work in certain cellular environments, including when DNA is packaged or unpackaged. The overlapping lesion substrates of AAG and ALKBH2 may help balance the need to repair mutagenic lesions against the generation of potentially mutagenic and/or cytotoxic intermediates such as AP sites and nicks. For example, DRR avoids the creation of the AP site generated by BER which has been shown to react with histone lysines leading to a strand break.[30] However, it remains unknown the context in which each repair pathway operates within the cellular environment.

In this study, we used a global population of NCP with εA lesions in a variety of translational and rotational positions to investigate and compare the activities of AAG

and ALKBH2. We utilized a combinatorial approach of hydroxyl radical footprinting (HRF) and enzymatic reactions to evaluate the repair profiles of both AAG and ALKBH2 in strongly positioned nucleosomes (**Figure 2.3**). We found that while only AAG has, at some sites, full activity on εA in the NCP, ALKBH2 is better at repairing occluded εA lesions. Through molecular modeling, we hypothesize that these differential repair profiles may be the result of steric interactions with the histone core and some of the structural distortions caused by these two enzymes.

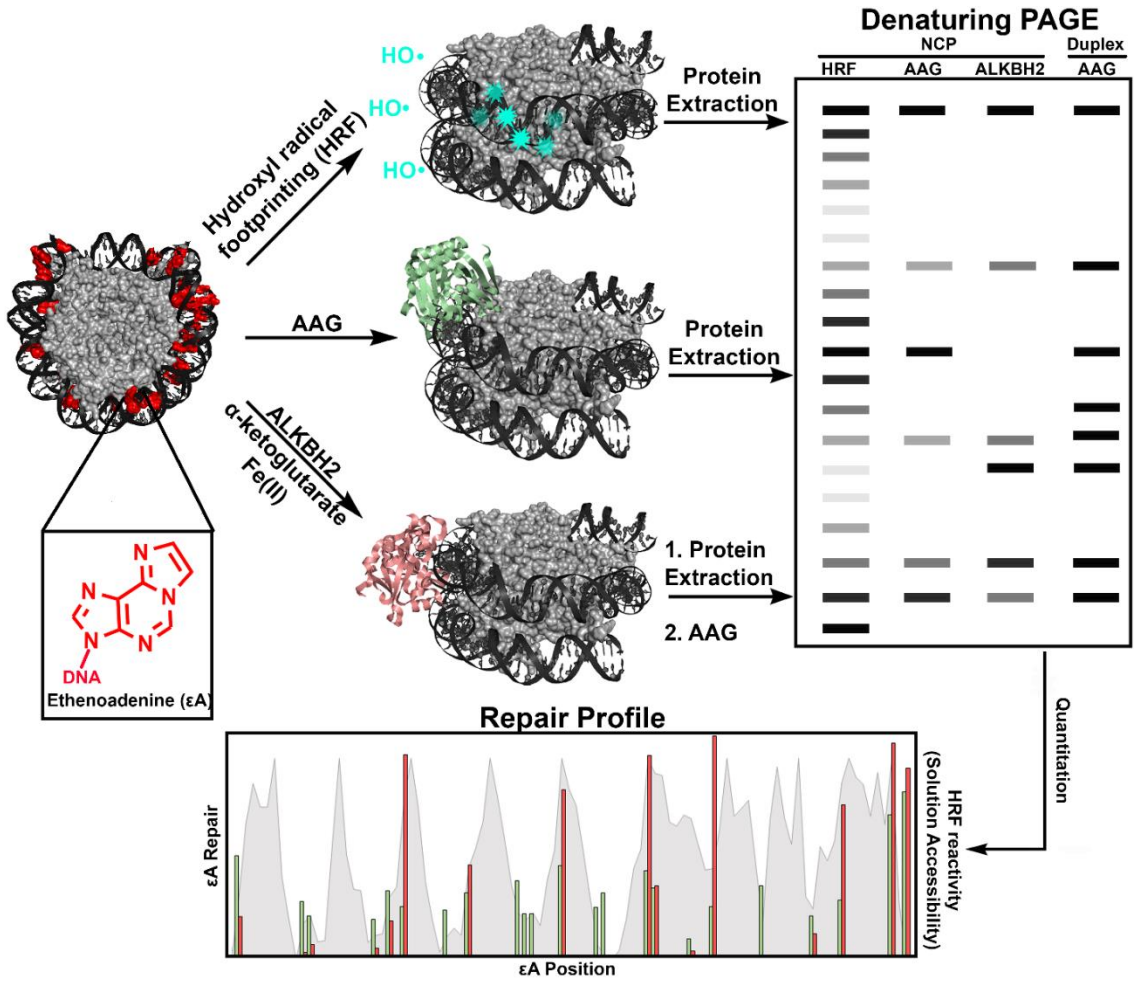

Figure 2.3 Overall workflow to establish the repair profiles of AAG and ALKBH2 in strongly positioned NCPs. NCPs with εA distributed globally throughout the NCP were assembled. Notably, each NCP contains only a single εA lesion but the population of NCP has εA in a variety of locations. The NCP were treated in three ways. The top shows establishing the solution accessibility of the εA lesions by hydroxyl radical footprinting. The middle shows the treatment of NCPs with AAG to reveal the εA sites that are repaired by BER. The bottom shows the two-step process for revealing DRR by ALKBH2. First, the NCPs are treated with ALKBH2 and its cofactors. The histone proteins are then extracted and the liberated DNA is treated with AAG to reveal sites that were not repaired, and by comparison to controls, the εA sites that were repaired by ALKBH2. The data is quantitated and combined to reveal the repair profile of εA in strongly positioned NCPs.

2.3 Materials and Methods

2.3.1 Oligonucleotide Synthesis and Purification

All oligonucleotides used in this study were synthesized on a MerMade 4 DNA synthesizer (BioAutomation). All reagents were purchased from Glen Research. We used the 145 bp Widom 601 nucleosome positioning sequence (**Table 2.1**) as the unincorporated duplex control and to assemble NCP. Base pairs are numbered starting with the first base of the 5′-end of the "I" strand. The 145 mer oligonucleotide containing εA was synthesized on 1400 Å controlled pore glass beads using phosphoramidites with ultramild protecting groups and deprotected according to the manufacturer's specifications. A Poisson distribution was utilized to substitute εA for A throughout the "I" strand, similar to recent reports.[31-33] We accomplished this distribution by using an εA and A phosphoramidite mixture during the synthesis, with the molar ratio determined by the Poisson distribution ($\lambda = 0.355$). The resulting DNA population contains either 0 or 1 εA lesion per 145 mer oligonucleotide with only 5% containing two or more lesions. The final trityl group was removed on the synthesizer and the DNA cleaved from the beads by incubation in NH_4OH at room temperature for 2 h. The DNA was then purified by 8% denaturing polyacrylamide gel electrophoresis (PAGE).

Table 2.1 DNA sequences used in this study

Name	Length	Sequence (5′ to 3′)
"I" strand	145mer	ATCAGAATCCCGGTGCCGAGGCCGCTCAATTGGTCGTAGACAG CTCTAGCACCGCTTAAACGCACGTACGCGCTGTCCCCCGCGTTT TAACCGCCAAGGGGATTACTCCCTAGTCTCCAGGCACGTGTCA GATATATACATCGAT
"J" strand	145mer	ATCGATGTATATATCTGACACGTGCCTGGAGACTAGGGAGTAA TCCCCTTGGCGGTTAAAACGCGGGGGACAGCGCGTACGTGCGT TTAAGCGGTGCTAGAGCTGTCTACGACCAATTGAGCGGCCTCG GCACCGGGATTCTGAT

IS1	23mer	ATCAGAATCCCGGTGCCGAGGCC
IS2	92mer	ATCAGAATCCCGGTGCCGAGGCCGCTCAATTGGTCGTAGACAG CTCTAGCACCGCTTAAACGCACGTACGCGCTGTCCCCCGCGTTT TAACC
J1	45mer	ATCGATGTATATATCTGACACGTGCCTGGAGACTAGGGAGTAA TC
J2	65mer	CCCTTGGCGGTTAAAACGCGGGGGACAGCGCGTACGTGCGTTT AAGCGGTGCTAGAGCTGTCTAC
J3	35mer	GACCAATTGAGCGGCCTCGGCACCGGGATTCTGAT
JS12	30mer	TTTAACCGCCAAGGGGATTACTCCCTAGTC
JS23	32mer	GCCGCTCAATTGGTCGTAGACAGCTCTAGCAC

The complementary 145 mer was prepared using a ligation strategy (**Figure 2.4**). The component oligonucleotides for ligation were synthesized using standard phosphoramidite protecting groups and the final trityl group was retained. Reverse-phase HPLC purification at 90 °C was used to purify the oligonucleotides with a trityl group (Agilent PLRP-S column, 250 mm × 4.6 mm; A = 100 mM triethylammonium acetate [TEAA] in 5% aqueous MeCN, B = 100 mM TEAA in MeCN; 5:95 to 35:65 of A:B over 30 min, 35:65 to 5:95 of A:B over 5 min at 1 mL/min, retention times ranged from 24-29 minutes). Incubation in 20% v/v aqueous glacial acetic acid for 1 h at room temperature removed the trityl group and a second HPLC purification at 90 °C was performed (Agilent PLRP-S column, 250 mm × 4.6 mm; A = 100 mM triethylammonium acetate [TEAA] in 5% aqueous MeCN, B = 100 mM TEAA in MeCN; 0:100 to 15:85 of A:B over 35 min, 15:85 to 35:65 of A:B over 5 min at 1 mL/min, retention times ranged from 28-32 minutes). Electrospray ionization mass spectrometry was used to verify the identity of the component oligonucleotides. Five nmol of each component oligonucleotide J2 and J3 (Scheme S2) were 5′-phosphorylated using 2 mM ATP and 30 units T4 kinase (New England Biolabs). These phosphorylated components were then combined in equal molar

amounts with component J1 and 10% excess of two scaffolding oligonucleotides, JS12 and JS23, and annealed by heating to 95°C for 5 min and cooling at 1°C per min to room temperature in 50 mM NaCl and 20 mM Tris (pH 8.0). These annealed oligonucleotides were then ligated at room temperature overnight using 4800 units T4 DNA ligase (New England Biolabs). The product of the ligation reaction was then purified using 8% denaturing PAGE.

Figure 2.4 Ligation scheme for complementary J strand sequence. Five nmol of phosphorylated J2 and J3 was mixed with 5 nmol J1 and 5.5 nmol JS12 and JS23 and annealed. The annealed sample was then treated with ligase to assemble 145 mer complementary DNA. The ligation reaction was purified by 8% denaturing PAGE.

The two single-stranded internal standards, IS1 and IS2, used for normalizing band quantification in the AAG and ALKBH2 analyses, were designed as a 23 mer and a 92 mer (**Table 2.1**) such that they would not co-migrate with any εA cleavage product. They were synthesized as described above and purified by 12% and 8% denaturing PAGE, respectively.

2.3.2 Reconstitution of Global εA Nucleosome Core Particles

Recombinant *Xenopus laevis* histones were individually expressed and purified, and subsequently assembled into octamers.[34, 35] NCPs were reconstituted by dialyzing the radiolabeled εA-containing duplex population and histone octamer together via salt gradient, as described previously.[34] Briefly, a 7% molar excess of histone octamer (0.535 μM octamer) was added to radiolabeled εA containing 145 bp duplex (0.5 μM DNA) in

buffer (10 mM Tris-HCl [pH 7.5], 1 mM EDTA, 1 mM dithiothreitol [DTT], 2 M NaCl, 500 μg/mL BSA) in a Slide-a-Lyzer dialysis device (0.1 mL capacity, 3.5 kDa MWCO; Thermo Fisher Scientific). The dialysis device started in a buffer of 10 mM Tris-HCl (pH 7.5), 1 mM EDTA, 1 mM DTT, 2 M NaCl at 4 °C. The device was placed in buffers containing decreasing concentrations of NaCl (1.2 M, 1.0 M, 0.6 M, 0 M) at hourly intervals. The final dialysis proceeded for 3 h and then the NCPs were filtered with a 0.22 μm cellulose acetate centrifuge tube filter (Corning Costar) to remove insoluble particles. NCP formation and relative purity were analyzed using a 7% native PAGE (60:1 acrylamide:bisacrylamide; 0.25x TBE) run for 3 h at 160 V at 4 °C (**Figure 2.5**). Only NCPs containing ≤ 5% duplex DNA were used in further studies.

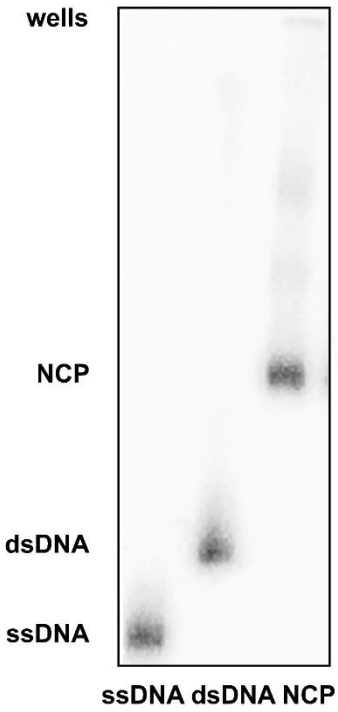

Figure 2.5 Native PAGE Analysis of εA Containing NCP. Representative native PAGE showing successful NCP formation as indicated by slower band migration in the NCP lane relative to the unincorporated duplex (dsDNA) lane. Only NCPs containing <5% dsDNA were used in these studies.

2.3.3 Hydroxyl Radical Footprinting

Hydroxyl radical footprinting was utilized to determine the relative solution accessibility of nucleobases in the NCP. A modified version of the method of Tullius[36, 37] was used to ensure single-hit conditions. Briefly, 7.5 μL of each 1 mM Fe(II)-EDTA, 10 mM sodium ascorbate, and 0.12% w/v aqueous hydrogen peroxide were combined with 5 pmol NCPs in 52.5 μL buffer (10 mM Tris-HCl [pH 7.5], 1 mM EDTA). This mixture was incubated in the dark at room temperature for 10 min and then quenched with 16 μL 1 mM EDTA in 25% v/v glycerol. This quenched sample was immediately loaded onto a 7% native PAGE (60:1 acrylamide:bisacrylamide; 0.25x TBE) and run for 3 h at 155 V at 4 °C. The gel bands containing NCPs were excised and eluted into buffer (0.3 M NaOAc, 1 mM Tris-HCl [pH 8.0], 1 mM EDTA) for 18-24 h at 37°C with gentle shaking (60 rpm). The eluent was then concentrated using a centrifugal concentrator (Sartorius Viaspin Turbo 15, 5 kDa MWCO) and filtered using a 0.22 μm cellulose acetate syringe filter. The samples was extracted with equal volume addition of 25:24:1 phenol:chloroform:isoamyl alcohol (PCI) and the aqueous layer was concentrated by SpeedVac evaporation. Following the addition of 40 μL co-precipitation agent (0.5 mg/mL tRNA in 300 mM NaOAc [pH 8.0], 1 mM EDTA), samples were desalted with ethanol precipitation. Samples were resuspended in a 1:1 mixture of formamide and water for denaturing PAGE. Cleavage fragments were resolved by 8% denaturing PAGE and quantitated using SAFA[38] gel analysis software.

The determination of solution accessibilities of nucleobases was achieved by normalization to the highest band intensity within a helical turn. Briefly, the band intensities were plotted against base position to identify the peaks and valleys

corresponding to OUT and IN locations respectively. The identified peaks with the highest band intensity were assigned as the most OUT position within a helical turn and assigned a value of 1. The band intensity of the five bases flanking each side of this OUT position were then normalized to this value to give the solution accessibility within the helical turn. This normalization allows for direct comparison of rotational positioning throughout all bases in the NCP. Highly solution-accessible (OUT) positions were defined as those with a ratio greater than or equal to 0.7; medium solution-accessible (MID) positions with a ratio range from 0.3-0.7; low solution accessibility (IN) positions were defined as those with a ratio less than 0.3.

2.3.4 Enzymatic Reactions

Human AAG was purchased from New England Biolabs, and the total enzyme concentration was determined by Bradford assay using γ-globulin standards (Bio-Rad Laboratories). Human ALKBH2 was expressed, purified and quantified as previously described.[39, 40] To assess the activity of ALKBH2 or AAG, 1 pmol substrate (either duplex DNA or NCPs) were mixed with 40 pmol ALKBH2 or AAG in a total volume of 20 μL of the reaction buffer (20 mM Tris, 50 mM NaCl, 150 mM KCl, 1 mM DTT, 100 μg/mL BSA, 1.5 mM α-ketoglutarate disodium salt, 3 mM sodium ascorbate, 50 mM HEPES (pH 8), and 100 μM $Fe(NH_4)_2(SO_4)_2 \bullet (H_2O)_6$). The reaction buffer was the same for both enzymes to ensure a direct comparison of repair with the same biophysical characteristics of the NCP in each instance. The samples were incubated for 1 h at 37 °C along with a negative control sample (no enzyme). After the incubation, AAG treated samples were quenched with 20 μL of 1M NaOH which had been spiked with the radiolabeled internal standards and heated to at 90 °C for 3 min. The internal standards were added based on

radioactive counts. Briefly, the counts per each εA site were calculated and multiplied by 1.7 to determine how many counts of the internal standards were added. ALKBH2 treated samples were quenched with a final concentration 25 mM EDTA and heated at 95 °C for 5 min. For both the AAG and ALKBH2 samples, the protein and DNA were then separated using an extraction with PCI. For AAG treated samples, the aqueous layer was supplemented with 40 μL co-precipitation agent (0.5 mg/mL tRNA in 300 mM NaOAc [pH 8.0], 1 mM EDTA) and 600 μL ethanol before being placed on dry ice for 30 min. For the ALKBH2 treated samples, the aqueous phase was supplemented with 40 μL 0.5 M sodium acetate and 600 μL ethanol and placed on dry ice for 30 min. The ALKBH2 treated samples were then reconstituted in 20 mM Tris (pH 8.0), 50 mM NaCl, 150 mM KCl, 1 mM DTT, 100 μg/mL BSA, 40 pmol of AAG was added, and the sample was incubated for 1 h at 37 °C. Another sample was kept as a negative control to reveal background damage during workup and was not treated with AAG. These samples were then quenched by 0.5 M NaOH, heated to 90 °C for 3 min. These samples were then supplemented with 40 μL co-precipitation agent (0.5 mg/mL tRNA in 300 mM NaOAc [pH 8.0], 1 mM EDTA) and 600 μL ethanol before being placed on dry ice for 30 min. All samples were resuspended in 50% v/v formamide:water, split in half, and loaded onto an 8% gel (**Figure 2.6**). One half of the samples were loaded to resolve bands 19-64, run 2 h at 80 W. The other half of the samples were loaded to resolve of bands 89-132, run 4 h at 80 W.

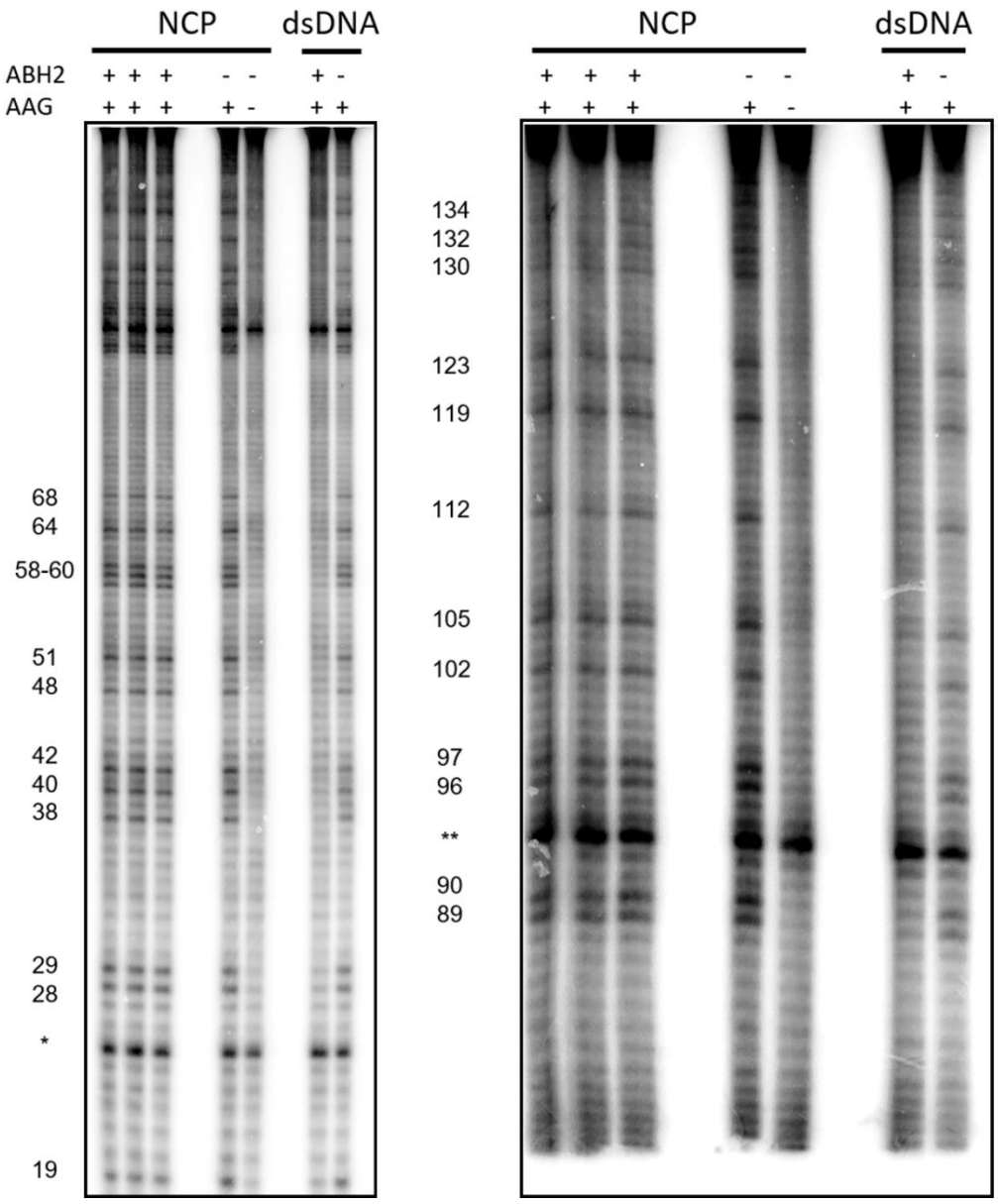

Figure 2.6 Denaturing PAGE analysis of AAG and ALKBH2 Activity in NCPs and Duplex. Evaluation of ALKBH2 activity on NCPs and Duplex containing globally substituted εA lesions. Samples were incubated with 2000 nM ALKBH2 for 1 h at 37 °C. The proteins were extracted, and samples were incubated with 2000 nM AAG for 1 h at 37 °C. NaOH catalyzed strand breaks were used to visualize εA still present for AAG treatment. Each data set consists of the following lanes: three replicates of ALKBH2 treated NCPs, duplex liberated from NCPs and treated with AAG, a no enzyme NCP sample, duplex treated with ALKBH2 and then AAG, and duplex treated with only AAG. The internal standards are indicated by the asterisks on the gel.

The gels were visualized by phosphorimagery and the bands were quantified using SAFA software. The band intensities were normalized using the internal standards. Sites 19-64 were normalized with the 23 mer standard, and sites 89-132 were normalized using the 92 mer standard. The no enzyme control was used to subtract background from enzyme-treated samples. For each site, the ratio of corrected band intensity in the NCPs to the duplex was used to determine the NCP/Duplex (NCP/DUP) ratio for AAG activity. An NCP/DUP value of 1 indicates activity that is comparable to duplex, while a value below one indicates lower activity relative to duplex. As a result of εA repair to A by ALKBH2, the DNA is no longer a substrate for AAG and does not generate a strand break under strongly basic conditions. Thus, we measured the loss of density in bands in ALKBH2-treated samples as compared to AAG only treatments. As ALKBH2 activity increased, we found that there was a corresponding drop in band density after AAG treatment. For ALKBH2, a value of 1 indicates a lack of repair while a value lower than 1 indicates repair by ALKBH2. To allow a direct comparison to AAG, this NCP/DUP value was then subtracted from 1 to convert to ALKBH2 repair. The standard error (SE) of NCP/DUP was calculated using $SE = \sigma/\sqrt{(n)}$, where σ is the standard deviation of the population and n is the sample size. For both AAG and ALKBH2, sites 19-123, n=5 and for sites 130 and 132, n=3.

2.3.5 Molecular Modeling

Molecular models were used to approximate enzyme binding to NCPs. The crystal structure of DNA-bound AAG (PDB: 1EWN, resolution 2.1 Å) or ALKBH2 (PDB 3RZK, resolution 2.8 Å) were aligned with the NCP crystal structure (PDB: 3LZ0, resolution 2.5 Å) using PyMOL. The alignment was performed using the phosphate

atoms of the five base pairs on either side of the lesion aligned with the five base pairs on either side of the site of interest (either site 42 or 64) using the "pair_fit" function of PyMOL. Color ramps were then applied to the surface representation of each enzyme to map the proximity to the histone core.

2.4 Results

2.4.1 Preparation of NCP Containing Globally Substituted εA Lesions

To investigate the εA repair profiles of AAG and ALKBH2, we prepared NCPs using the Widom 601 DNA sequence.[41] The 601 sequence is a strong positioning sequence which binds the histone octamer in a single translational and rotational position and provides a homogeneous population of NCPs for repair studies. Crystal structures of the 601 NCP are also available for reference.[41] Using methods we reported previously,[31-33] εA lesions were incorporated at A sites in the "I" strand of the 601 DNA to create εA:T base pairs throughout the sequence. We utilized a Poisson distribution to determine the molar ratio of A to εA building blocks such that 95% of the synthesized DNA sequences contain no more than one εA.

2.4.2 Rotational Position of DNA in NCP

We utilized HRF to establish the rotational position of each nucleobase and εA lesion.[37] The hydroxyl radical abstracts preferentially the C5' hydrogen of the sugar-phosphate backbone, which is located in the minor groove. For DNA packaged in NCPs, the regions of most intense strand cleavage indicate that the minor groove is solvent exposed and, thus, the major groove is facing the histone core and is protected from hydroxyl radicals. Therefore, a characteristic of DNA packaged in NCPs is an oscillating

pattern of high and low reactivity towards hydroxyl radicals. This pattern is observed in **Figure 2.7**.

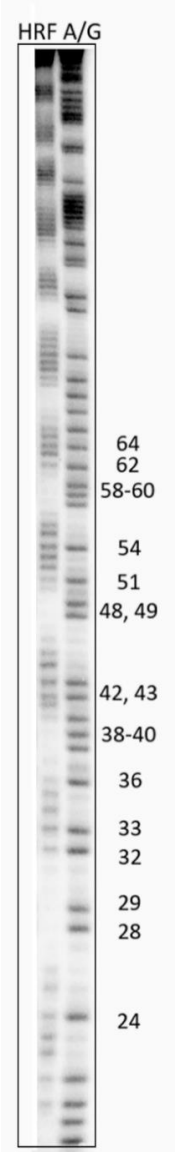

Figure 2.7 Hydroxyl Radical Footprinting of NCPs. Representative HRF denaturing PAGE used to assign solution accessibilities to each base position in the NCPs. The oscillatory pattern of bands in the HRF lane reflects the rotational position of DNA in the NCP. Areas with dark bands are not protected by the histone proteins and are thus OUT towards solution. Areas with no bands are areas protected from cleavage and are located IN. MID sites are lighter bands between the areas of very dark and very light bands. Lane A/G is the Maxam-Gilbert sequencing reaction (A+G).

Quantitation of the HRF confirms variable levels of solution accessibility throughout the DNA (**Table 2.2**). At OUT sites, defined here as having solution accessibility of greater than or equal to 0.7 when normalized within a helical turn, nucleobases are most solution accessible to hydroxyl radicals. The IN sites are defined as having solution accessibility less than 0.3; these sites are the least susceptible to cleavage by hydroxyl radicals because they are protected by the proximity of the histone proteins. The MID sites have solution accessibility between 0.3 and 0.7, exhibiting moderate protection by the histone proteins. The εA lesions are in a variety of rotational and translational positions that allows for a global analysis of the effects of geometric position on repair. Of the εA sites evaluated in this work, 8 are OUT, 4 are MID, and 11 are IN; these 23 lesion sites are also distributed throughout various translation positions in the NCP.

Table 2.2 Rotational Position of εA lesions. HRF reactivity used to assign rotational positions. These values are derived from band intensities measured from gels provided in Figure 2.6.

εA Position	**Solution Accessibility Normalized within Helical Turn**	**Relative Rotational Position**
90	0.02	
89	0.07	
48	0.11	
38	0.12	
112	0.18	
28	0.18	**IN**
59	0.20	
29	0.22	
58	0.23	
60	0.23	
119	0.25	

19	0.30	**MID**
40	0.31	
51	0.45	
105	0.45	
132	0.70	**OUT**
102	0.70	
42	0.78	
123	0.88	
97	0.93	
64	1.00	
96	1.00	
130	1.00	

2.4.3 Excision Activity of AAG in NCP Correlates with Rotational Position

AAG is known to remove εA from duplex DNA that is not incorporated into an NCP (unincorporated duplex).[42-44] Therefore, at each εA site, the ratio of excision from NCP relative to unincorporated duplex (NCP/DUP) is plotted (**Figure 2.8A**, striped bars). A ratio of 1 reflects comparable excision activity in NCP and unincorporated duplex DNA. We find that AAG glycosylase activity in NCP correlates strongly with rotational position (**Figure 2.8B**, open circles), in agreement with previous reports.[31] Most OUT sites (42, 64, 96, 123, 130, 132) exhibit high AAG activity as defined by NCP/DUP > 0.6. The only notable exceptions are sites 97 and 102 where relatively low levels of excision below 0.4 are observed in NCP. Consistent with the correlation between rotational position and excision activity, IN sites (19, 38, 48, 58, 59, 89, 90, 112) exhibit low AAG activity with NCP/DUP < 0.2. AAG exhibits a wider range of activity at MID sites with most NCP/DUP ranging from 0.1-0.6. However, site 105 exhibits a much higher activity, reaching 1. Furthermore, sites located towards the 3′-end of the "I" strand, near the DNA entry/exit region, generally exhibit higher levels of AAG activity than observed at other locations in the NCP. Importantly, native PAGE analysis

demonstrates that NCPs remain intact after incubation with AAG and that the glycosylase does not act by removing DNA from histones.

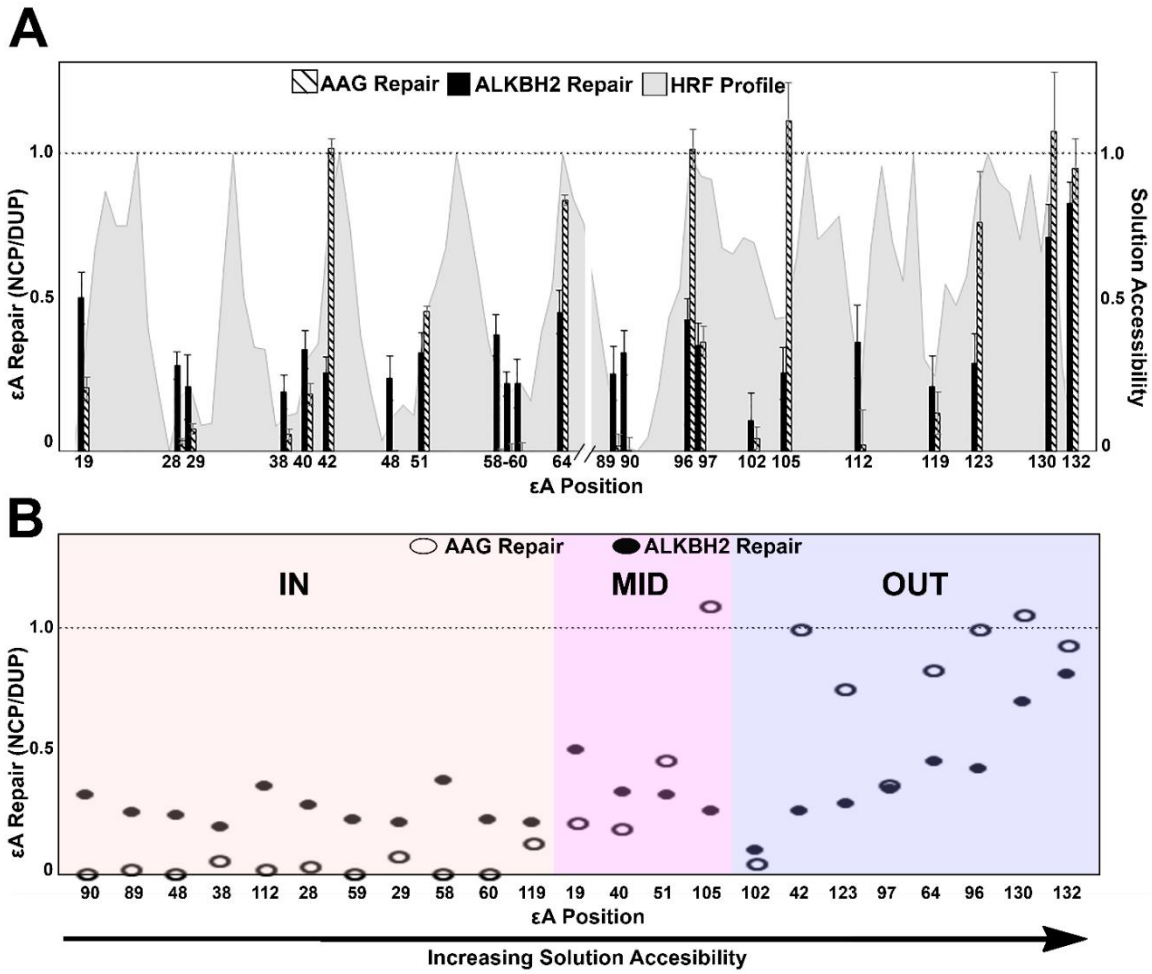

Figure 2.8 Repair profiles for AAG and ALKBH2. **(A)** The amount of εA excision for AAG (striped bars) and repair by ALKBH2 (solid bars) are plotted with solution accessibility as established by HRF (gray area) **(B)** Excision of εA by AAG (open circles) and repair by ALKBH2 (solid circles) plotted as a function of increasing solution accessibility.

2.4.4 Repair of εA by ALKBH2 is Unhindered in Duplex DNA but Suppressed in NCP

The ability of ALKBH2 to repair εA was markedly different between unincorporated duplex and NCP. εA was repaired at all 23 sites evaluated in

unincorporated duplex, with all εA lesions repaired at least 70% (**Figure 2.9**). In contrast, only sites 19, 130, and 132 in the NCP have NCP/DUP ≥ 0.5 and no εA lesions are repaired as readily as in unincorporated duplex (**Figure 2.8A**, black bars). Furthermore, while OUT sites (such as sites 42, 64, and 96) show somewhat higher repair activity than MID or IN sites, this correlation with rotational position is much weaker than observed for AAG and was not observed at all OUT sites (**Figure 2.8B**, black circles). It is notable that at site 97, the decrease in activity for AAG upon incorporation of the DNA into an NCP is not observed for ALKBH2 and, therefore, direct repair is comparable to AAG excision at this OUT site. In comparison to AAG, ALKBH2 exhibits greater activity at IN sites with all 11 IN sites exhibiting NCP/DUP ≥ 0.2. However, none of these IN sites reached NCP/DUP ≥ 0.4. Similar to AAG, native PAGE analysis demonstrates that NCPs remain intact after incubation with ALKBH2.

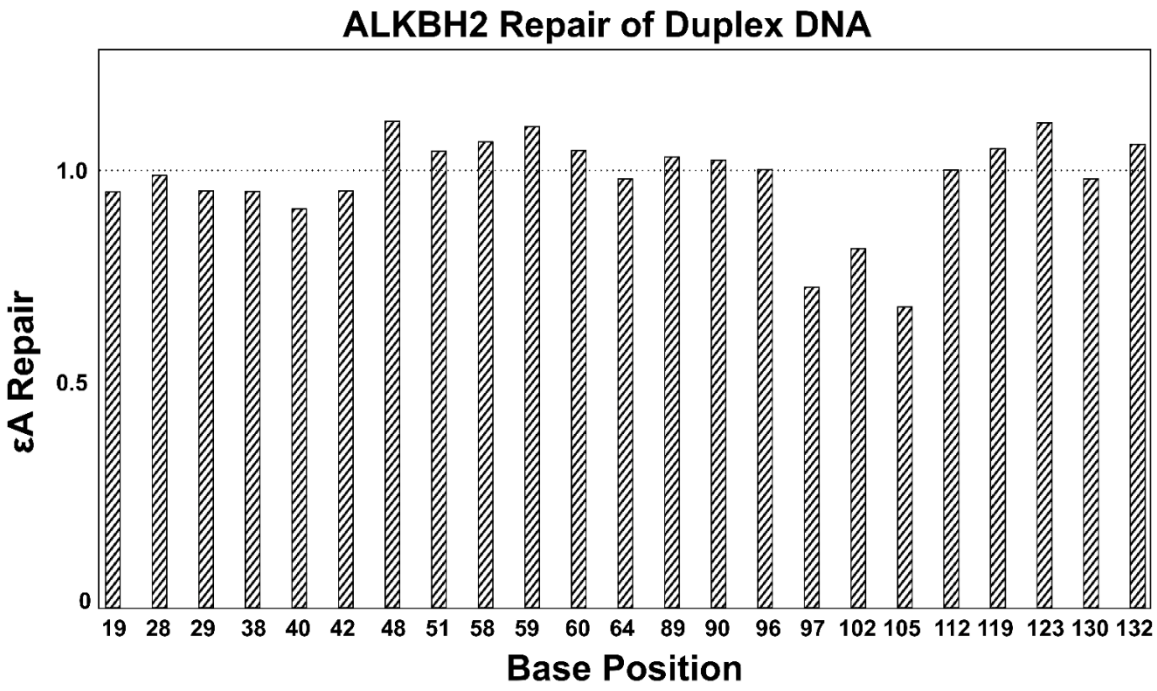

Figure 2.9 Repair of εA lesions by ALKBH2 in duplex DNA. ALKBH2 repair of εA in unincorporated duplex at various positions. The repair total was determined by subtracting AAG activity after ALKBH2 treatment from the same amount of duplex DNA treated only with AAG. This value was then subtracted from 1 to represent the repair activity of ALKBH2. A value of 1 indicates full repair and a value of 0 represents a total lack of ALKBH2 repair.

2.4.5 ALKBH2 Exhibits Greater Steric Interactions with the Histone Core than AAG

The εA lesions at OUT sites 42 and 64 were chosen for more in-depth molecular modeling because despite having the same rotational orientation, AAG exhibits higher repair activity at site 42, while ALKBH2 has higher repair at site 64. Our enzyme docking analysis shows that for sites 42 and 64, steric influences play a pronounced role in enzymatic activity, particularly for ALKBH2 (**Figure 2.10**). Minimal steric clash is observed between the histone core and AAG when binding at site 42 where excision of εA is complete as evidenced by the near lack of yellow and red in the proximity map (**Figure 2.10D**, top). In fact, no AAG amino acid residues are within 5 Å of the histone

octamer at site 42. In comparison, a steric clash between the histone core and AAG is seen when AAG is docked at site 64 as observed by the 13 amino acid residues within 5 Å of the histone core (**Figure 2.10D**, bottom); notably, AAG still demonstrates a NCP/DUP of 0.84.

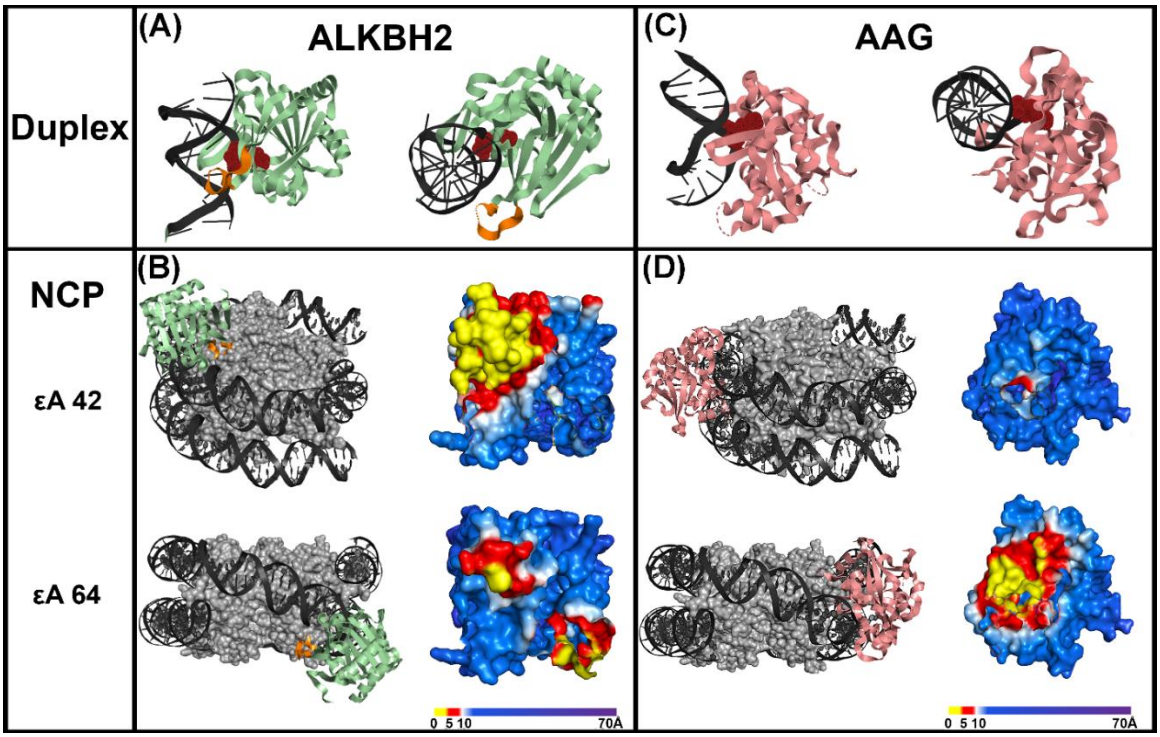

Figure 2.10 Molecular modeling of steric interactions between ALKBH2 and AAG upon substrate binding. **(A)** ALKBH2-duplex co-crystal structure (PDB: 3RZK) (left is side view; right is view down helical axis of DNA). εA is in red and can be seen flipped into the active site. The long loop is highlighted in orange. **(B)** ALKBH2-duplex co-crystal structure (PDB: 3RZK) merged with the NCP (PDB: 3LZ0) at εA sites 42 (top) and 64 (bottom). ALKBH2 surface models are rotated and enlarged to show the NCP binding face and colored according to the distance to the histone core. Amino acids within 5 Å of the histones are in yellow, those between 5 and 10Å are in red, and further distances are in blue. **(C)** AAG-duplex co-crystal structure (PDB: 1EWN) (left is side view; right is view down helical axis of DNA). εA is in red and can be seen flipped into the active site. **(D)** AAG-duplex co-crystal structure (PDB: 1EWN) merged with the NCP (PDB: 3LZ0) at εA sites 42 (top) and 64 (bottom). AAG surface models are rotated and enlarged to show the NCP binding face and colored according to the distance to the histone core.

In contrast, ALKBH2 has a NCP/DUP of only 0.25 at site 42 where there is substantial steric clash of 15 amino acid residues within 5Å of the octamer core, all residing within the long loop of ALKBH2 (**Figure 2.10B**, top).[25] At site 64, where there is only a single amino acid from the long loop within 5Å of the histones (**Figure 2.10B**, bottom), there is enhanced repair activity that increases NCP/DUP to 0.40.

2.5 Discussion

In this work, we compare the global repair profiles of AAG and ALKBH2 acting on εA lesions distributed throughout a strongly positioned NCP, encompassing different microenvironments with varying geometric positions. As observed previously, εA removal by AAG is highly correlated with rotational position.[31] This result is consistent with the general trend that has been observed previously for other glycosylases acting on strongly positioned NCPs. We have reported that OGG1,[33, 45] UDG,[32, 45] TDG,[46] and AAG[31, 45] exhibit activity at sites facing OUT from the histone core. These findings are also consistent with results reported by other groups.[47-50] An alternate approach to repair εA lesions is DRR by the AlkB family enzymes. Overall, we found substantial inhibition of ALKBH2 across the NCP, even at OUT sites. Intriguingly, all but one IN site (site 28) exhibit higher activity by ALKBH2 than AAG, albeit modest activity. These data suggest that while the ALKBH2 repair is more broadly inhibited in NCPs compared to AAG, ALKBH2 has higher activity on occluded sites that are poorly excised by AAG. Notably, ALKBH2 does not greatly distort DNA upon binding (**Figure 2.10A**) and may be easier to accommodate than the 22° angle pinching of the DNA observed for AAG[12] (**Figure 2.10C, left**). We hypothesize that the lesser distortion of the DNA helix by ALKBH2 leads to its higher activity at occluded sites compared to AAG. However, neither enzyme

demonstrates an ability to completely repair occluded lesions, indicating that these sites may represent mutational hotspots in the absence of structural changes to the NCP or external factors to enhance accessibility.

Our NCP system with εA in a variety of positions also allows us to consider the role of DNA sequence context on the activity of AAG and ALKBH2. We did not observe any significant sequence context effects for either AAG or ALKBH2, although it should be noted that these results are not a comprehensive study of all possible sequence contexts of εA (**Table 2.3**). This result is consistent with previous reports of AAG excision of εA being independent of sequence context.[11] Rather than sequence context, the rotational orientation of εA seems to be the dominant factor in predicting both enzymes' ability to initiate repair.

Table 2.3 Sequence Context of εA lesions.

εA Position	AAG Excision (NCP/DUP)	ALKBH2 Repair (NCP/DUP)	Sequence Context (X= εA)	Rotational Position
29	0.07±0.02	0.22±0.11	5'-AXT-3'	IN
59	0.00±0.03	0.23±0.04	AXA	IN
60	0.00±0.03	0.23±0.08	AXC	IN
90	0.00±0.04	0.33±0.07	AXC	IN
97	0.37±0.05	0.36±0.08	AXG	OUT
28	0.03±0.01	0.29±0.05	CXA	IN
42	1.02±0.03	0.26±0.06	CXG	OUT
51	0.47±0.02	0.33±0.08	CXC	MID
64	0.84±0.02	0.47±0.07	CXC	OUT
96	1.02±0.07	0.44±0.07	CXA	OUT
119	0.13±0.07	0.22±0.10	CXG	IN
123	0.77±0.17	0.29±0.10	CXC	OUT
130	1.08±0.20	0.72±0.11	CXG	OUT
19	0.21±0.04	0.51±0.09	GXG	MID
40	0.19±0.04	0.34±0.04	GXC	MID

102	0.04±0.04	0.10±0.09	GXT	OUT
132	0.95±0.10	0.83±0.07	GXT	OUT
38	0.06±0.02	0.20±0.06	TXG	IN
48	0.00±0.01	0.25±0.05	TXG	IN
58	0.00±0.01	0.39±0.07	TXA	IN
89	0.02±0.04	0.26±0.09	TXA	IN
105	1.11±0.13	0.26±0.09	TXC	MID
112	0.02±0.12	0.37±0.12	TXG	IN

Modelling of AAG and ALKBH2 docked at OUT sites provides insight into binding of these two enzymes to NCP substrates. Steric interactions between the histone core and the long loop of ALKBH2 (**Figure 2.10**, highlighted in orange), which is known to play an essential role in substrate binding,[25] modulate binding to the NCP. The stronger steric interactions with the long loop at OUT sites lead to diminished ALKBH2 activity as can be seen by comparing sites 42 and 64. Notably, this modeling does not account for the dynamic histone tails that could also modulate binding of repair enzymes. It is intriguing to consider that the H2B and H4 tails near site 97 may contribute to the unexpectedly low amount of excision by AAG at this location as histone tails have been shown to alter the structure and dynamics of damaged DNA.[51, 52] The H2B tail is also near site 102 and may account for the unexpected lower levels of εA excision by AAG. However, the unexpectedly high excision at site 105 indicates that the microenvironment generated by the H2B tail may have more complex and nuanced effects that include local structural changes, sterics, and electrostatics. These effects may be beneficial or inhibitory for different nucleobases that exist in a similar microenvironment.

DNA located near the entry/exit region of the NCP is known to transiently and spontaneously unwrap and expose otherwise occluded lesion sites. In particular, the 3′-end of the Widom 601 “I” strand has been shown to unwrap preferentially.[53] The high

levels of activity for both enzymes at sites 123, 130, and 132 is likely due to this asymmetric unwrapping. While the kinetics of unwrapping have not been measured in the presence of a DNA binding enzyme, the histone chaperone Nap1 has been shown to exploit unwrapping to promote H2A-H2B dimer eviction.[54] Furthermore, it has been demonstrated that unwrapping is rate-limiting for endonuclease III-like protein 1 (NTH1).[55, 56] These results agree with our earlier reports that solution accessibility does not correlate with glycosylase activity in certain translational regions.[32, 33, 45] Specifically, excision of U by UDG[32] and excision of 8-oxo-G by OGG1[33] are enhanced at the DNA entry/exit regions and was attributed to the unwrapping of the DNA. However, this observation is not universal and is dependent upon the specific glycosylase, as NEIL1 has been reported to be unable to exploit this unwrapping due to its high affinity for undamaged bases.[55]

Our results are also consistent with reports that demonstrated accumulation of alkylation damage in yeast at IN sites in genomic DNA.[57] Decreased repair at these sites is further indicated in an analysis of human tumors, in which mutational hotspots were observed at IN sites.[58] Taken together these data suggest that an alternate means of accessing occluded lesions, such as chromatin remodelers or histone modifications, may be required. Indeed, H2B[59] and H3[60] acetylation has been shown to enhance DNA unwrapping and acetylation has been observed to occur as part of the DNA damage response.[61] Furthermore, incorporation of histone variants has been demonstrated to enhance the initiation of BER of uracil lesions.[32] Finally, it was recently shown that AAG forms a complex with RNA polymerase II and may utilize localized chromatin decondensation to access otherwise occluded lesions.[62]

Further understanding of the molecular mechanisms of εA repair is essential to understand and inform clinical impacts. Abnormal expression of both AAG and ALKBH2 have been observed in cancer pathologies. Overexpression of AAG has been associated with both decreased sensitivity to various chemotherapeutic agents in mouse embryonic stem cells and increased sensitivity in breast cancer cells.[10, 63] ALKBH2 also has clinical significance, as its knockdown in bladder cancer tissues limited tumor development, while downregulation led to increased sensitivity to alkylating agents and chemotherapeutics.[64] The potential for AlkB homolog inhibitors to serve as anticancer agents has also been investigated.[40] However, the potential obstacles to the activity of these enzymes, such as the packaging of DNA into the NCP, need to be better understood to inform future therapies.

2.6 References

1. Levine, R. L.; Yang, I.-Y.; Hossain, M.; Pandya, G. A.; Grollman, A. P.; Moriya, M. (2000) Mutagenesis induced by a single 1,*N6*-ethenodeoxyadenosine adduct in human cells. *Cancer Res. 60* (15), 4098-4104.

2. El Ghissassi, F.; Barbin, A.; Nair, J.; Bartsch, H. (1995) Formation of 1,*N6*-ethenoadenine and 3,*N4*-ethenocytosine by lipid peroxidation products and nucleic acid bases. *Chem. Ress. Toxicol. 8* (2), 278-283.

3. Guengerich, F. P.; Crawford, W. M.; Watanabe, P. G. (1979) Activation of vinyl chloride to covalently bound metabolites: roles of 2-chloroethylene oxide and 2-chloroacetaldehyde. *Biochemistry 18* (23), 5177-5182.

4. Nair, U.; Bartsch, H.; Nair, J. (2007) Lipid peroxidation-induced DNA damage in cancer-prone inflammatory diseases: A review of published adduct types and levels in humans. *Free Radic. Biol. Med. 43* (8), 1109-1120.

5. Barbin, A. (200) Etheno-adduct-forming chemicals: from mutagenicity testing to tumor mutation spectra. *Mutat. Res. Rev. Mutat., 462* (2), 55-69.

6. Schermerhorn, K. M.; Delaney, S. (2014) A chemical and kinetic perspective on base excision repair of DNA. *Acc. Chem. Res. 47* (4), 1238-1246.

7. O'Brien, P. J.; Ellenberger, T. (2004) Dissecting the broad substrate specificity of Human 3-Methyladenine-DNA Glycosylase. *J. Biol. Chem. 279* (11), 9750-9757.

8. Ayala-García, V. M.; Valenzuela-García, L. I.; Setlow, P.; Pedraza-Reyes, M. (2016) Aag hypoxanthine-DNA glycosylase is synthesized in the forespore compartment and involved in counteracting the genotoxic and mutagenic effects of hypoxanthine and alkylated bases in DNA during *Bacillus subtilis* Sporulation. *J. Bacteriol.198* (24), 3345-3354.

9. Glassner, B. J.; Rasmussen, L. J.; Najarian, M. T.; Posnick, L. M.; Samson, L. D. (1998) Generation of a strong mutator phenotype in yeast by imbalanced base excision repair. *Proc. Natl. Acad. Sci. U.S.A. 95* (17), 9997-10002.

10. Allan, J. M.; Engelward, B. P.; Dreslin, A. J.; Wyatt, M. D.; Tomasz, M.; Samson, L. D. (1998) Mammalian 3-methyladenine DNA glycosylase protects against the toxicity and clastogenicity of certain chemotherapeutic DNA cross-linking agents. *Cancer Res.*, *58* (17), 3965-3973.

11. Wolfe, A. E.; O'Brien, P. J. (2009) Kinetic mechanism for the flipping and excision of 1,N(6)-ethenoadenine by human alkyladenine DNA glycosylase. *Biochemistry 48* (48), 11357-11369.

12. Lau, A. Y.; Scharer, O. D.; Samson, L.; Verdine, G. L.; Ellenberger, T. (1998) Crystal structure of a human alkylbase-DNA repair enzyme complexed to DNA: mechanisms for nucleotide flipping and base excision. *Cell 95* (2), 249-58.

13. Aravind, L.; Koonin, E. V. (2001) The DNA-repair protein AlkB, EGL-9, and leprecan define new families of 2-oxoglutarate- and iron-dependent dioxygenases. *Genome Biol. 2* (3), research0007.1.

14. Sedgwick, B. (2004) Repairing DNA-methylation damage. *Nat. Rev. Mol. Cell Biol. 5* (2), 148-157.

15. Delaney, J. C.; Smeester, L.; Wong, C.; Frick, L. E.; Taghizadeh, K.; Wishnok, J. S.; Drennan, C. L.; Samson, L. D.; Essigmann, J. M. (2004) AlkB reverses etheno DNA lesions caused by lipid oxidation in vitro and in vivo. *Nat. Struct. Mol. Biol. 12* (10), 855-860.

16. Mishina, Y.; Yang, C.-G.; He, C. (2005) Direct repair of the exocyclic DNA adduct 1,N6-ethenoadenine by the DNA repair AlkB proteins. *J. Am. Chem. Soc. 127* (42), 14594-14595.

17. Ougland, R.; Rognes, T.; Klungland, A.; Larsen, E. (2015) Non-homologous functions of the AlkB homologs. *J. Mol. Cell Biol. 7* (6), 494-504.

18. Aas, P. A.; Otterlei, M.; Falnes, P. Ø.; Vågbø, C. B.; Skorpen, F.; Akbari, M.; Sundheim, O.; Bjørås, M.; Slupphaug, G.; Seeberg, E.; Krokan, H. E. (2003) Human

and bacterial oxidative demethylases repair alkylation damage in both RNA and DNA. *Nature 421* (6925), 859-863.

19. Duncan, T.; Trewick, S. C.; Koivisto, P.; Bates, P. A.; Lindahl, T.; Sedgwick, B. (2002) Reversal of DNA alkylation damage by two human dioxygenases. *Proc. Natl. Acad. Sci. U.S.A 99* (26), 16660-16665.

20. Ringvoll, J.; Nordstrand, L. M.; Vågbø, C. B.; Talstad, V.; Reite, K.; Aas, P. A.; Lauritzen, K. H.; Liabakk, N. B.; Bjørk, A.; Doughty, R. W.; Falnes, P. Ø.; Krokan, H. E.; Klungland, A. (2006) Repair deficient mice reveal mABH2 as the primary oxidative demethylase for repairing 1meA and 3meC lesions in DNA. *EMBO J. 25* (10), 2189-2198.

21. Fedeles, B. I.; Singh, V.; Delaney, J. C.; Li, D.; Essigmann, J. M. (2015) The AlkB Family of Fe(II)/alpha-ketoglutarate-dependent dioxygenases: repairing nucleic acid alkylation damage and beyond. *J. Biol. Chem* (34), 20734-42.

22. van den Born, E.; Omelchenko, M. V.; Bekkelund, A.; Leihne, V.; Koonin, E. V.; Dolja, V. V.; Falnes, P. Ø. (2008) Viral AlkB proteins repair RNA damage by oxidative demethylation. *Nucleic Acids Res. 36* (17), 5451-5461.

23. Sedgwick, B.; Bates, P. A.; Paik, J.; Jacobs, S. C.; Lindahl, T. (2007) Repair of alkylated DNA: Recent advances. *DNA Repair 6* (4), 429-442.

24. Drabløs, F.; Feyzi, E.; Aas, P. A.; Vaagbø, C. B.; Kavli, B.; Bratlie, M. S.; Peña-Diaz, J.; Otterlei, M.; Slupphaug, G.; Krokan, H. E. (2004) Alkylation damage in DNA and RNA—repair mechanisms and medical significance. *DNA Repair 3* (11), 1389-1407.

25. Yang, C.-G.; Yi, C.; Duguid, E. M.; Sullivan, C. T.; Jian, X.; Rice, P. A.; He, C. (2008) Crystal structures of DNA/RNA repair enzymes AlkB and ABH2 bound to dsDNA. *Nature 452* (7190), 961-965.

26. Luger, K.; Mäder, A. W.; Richmond, R. K.; Sargent, D. F.; Richmond, T. J. (1997) Crystal structure of the nucleosome core particle at 2.8 Å resolution. *Nature 389* (6648), 251-260.

27. Eickbush, T. H.; Moudrianakis, E. N. (1978) The histone core complex: an octamer assembled by two sets of protein-protein interactions. *Biochemistry 17* (23), 4955-4964.

28. Lee, J. Y.; Lee, J.; Yue, H.; Lee, T. H. (2015) Dynamics of nucleosome assembly and effects of DNA methylation. *J. Biol. Chem 290* (7), 4291-303.

29. Zhou, K.; Gaullier, G.; Luger, K. (2019) Nucleosome structure and dynamics are coming of age. *Nat. Struct. Mol. Biol. 26* (1), 3-13.

30. Sczepanski, J. T.; Wong, R. S.; McKnight, J. N.; Bowman, G. D.; Greenberg, M. M. (2010) Rapid DNA–protein cross-linking and strand scission by an abasic site in a nucleosome core particle. *Proc. Natl. Acad. Sci. U.S.A 107* (52), 22475-22480.

31. Kennedy, E. E.; Li, C.; Delaney, S. (2019) Global repair profile of human alkyladenine DNA glycosylase on nucleosomes reveals DNA packaging effects. *ACS Chem. Biol. 14* (8), 1687-1692.

32. Li, C.; Delaney, S. (2019) Histone H2A variants enhance the initiation of base excision repair in nucleosomes. *ACS Chem. Biol. 14* (5), 1041-1050.

33. Bilotti, K.; Tarantino, M. E.; Delaney, S. (2018) Human oxoguanine glycosylase 1 removes solution accessible 8-oxo-7,8-dihydroguanine lesions from globally substituted nucleosomes except in the dyad region. *Biochemistry 57* (9), 1436-1439.

34. Luger, K.; Rechsteiner, T. J.; Richmond, T. J. (1999) Expression and purification of recombinant histones and nucleosome reconstitution. *Methods Mol. Biol. 119*, 1-16.

35. Luger, K.; Rechsteiner, T. J.; Richmond, T. J. (1999) Preparation of nucleosome core particle from recombinant histones. *Methods Enzymol. 304*, 3-19.

36. Hayes, J. J.; Tullius, T. D.; Wolffe, A. P. (1990) The structure of DNA in a nucleosome. *Proc. Natl. Acad. Sci. U.S.A 87* (19), 7405-7409.

37. Jain, S. S.; Tullius, T. D. (2008) Footprinting protein–DNA complexes using the hydroxyl radical. *Nat. Protoc. 3* (6), 1092-1100.

38. Das, R.; Laederach, A.; Pearlman, S. M.; Herschlag, D.; Altman, R. B. (2005) SAFA: semi-automated footprinting analysis software for high-throughput quantification of nucleic acid footprinting experiments. *RNA 11* (3), 344-54.

39. Chen, F.; Tang, Q.; Bian, K.; Humulock, Z. T.; Yang, X.; Jost, M.; Drennan, C. L.; Essigmann, J. M.; Li, D. (2016) Adaptive response enzyme AlkB preferentially repairs 1-methylguanine and 3-methylthymine adducts in double-stranded DNA. *Chem. Res.Toxicol. 29* (4), 687-693.

40. Chen, F.; Bian, K.; Tang, Q.; Fedeles, B. I.; Singh, V.; Humulock, Z. T.; Essigmann, J. M.; Li, D. (2017) Oncometabolites d- and l-2-hydroxyglutarate inhibit the AlkB family DNA repair enzymes under physiological conditions. *Chem. Res. Toxicol. 30* (4), 1102-1110.

41. Vasudevan, D.; Chua, E. Y. D.; Davey, C. A. (2010) Crystal structures of nucleosome core particles containing the '601' strong positioning sequence. *J. Mol. Biol. 403* (1), 1-10.

42. Samson, L.; Derfler, B.; Boosalis, M.; Call, K. (1991) Cloning and characterization of a 3-methyladenine DNA glycosylase cDNA from human cells whose gene maps to chromosome 16. *Proc. Natl. Acad. Sci. U.S.A 88* (20), 9127-9131.

43. Chakravarti, D.; Ibeanu, G. C.; Tano, K.; Mitra, S. (1991) Cloning and expression in Escherichia coli of a human cDNA encoding the DNA repair protein N-methylpurine-DNA glycosylase. *J. Biol. Chem. 266* (24), 15710-15715.

44. Riazuddin, S.; Lindahl, T. (1978) Properties of 3-methyladenine-DNA glycosylase from Escherichia coli. *Biochemistry 17* (11), 2110-2118.

45. Olmon, E. D.; Delaney, S. (2017) Differential ability of five DNA glycosylases to recognize and repair damage on nucleosomal DNA. *ACS Chem. Biol. 12* (3), 692-701.

46. Tarantino, M. E.; Dow, B. J.; Drohat, A. C.; Delaney, S. (2018) Nucleosomes and the three glycosylases: High, medium, and low levels of excision by the uracil DNA glycosylase superfamily. *DNA Repair 72*, 56-63.

47. Beard, B. C.; Wilson, S. H.; Smerdon, M. J. (2003) Suppressed catalytic activity of base excision repair enzymes on rotationally positioned uracil in nucleosomes. *Proc. Natl. Acad. Sci. U.S.A 100* (13), 7465-70.

48. Cole, H. A.; Tabor-Godwin, J. M.; Hayes, J. J. (2010) Uracil DNA glycosylase activity on nucleosomal DNA depends on rotational orientation of targets. *J. Biol. Chem. 285* (4), 2876-85.

49. Hinz, J. M.; Rodriguez, Y.; Smerdon, M. J. (2010) Rotational dynamics of DNA on the nucleosome surface markedly impact accessibility to a DNA repair enzyme. *Proc. Natl. Acad. Sci. U.S.A 107* (10), 4646-4651.

50. Prasad, A.; Wallace, S. S.; Pederson, D. S. (2007) Initiation of base excision repair of oxidative lesions in nucleosomes by the human, bifunctional DNA glycosylase NTH1. *Mol. Cell Biol. 27* (24), 8442-8453.

51. Cai, Y.; Fu, I.; Geacintov, N. E.; Zhang, Y.; Broyde, S. (2018) Synergistic effects of H3 and H4 nucleosome tails on structure and dynamics of a lesion-containing DNA: Binding of a displaced lesion partner base to the H3 tail for GG-NER recognition. *DNA Repair 65*, 73-78.

52. Fu, I.; Cai, Y.; Zhang, Y.; Geacintov, N. E.; Broyde, S. (2016) Entrapment of a histone tail by a DNA lesion in a nucleosome suggests the lesion impacts epigenetic marking: a molecular dynamics study. *Biochemistry 55* (2), 239-242.

53. Ngo, Thuy T. M.; Zhang, Q.; Zhou, R.; Yodh, Jaya G.; Ha, T. (2015) Asymmetric unwrapping of nucleosomes under tension directed by DNA local flexibility. *Cell 160* (6), 1135-1144.

54. Lee, J.; Lee, T.-H. (2017) Single-molecule investigations on histone H2A-H2B dynamics in the nucleosome. *Biochemistry 56* (7), 977-985.

55. Odell, I. D.; Newick, K.; Heintz, N. H.; Wallace, S. S.; Pederson, D. S. (2010) Non-specific DNA binding interferes with the efficient excision of oxidative lesions from chromatin by the human DNA glycosylase, NEIL1. *DNA Repair 9* (2), 134-143.

56. Maher, R. L.; Prasad, A.; Rizvanova, O.; Wallace, S. S.; Pederson, D. S. (2013) Contribution of DNA unwrapping from histone octamers to the repair of oxidatively damaged DNA in nucleosomes. *DNA Repair 12* (11), 964-971.

57. Mao, P.; Brown, A. J.; Malc, E. P.; Mieczkowski, P. A.; Smerdon, M. J.; Roberts, S. A.; Wyrick, J. J. (2017) Genome-wide maps of alkylation damage, repair, and mutagenesis in yeast reveal mechanisms of mutational heterogeneity. *Genome Res. 27* (10), 1674-1684.

58. Pich, O.; Muinos, F.; Sabarinathan, R.; Reyes-Salazar, I.; Gonzalez-Perez, A.; Lopez-Bigas, N. (2018) Somatic and germline mutation periodicity follow the orientation of the DNA minor groove around nucleosomes. *Cell 175* (4), 1074-1087.e18.

59. Fu, I.; Cai, Y.; Geacintov, N. E.; Zhang, Y.; Broyde, S. (2017) Nucleosome histone tail conformation and dynamics: impacts of lysine acetylation and a nearby minor groove benzo[a]pyrene-derived lesion. *Biochemistry 56* (14), 1963-1973.

60. Gansen, A.; Tóth, K.; Schwarz, N.; Langowski, J. (2015) Opposing roles of H3- and H4-acetylation in the regulation of nucleosome structure—a FRET study. *Nucleic Acids Res. 43* (3), 1433-1443.

61. van Attikum, H.; Gasser, S. M. (2009) Crosstalk between histone modifications during the DNA damage response. *Trends Cell Biol. 19* (5), 207-217.

62. Montaldo, N. P.; Bordin, D. L.; Brambilla, A.; Rösinger, M.; Fordyce Martin, S. L.; Bjørås, K. Ø.; Bradamante, S.; Aas, P. A.; Furrer, A.; Olsen, L. C.; Kunath, N.; Otterlei, M.; Sætrom, P.; Bjørås, M.; Samson, L. D.; van Loon, B. (2019) Alkyladenine DNA glycosylase associates with transcription elongation to coordinate DNA repair with gene expression. *Nat. Commun. 10* (1), 5460.

63. Rinne, M.; Caldwell, D.; Kelley, M. R. (2004) Transient adenoviral *N*-methylpurine DNA glycosylase overexpression imparts chemotherapeutic sensitivity to human breast cancer cells. *Mol. Cancer Ther. 3* (8), 955-967.

64. Pilžys, T.; Marcinkowski, M.; Kukwa, W.; Garbicz, D.; Dylewska, M.; Ferenc, K.; Mieczkowski, A.; Kukwa, A.; Migacz, E.; Wołosz, D.; Mielecki, D.; Klungland, A.; Piwowarski, J.; Poznański, J.; Grzesiuk, E. (2019) ALKBH overexpression in head and neck cancer: potential target for novel anticancer therapy. *Sci. Rep. 9* (1), 13249.

Chapter 3: Histone Tails Modulate AAG Excision Activity in Nucleosome core Particles†

†Adapted from:

Paul J. Caffrey and Sarah Delaney

Nucleosome Core Particles Lacking H2B or H3 Tails Are Altered Structurally and Have Differential Base Excision Repair Fingerprints

Biochemistry (**2021**) 60 (3): 210-219. doi: 10.1021/acs.cbiochemhemrestoc.0c00877

3.1 Abstract

A recently discovered post-translational modification of histone proteins is the irreversible proteolytic clipping of the histone N-terminal tail domains. This modification is involved in regulation of various biological process, including the DNA damage response. In this work, we use chemical footprinting to characterize the structural alterations to nucleosome core particles (NCPs) that result from lack of the histone H2B or H3 tails. We also examine the influence of these histone tails on excision of the mutagenic lesion 1,N^6-ethenoadenine (εA) by the repair enzyme alkyladenine DNA glycosylase (AAG). We found that absence of the H2B or H3 tail results in altered DNA periodicity relative to native NCPs. We correlated these structural alterations to εA excision by utilizing a global analysis of 21 εA sites in NCPs and unincorporated duplex DNA. In comparison to native NCPs, there is enhanced excision of εA in tailless H2B NCPs in regions which undergo DNA unwrapping. This enhanced excision is not observed for tailless H3 NCPs, rather, excision is inhibited in more static areas of the NCP not prone to unwrapping. Our results support *in vivo* observations of alkylation damage profiles and the potential role of tail clipping as a mechanism to overcome physical obstructions caused by packaging in NCPs, but also reveal potential inhibition of repair by tail clipping in some locations. Taken together these results further our understanding of how base excision repair can be facilitated or diminished by histone tail removal and contributes to understanding the underlying mechanism that lead to mutational hotspots.

3.2 Introduction

In most eukaryotic organisms, DNA is organized into chromatin. The base unit of packaging in chromatin is the nucleosome core particle (NCP). The NCP is comprised of 145-147 base pairs of DNA wrapped approximately 1.7 times around a histone protein core.[1] The histone core is formed by two copies of each of the proteins H2A, H2B, H3, and H4.[2] Each histone contains a highly structured globular core and an N-terminal disordered tail.[1] There is also a 2-fold rotational axis of pseudosymmetry in the NCP known as the dyad axis. Notably, an NCP is not a static structure but rather a dynamic one where DNA is transiently exposed through unwrapping at the entry/exit points,[3, 4] histone variants can be exchanged for the canonical versions,[5] and histones undergo posttranslational modifications (PTMs).[6, 7] Besides reversible PTMs such as methylation, phosphorylation, and acetylation, proteolytic clipping of the histone tails has been identified as an irreversible modification.[8, 9]

Clipping of the histone tails, particularly H2B and H3, alters the NCP structure and DNA accessibility. It has been shown that the absence of the H3 tail promotes DNA unwrapping and H2A/H2B dimer eviction.[10, 11] Absence of the H2B tail has also been demonstrated to promote DNA unwrapping,[10] putatively via elimination of interactions between the H2B and H3 tails that inhibit unwrapping.[12] Trypsin catalyzed removal of histone tails enhances binding of the GAL4 transcription factor and DNA digestion by restriction enzymes,[13] demonstrating an increase in physical accessibility of DNA in the absence of histone tails. Furthermore, tail removal has been shown to alter the translational positioning of DNA, even when removal was conducted after NCP assembly.[13, 14]

By altering chromatin structure and DNA accessibility, histone tails can play key roles in regulating biological processes. One result of tail clipping is the erasure of PTMs. Moreover, histone clipping itself serves to activate gene expression in yeast,[15] promote cell differentiation,[16] increase the rate of transcriptional elongation by RNA polymerase,[17] alleviate pausing at promoter regions,[18] and serves as an epigenetic marker.[19] H3 clipping has also been shown to occur under DNA damaging conditions, implicating histone clipping in the DNA damage response.[20]

Single- and double-strand breaks, inter- and intra-strand crosslinks, abasic sites, and modification of the bases are all potential consequences of DNA damaging agents.[21] These various forms of damage are repaired by different pathways. Modified bases, referred to here as lesions, are repaired by the base excision repair (BER) pathway. One mutagenic lesion repaired by the BER pathway is 1,N^6-ethenoadenine (εA, Figure 1).[22, 23] εA is generated both as a byproduct of endogenous lipid peroxidation and exogenous exposure to vinyl chloride.[24, 25] εA levels are elevated in tissues from individuals with chronic inflammatory diseases associated with carcinogenesis as well as cancerous tissues.[26]

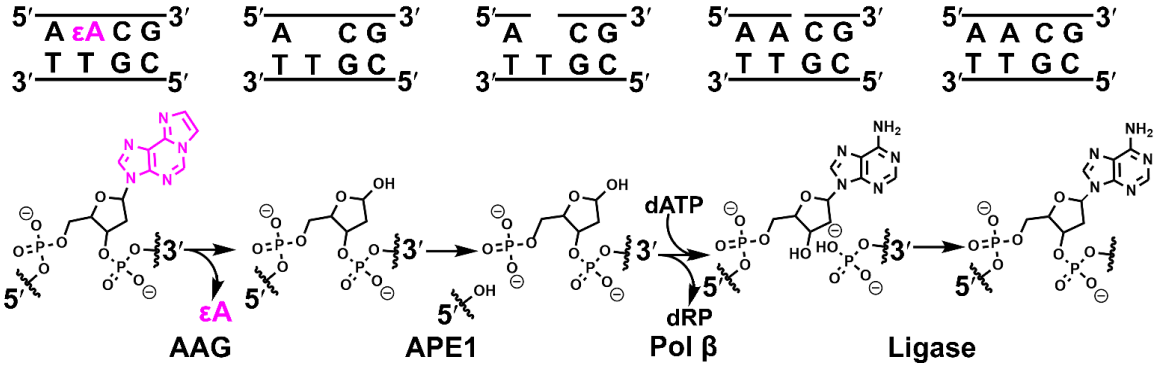

Figure 3.1 Base excision repair of 1,N^6-ethenoadenine (εA). The εA lesion is shown in pink along with the four steps of the repair catalyzed by AAG, APE1, pol β, and DNA ligase, respectively.

The BER pathway is comprised of several enzymes that catalyze the excision of a lesion and subsequent insertion of an unmodified nucleotide. Alkyladenine glycosylase (AAG) is responsible for excision of alkylated bases, including εA.[27] Excision of εA by AAG results in an apurinic/apyrimidinic (AP) site which is then processed by downstream enzymes that complete the repair.[21]

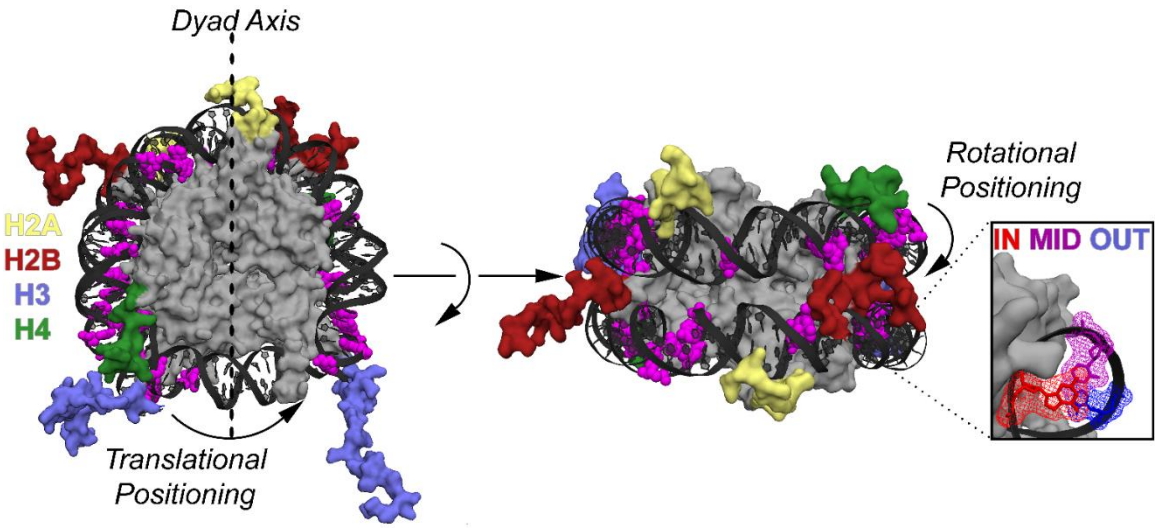

Figure 3.2 Global distribution of εA lesions in the NCP. The image was created by merging the crystal structure of a 601 NCP lacking histone tails (PDB: 3lz0) with one including tails but with a different DNA sequence (PDB: 1kx5). The location of εA lesions are highlighted in pink. The globular domains of the histones are in gray. The N-terminal tails of each histone are highlighted: H2A (yellow), H2B (red), H3 (blue) and H4 (green). On the left is a top-down view of the NCP with the dyad axis indicated with a dashed line. On the right is a side view after rotating the NCP 90°. Rotational position of bases is shown with examples of IN, MID, and OUT bases provided.

When considering the activity of BER enzymes in an NCP, unlike unpackaged duplex DNA, the geometric positioning of the lesion is important. The dyad axis acts as a reference point in defining the translational position of a lesion (**Figure 3.2**). Besides translational positioning, a lesion can be defined by its rotational orientation which can be described as outwards towards solution (OUT), inwards towards the histone core (IN), or somewhere in between (MID). Further microenvironments are created by the DNA

superhelices, histone tails, and areas of transient unwrapping of DNA from the histone core.

In this work, we use chemical footprinting techniques to show that NCPs lacking either the H2B or H3 tail have structures distinct from NCPs with intact tails. We also demonstrate that these structural differences manifest in differential excision of εA by AAG. Excision is enhanced in the entry/exit regions of NCPs lacking H2B tails, but inhibition is seen in less dynamic areas of the NCPs lacking H3 tails. Taken together, these results implicate tail removal as a potential modulator of BER initiation in chromatin.

3.3 Materials and Method

3.3.1 Oligonucleotide Synthesis and Purification

All oligonucleotides used in this study were synthesized on a MerMade 4 DNA synthesizer (BioAutomation). We used the 145 bp Widom 601 nucleosome positioning sequence (**Table 3.1**) as the unincorporated duplex control and to assemble NCPs. Synthesis of the 145 mer oligonucleotide containing εA was conducted on 1,400 Å controlled pore glass beads (BioAutomation) using phosphoramidites with ultramild protecting groups (Glen Research). Deprotection was performed according to the manufacturer's specifications. εA substitution for A throughout the "I" strand was conducted utilizing a Poisson distribution, as described in recent reports.[28-30] The molar ratio determined by the Poisson distribution ($\lambda = 0.355$) was used to determine the correct mixture of A and εA phosphoramidites. This synthetic strategy yields a DNA population containing either 0 or 1 εA lesion per 145 mer oligonucleotide while minimizing strands containing two or more lesions to 5% of the population. Numbering starts with the first

base of the 5′-end of the "I" strand. The final trityl group was removed on the synthesizer, and the DNA cleaved from the solid support by incubation in NH_4OH at room temperature for 2 h. The DNA was then purified via the crush and soak method utilizing 8% denaturing polyacrylamide gel electrophoresis (PAGE).

Table 3.1 DNA Sequences used in this study

Name	Length	Sequence (5′ to 3′)
"I" strand	145mer	ATCAGAATCCCGGTGCCGAGGCCGCTCAATTGGTCGTAGACAG CTCTAGCACCGCTTAAACGCACGTACGCGCTGTCCCCCGCGTTT TAACCGCCAAGGGGATTACTCCCTAGTCTCCAGGCACGTGTCA GATATATACATCGAT
"J" strand	145mer	ATCGATGTATATATCTGACACGTGCCTGGAGACTAGGGAGTAA TCCCCTTGGCGGTTAAAACGCGGGGGACAGCGCGTACGTGCGT TTAAGCGGTGCTAGAGCTGTCTACGACCAATTGAGCGGCCTCG GCACCGGGATTCTGAT
IS1	23mer	ATCAGAATCCCGGTGCCGAGGCC
IS2	92mer	ATCAGAATCCCGGTGCCGAGGCCGCTCAATTGGTCGTAGACAG CTCTAGCACCGCTTAAACGCACGTACGCGCTGTCCCCCGCGTTT TAACC
J1	45mer	ATCGATGTATATATCTGACACGTGCCTGGAGACTAGGGAGTAA TC
J2	65mer	CCCTTGGCGGTTAAAACGCGGGGGACAGCGCGTACGTGCGTTT AAGCGGTGCTAGAGCTGTCTAC
J3	35mer	GACCAATTGAGCGGCCTCGGCACCGGGATTCTGAT
JS12	30mer	TTTAACCGCCAAGGGGATTACTCCCTAGTC
JS23	32mer	GCCGCTCAATTGGTCGTAGACAGCTCTAGCAC

A ligation strategy was utilized to prepare the complementary 145 mer (**Figure 3.3**). The component oligonucleotides for ligation were synthesized using standard phosphoramidite protecting groups with the final trityl group retained. Reverse-phase HPLC purification at 90 °C was used to purify the oligonucleotides (Agilent PLRP-S column, 250 mm × 4.6 mm; A = 100 mM triethylammonium acetate [TEAA] in 5% aqueous MeCN, B = 100 mM TEAA in MeCN; 5:95 to 35:65 A:B over 30 min, 35:65 to

5:95 A:B over 5 min at 1 mL/min). Removal of the trityl group was accomplished by incubation in 20% v/v aqueous glacial acetic acid for 1 h at room temperature. Subsequently, a second HPLC purification at 90 °C was performed (Agilent PLRP-S column, 250 mm × 4.6 mm; A = 100 mM triethylammonium acetate [TEAA] in 5% aqueous MeCN, B = 100 mM TEAA in MeCN; 0:100 to 15:85 A:B over 35 min, 15:85 to 35:65 A:B over 5 min at 1 mL/min). Electrospray ionization mass spectrometry was used to verify the identity of the component oligonucleotides. Five nmol of each component oligonucleotide J2 and J3 were 5′-phosphorylated using 2 mM ATP and T4 kinase (New England Biolabs). These phosphorylated components were then combined in equal molar amounts with component J1 and 10% excess of two scaffolding oligonucleotides, JS12 and JS23, and annealed by heating to 95 °C for 5 min and cooling at 1°C per min in 50 mM NaCl and 20 mM Tris (pH 8.0). These annealed oligonucleotides were then ligated at room temperature overnight using 4,800 units T4 DNA ligase in buffer (50 mM Tris-HCl, 10 mM NaCl, 10 mM $MgCl_2$, 10 mM DTT, 1 mM ATP, pH: 7.5). The product of the ligation reaction was then purified using 8% denaturing PAGE.

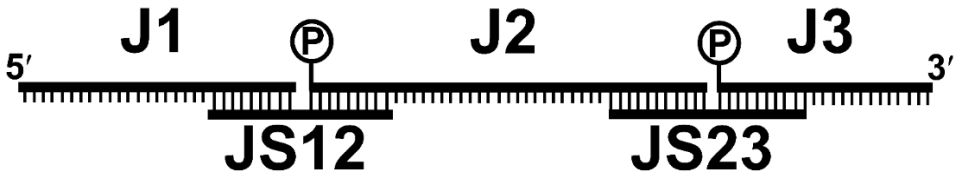

Figure 3.3 Ligation scheme for complementary J strand sequence. Five nmol of phosphorylated J2 and J3 was mixed with 5 nmol J1 and 5.5 nmol JS12 and JS23 and annealed. The annealed sample was then treated with ligase to assemble 145 mer complementary DNA. The ligation reaction was purified by 8% denaturing PAGE.

For normalization of AAG glycosylase excision data (*vide infra*), a 23 mer (IS1) and a 92 mer (IS2) were designed as internal standards such that they would not co-

migrate with any εA cleavage product. They were synthesized as described above and purified by 12% and 8% denaturing PAGE, respectively.

3.3.2 Reconstitution of Global εA Nucleosome Core Particles

Recombinant *Xenopus laevis* histones were expressed and purified individually before assembly into octamers.[31, 32] The globular *X. laevis* H2B protein (residues 24-122) and H3 protein (residues 38-135) were purchased from The Histone Source (Colorado State University). NCPs were reconstituted as described previously[31] via salt gradient dialysis of the radiolabeled εA-containing duplex population and histone octamer. Briefly, a molar excess of histone octamer was added to εA containing 145 bp duplex with a ^{32}P radiolabel attached at the 5'-end (10.05 pmol octamer to 10.00 pmol DNA for gH3 NCP, 10.10:10.00 pmol for native NCP, and 10.15:10.00 pmol for gH2B NCP) in buffer (10 mM Tris-HCl [pH 7.5], 1 mM EDTA, 1 mM dithiothreitol [DTT], 2 M NaCl, 500 μg/mL BSA) in a Slide-a-Lyzer dialysis device (0.1 mL capacity, 3.5 kDa MWCO; Thermo Fisher Scientific). The dialysis device started in a buffer of 10 mM Tris-HCl (pH 7.5), 1 mM EDTA, 1mM dithiothreitol (DTT), 2 M NaCl at 4 °C before transfer to buffers containing decreasing concentrations of NaCl (1.2 M, 1.0 M, 0.6 M, 0 M) at hourly intervals. The final dialysis in 0 M buffer was conducted for 3 h and then the NCPs were filtered with a 0.45 μm cellulose acetate centrifuge tube filter (Corning Costar) to remove insoluble particles. NCP formation and relative purity were analyzed using a 7% native PAGE (60:1 acrylamide: bisacrylamide; 0.25X TBE) run for 3 h at 160 V in 4 °C (**Figure 3.4**). Only NCPs containing < 5% duplex were used in these studies.

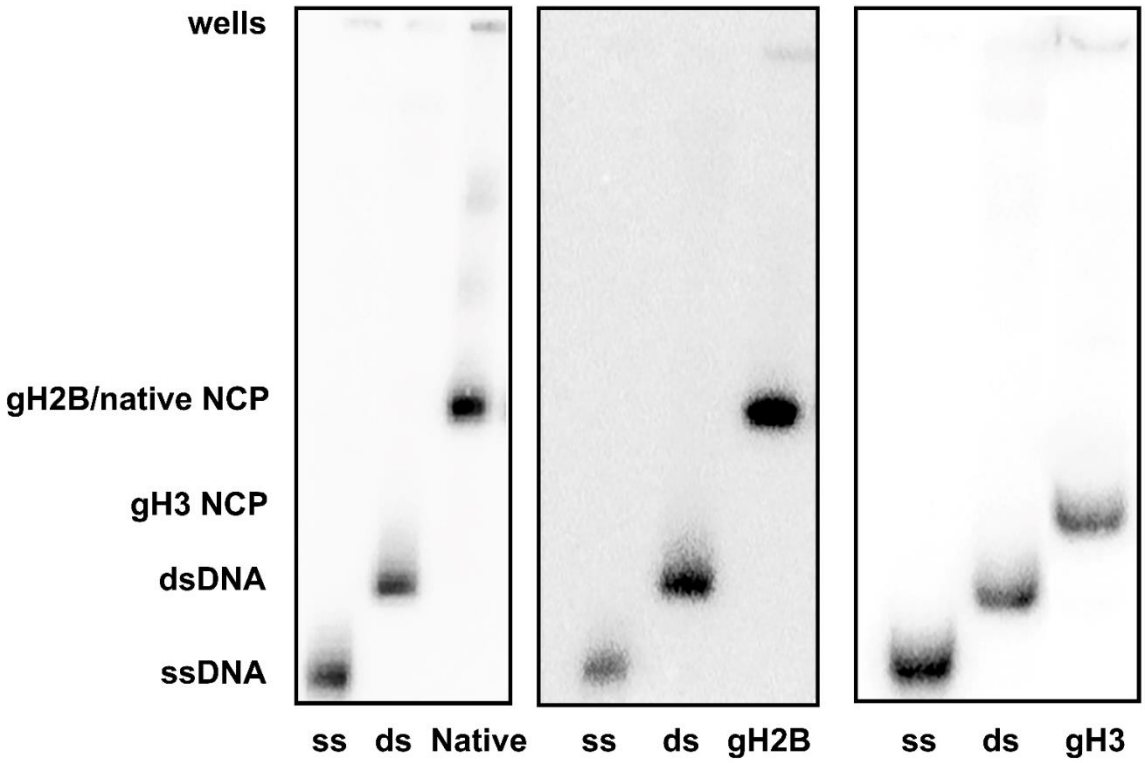

Figure 3.4 Native PAGE Analysis of εA Containing NCPs. Representative native PAGE gels showing successful NCP formation as indicated by slower band migration in the NCP lane relative to the unincorporated duplex (ds) lane. Separate gels were run for the native, gH2B, and gH3 NCPs respectively. Only NCPs containing <5% dsDNA were used in these studies.

3.3.3 Hydroxyl Radical Footprinting

To determine the rotational orientation of bases in the NCPs we utilized hydroxyl radical footprinting. To ensure single hit conditions we used a modified version of the method of Tullius.[33, 34] Briefly, 7.5 μL of each 1 mM Fe(II)-EDTA, 10 mM sodium ascorbate, and 0.12% w/v aqueous hydrogen peroxide were combined with 5 pmol NCPs in a total of 52.5 μL buffer (10 mM Tris-HCl [pH 7.5], 1 mM EDTA). This mixture was incubated in the dark at room temperature for 10 min and then quenched with 16 μL 1 mM EDTA in 25% v/v glycerol and immediately loaded onto a 7% native PAGE (60:1 acrylamide: bisacrylamide; 0.25x TBE) which was run for 3 h at 155 V at 4 °C. The gel

bands containing NCPs were excised and eluted into buffer (0.3 M NaOAc, 1 mM Tris-HCl [pH 8.0], 1 mM EDTA) for 18-24 h at 37°C with gentle shaking (60 rpm). The eluent was then concentrated using a centrifugal concentrator (Sartorius Viaspin Turbo 15, 5 kDa MWCO) and filtered using a 0.22 μm cellulose acetate syringe filter. The samples were extracted with equal volume addition of 25:24:1 phenol:chloroform:isoamyl alcohol (PCI) and the aqueous layer was concentrated by SpeedVac evaporation. Following the addition of 40 μL co-precipitation agent (0.5 mg/mL tRNA in 300 mM NaOAc [pH 8.0], 1 mM EDTA), samples were desalted with ethanol precipitation. Samples were resuspended in a 1:1 mixture of formamide and water for denaturing PAGE. Cleavage fragments were resolved by 8% denaturing PAGE (**Figure 3.5**) and quantitated using SAFA[35] gel analysis software. The highest band intensity within a helical turn was used to normalize the data and correct for loss of smaller DNA fragments during workup. To accomplish this normalization, the band intensities were plotted against base position to identify the maxima and minima corresponding to OUT and IN locations, respectively. The five bases flanking to each side of a maximum were divided by the maximum band intensity to normalize the values within each helical turn. A three-point smooth was then applied and MATLAB used for a single term Fourier fitting of bases 20-80 for each NCP to the following general equation: $f(x) = a0 + a1 * \cos(x * w) + b1 * \sin(x * w)$ where $a0,\ a1,$ and $b1$ are the Fourier coefficients and w is the fundamental frequency, w. Only fits with an R squared value of ≥ 0.7 were used for period determination. The period was determined using the following equation: $T = 2\pi/w$.

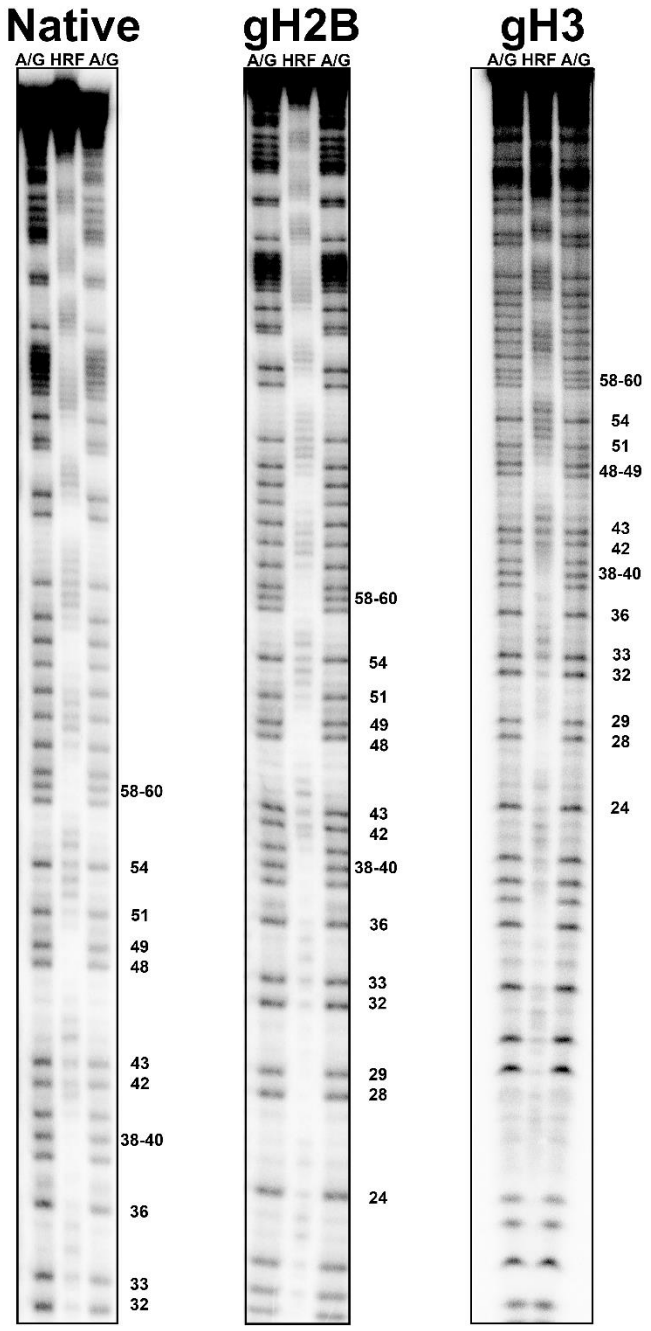

Figure 3.5 Hydroxyl Radical Footprinting of NCPs. Representative HRF denaturing PAGE gels from which rotational orientation of nucleobases was assigned. The oscillatory pattern of bands in the HRF lanes reflects the rotational position of DNA in the NCP. Quantitation of band intensity is provided in Figure 3. Lane A/G is the Maxam-Gilbert sequencing reaction (A+G) use for sequence alignment.

3.3.4 Enzymatic Reactions

Human AAG was purchased from New England Biolabs, and the total enzyme concentration determined by Bradford assay using γ-globulin standards (Bio-Rad Laboratories). AAG excision was assessed by mixing 1 pmol substrate (either duplex DNA or native, gH2B, or gH3 NCPs) with 40 pmol AAG in a total volume of 20 μL of the reaction buffer (20 mM Tris, 50 mM NaCl, 150 mM KCl, 1 mM DTT, 100 μg/mL BSA) and incubated for 1 h at 37 °C along with a negative control sample (no enzyme). After 1 h, samples were quenched with 20 μL of 1M NaOH which had been spiked with the radiolabeled internal standards and heated to at 90 °C for 3 min. PCI extraction separated the DNA from protein and the aqueous layer was supplemented with 40 μL co-precipitation agent (0.5 mg/mL tRNA in 300 mM NaOAc [pH 8.0], 1 mM EDTA) and 600 μL of ethanol before being placed on dry ice for 30 min. The ethanol was then separated from the DNA via centrifugation, removed with a pipette, and all samples were resuspended in 50% v/v formamide:water, split in half, and loaded onto an 0.6 mm, 8% PAGE gel (**Figure 3.6**). One half of the samples were loaded to resolve bands 19-64, run 2 h at 80 W. The other half of the samples were loaded to resolve of bands 89-123, run 4 h at 80 W.

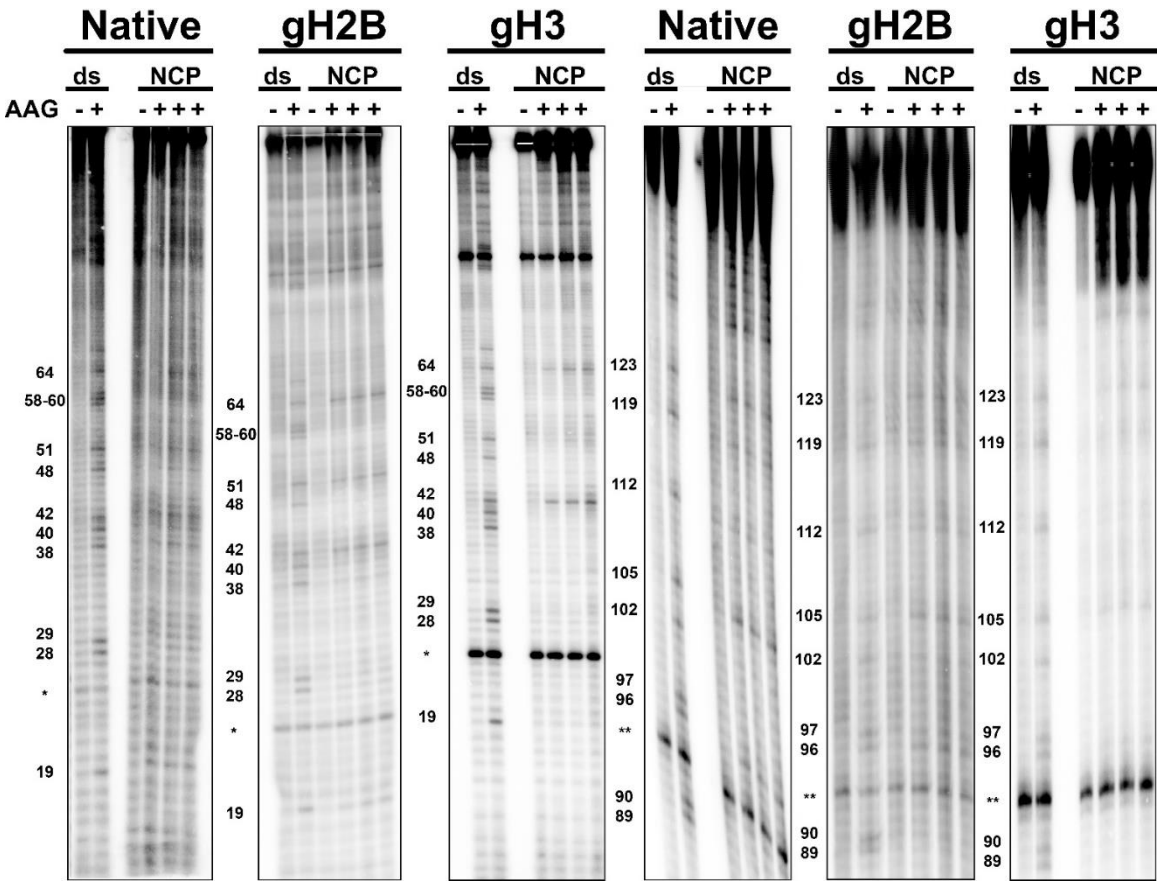

Figure 3.6 Denaturing PAGE analysis of AAG activity on NCPs and Duplex. Evaluation of AAG activity on NCPs and Duplex containing globally substituted εA lesions. All samples were incubated with 2000 nM AAG and 50 nM of either ds or NCP substrate for 1 h at 37 °C and then strand breaks were catalyzed by incubation with 0.5 M NaOH at 90 °C for 3 min to visualize successful εA excision. Each data set consists of the following lanes: a no enzyme duplex sample, duplex treated with AAG, a no enzyme NCP sample, and three replicates of AAG treated NCPs. The internal standards are indicated by the asterisks on the gel with a single asterisk and double asterisk corresponding to the 23 mer and 92 mer standards, respectively. The gels were aligned using SAFA software to allow for analysis of any slanted gels.

After phosphorimaging of the gels, SAFA software was used to quantitate band intensity. The internal standards were used for band normalization, sites 19-64 with the 23 mer standard and sites 89-123 with the 92 mer standard. The no enzyme control was used to subtract background from enzyme-treated samples. For each site, the ratio of corrected band intensity in the NCPs to the duplex was used to determine the

NCP/Duplex (NCP/DUP) ratio for AAG activity. An NCP/DUP value of 1 indicates excision that is comparable to duplex, while a value below one indicates lower excision in NCPs relative to duplex. The standard error (SE) of NCP/DUP was calculated using $SE = \sigma/\sqrt{(n)}$, where σ is the standard deviation of the population and n is the sample size. For all NCPs n=3. A two-tailed Welch's *t* test (α=0.05) was performed to obtain the p value at each εA site for NCP/DUP for each tailless NCP in comparison to native NCP/DUP. All statistical analyses were conducted using R. We considered $p < 0.05$ to be significant.

3.4 Results

3.4.1 Preparation of NCPs Containing Globally Substituted εA Lesions

To examine the effects of H2B and H3 tail deletion on the excision activity of AAG, NCPs were assembled using the Widom 601 DNA sequence and recombinant histones.[36] The NCPs had three combinations of histones: all full length histones (native NCP); native H2A, H3, H4 and globular (tailless) H2B domain (gH2B NCP); or native H2A, H2B, H4 and globular (tailless) H3 domain (gH3 NCP). Using the 601 DNA creates a homogenous population of NCPs as a substrate for biochemical studies, since it is a strong positioning sequence that reproducibly binds the histone octamer in a single translational and rotational position.[36] Furthermore, crystal structures of 601 NCPs, albeit without histone tails, are available for reference.[36]

εA lesions were incorporated throughout the "I" strand of the Widom 601 sequence to create a population of DNA containing εA:T base pairs, utilizing methods we reported previously.[28-30, 37] (The "I" strand designation is based on nomenclature used in the reported crystal structure of the 601 NCP.[36]) Briefly, a Poisson distribution was used

to determine the molar ratio of A to εA phosphoramidite building blocks used during chemical synthesis such that 95% of the synthesized DNA contain no more than a single εA. Overall, we examined excision of εA from 21 sites to define the repair fingerprint of AAG in native, gH2B, and gH3 NCPs.

3.4.2 Structural Differences in Native NCPs Compared to gH2B and gH3 NCPs

We utilized hydroxyl radical footprinting (HRF) to establish the rotational orientation of each base and determine the periodicity of DNA in the NCPs.[34] When DNA is packaged in an NCP, an oscillatory pattern of high and low reactivity towards hydroxyl radicals is observed. This pattern emerges from the preferential abstraction of C5' hydrogens of the sugar-phosphate backbone facing away from the histone core,[38] while C5' hydrogens facing towards the histone core are shielded and protected from hydroxyl radicals.

Quantitation of the HRF for each NCP confirms varying levels of solution accessibility throughout the DNA and establishes the rotational orientation of each base (**Figure 3.5, Figure 3.7, Table 3.2**). OUT sites, defined here as a maximum in the HRF profile, demonstrate the highest HRF reactivity. IN sites, defined here as a minimum in the HRF profile, exhibit the lowest HRF reactivity. MID sites, defined here as a being between a minimum and maximum in the HRF profile, demonstrate intermediate HRF reactivity. The distribution of rotational orientation of εA lesions varied and we examined AAG activity at 5 OUT, 5 MID, and 11 IN lesion sites (**Table 3.3**).

Table 3.2 HRF reactivity of εA lesions in various NCPs. These values are derived from band intensities quantitated in gels provided in Figure **3.5**.

εA Position	**Rotational Orientation**	**Native NCP**	**gH2B NCP**	**gH3 NCP**
19	IN	0.30	0.23	0.44
28	IN	0.11	0.06	0.05
29	IN	0.14	0.00	0.05
38	IN	0.09	0.28	0.10
40	MID	0.25	0.19	0.34
42	OUT	0.69	0.51	0.75
48	IN	0.08	0.01	0.00
51	MID	0.35	0.43	0.44
58	IN	0.24	0.24	0.19
59	IN	0.20	0.40	0.13
60	IN	0.18	0.47	0.23
64	OUT	0.78	0.64	0.77
89	IN	0.04	0.28	0.44
90	IN	0.01	0.24	0.36
96	OUT	0.80	0.57	0.77
97	OUT	0.92	0.72	0.79
102	MID	0.64	0.59	0.24
105	MID	0.49	0.65	0.65
112	MID	0.43	0.14	0.52
119	IN	0.35	0.32	N/A
123	OUT	0.80	0.45	N/A

Table 3.3 Translational position, rotational orientation, and AAG excision activity for native, gH2B, and gH3 NCPs. Statistical significance ($p < 0.05$) of εA excision relative to native NCP is indicated by *.

Translational Base Position	Rotational Orientation	AAG Excision Activity (NCP/DUP)		
		Native NCP	gH2B NCP	gH3 NCP
19	IN	0.21	0.21	0.02*
28	IN	0.03	0.08*	0.03
29	IN	0.07	0.07	0.02
38	IN	0.06	0.02	0.02
40	MID	0.19	0.01	0.03

42	OUT	1.02	0.91	0.63
48	IN	0.00	0.01	0.02
51	MID	0.47	0.55	0.12*
58	IN	0.00	0.04*	0.02
59	IN	0.00	0.03	0.04
60	IN	0.00	0.02	0.08
64	OUT	0.84	1.04*	0.67
89	IN	0.02	0.05	0.00
90	IN	0.00	0.01	0.00
96	OUT	1.02	0.78	0.33*
97	OUT	0.37	0.17	0.13
102	MID	0.04	0.27	0.12
105	MID	1.11	1.00	0.62
112	MID	0.02	0.44*	0.25
119	IN	0.13	0.61*	0.40
123	OUT	0.77	0.81	0.95

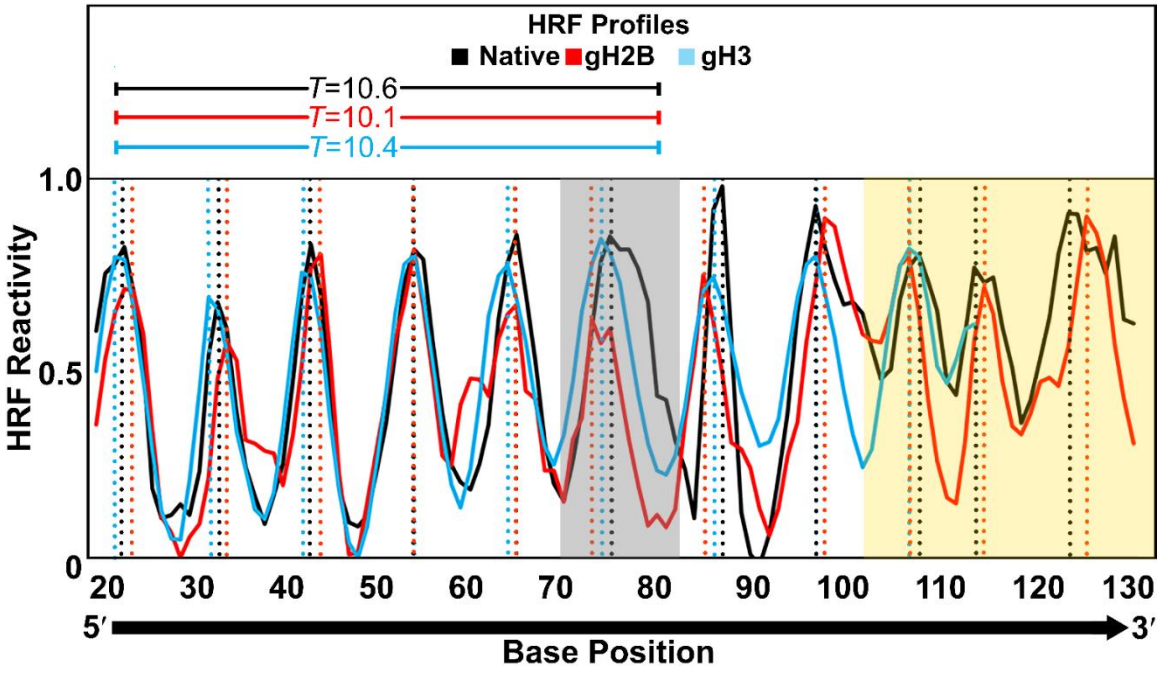

Figure 3.7 HRF profiles for native (black), gH2B (red), and gH3 (blue) NCPs with dashed vertical lines indicating maximum locations. The yellow highlighting indicates DNA near the entry/exit region in the NCP. Gray highlighting indicates the dyad region. The average periodicity (T) from bases 20-80 for each NCP is indicated.

Comparison of the HRF profiles of the native (black), gH2B (red), and gH3 (blue) NCPs reveals structural differences (**Figure 3.7**). The profiles of all three NCPs exhibit

the expected oscillatory pattern. However, there are differences in locations of the maxima and minima for many helical turns. For example, the native NCP has a maximum at position 33 (vertical black dashed line) while gH2B (red dashed) is at 32 and gH3 (blue dashed) at 34. Differences in locations of maxima and minima can be seen throughout the NCP, with the only shared maxima for all three NCPs at 54. Other shared maxima can be seen for gH2B and gH3 NCPs at 107; gH2B and native NCPs at 65; and gH3 and native NCPs at 97. Differences in the location of maxima and minima indicate differential stretching and compaction of the DNA in these NCPs.

Alterations to the shape of the HRF profiles are observed near the dyad axis (**Figure 3.7**, gray shaded region). The native NCP has a broad maximum while the gH2B and gH3 NCPs display narrower peaks. The broader maximum indicates an area facing OUT that is underwound in the native NCP relative to the gH2B and gH3 NCPs. Changes continue towards the 3'-end for all NCPs. A Fourier fit of bases 20-80 reveals that the average periodicity, the number of base pairs per helical turn, differs between the three NCPs: 10.6 bp/turn for native NCP, 10.1 bp/turn for gH2B NCP, and 10.4 bp/turn for the gH3 NCP. Poor fits for bases 90-130 and lack of data for gH2B NCPs beyond base 115 prevented a periodicity analysis for the 3'-end.

3.4.3 Excision of εA from Native NCPs Correlates with Rotational Orientation

AAG is known to remove εA from duplex DNA not packaged into NCPs (unincorporated duplex).[23, 39, 40] To determine the effects of incorporation into an NCP on εA excision we compared excision from each NCP as a ratio relative to unincorporated duplex (NCP/DUP). A ratio of 1 indicates that excision from NCPs is comparable to

unincorporated duplex, while a ratio less than 1 indicates inhibition of excision from NCPs.

The repair fingerprint of native NCPs demonstrates a strong correlation between rotational orientation and AAG excision (**Figure 3.8**, black bars; **Table 3.3**). Low AAG excision (NCP/DUP <0.2) is observed for IN sites. In contrast, high excision (NCP/DUP >0.6) is observed for most OUT sites with the notable exception being site 97 (**Figure 3.9**, black bars), with NCP/DUP of <0.4. MID sites demonstrate much more variability, with most NCP/DUP ranging between 0.1-0.6, except site 105 which reaches 1. This correlation between rotational orientation and excision is in agreement with previous reports.[28, 37]

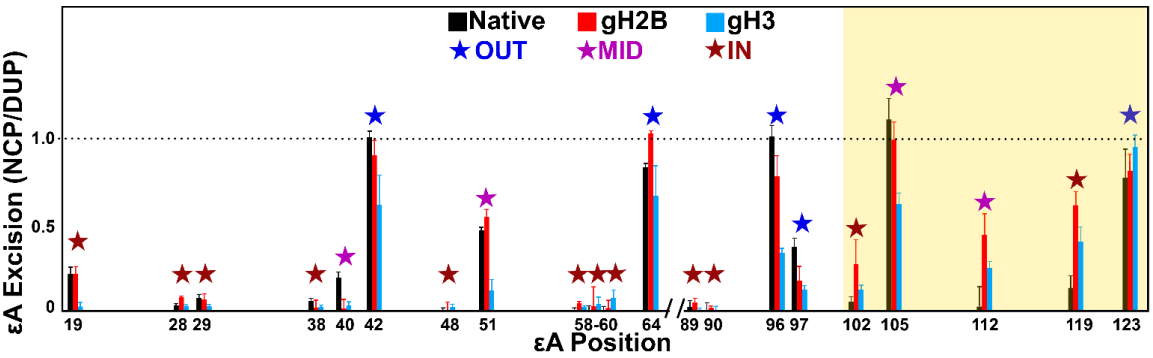

Figure 3.9. AAG excision activity for native (black), gH2B (red), and gH3 (blue) NCPs. Stars indicate rotational orientation: OUT (blue), MID (purple) and IN (dark red) as determined by HRF. The yellow highlighting indicates the region outside of the central DNA in the NCP.

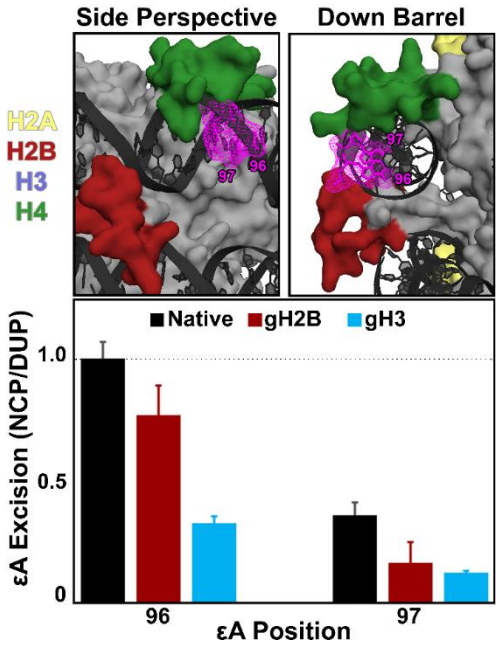

Figure 3.10. Location of εA sites 96 and 97 in the NCP compared to their excision activity. (Top) The side perspective (left) and down barrel perspective (right) of εA sites 96 and 97 are highlighted in the NCP. (Bottom) The AAG excision activity are shown for each NCP: native (black), gH2B (red), and gH3 (blue).

3.4.4 Excision of εA from gH2B

For the majority of εA lesions, excision is comparable or enhanced in gH2B compared to native NCPs (**Figure 3.9**, red bars; **Table 3.3**). Enhancement is particularly notable in the DNA entry/exit region (**Figure 3.9**, yellow shaded region). Like the native NCPs, there is a general correlation between rotational position and εA excision in the central region of the NCP (bases 19-97), with OUT sites exhibiting generally higher NCP/DUP values than IN or MID sites. There is a small, but significant enhancement of εA excision at OUT site 64 and IN sites 28 and 58 in the gH2B NCP. However, in contrast to native NCPs, the IN and MID sites located towards the 3'-end of the sequence (112 and 119) show 5 to 22-fold enhancement in excision (**Figure 3.11**, red bars). Sites 42, 48, and 51 are on the same DNA superhelix but on the opposite side of the H2B tail

but do not exhibit similar enhancement of excision. There are no sites that show significant inhibition in the gH2B NCP compared to native NCP.

3.4.5 Excision of εA from gH3 NCPs

Unlike the gH2B NCPs, which show a few sites of enhanced excision compared to native NCPs, gH3 NCPs show no significant enhancement at any site (**Figure 3.9**, blue bars; **Table 3.3**). In contrast, the AAG repair profile for gH3 NCPs displays inhibitory effects in the central part of the NCP compared to native NCPs (**Figure 3.9**, blue bars). Excision at IN (19), MID (51), and OUT (96; **Figure 3.10**) sites is inhibited and varies from 3 to 10-fold.

3.5 Discussion

In this work, we compare the global repair profiles of AAG on εA lesions distributed throughout native NCPs or those lacking H2B or H3 tails. As observed previously, εA removal by AAG is highly correlated with rotational orientation in the central region of the DNA in native NCPs.[28, 37] We also reported a similar trend for the glycosylases 8-oxo-7,8-dihydroguanine glycosylases (OGG1),[30, 41] uracil DNA glycosylase (UDG),[29, 41] and thymine DNA glycosylase (TDG).[42] A correlation between rotational orientation of a lesion and glycosylase activity has also been reported by other groups.[43-46]

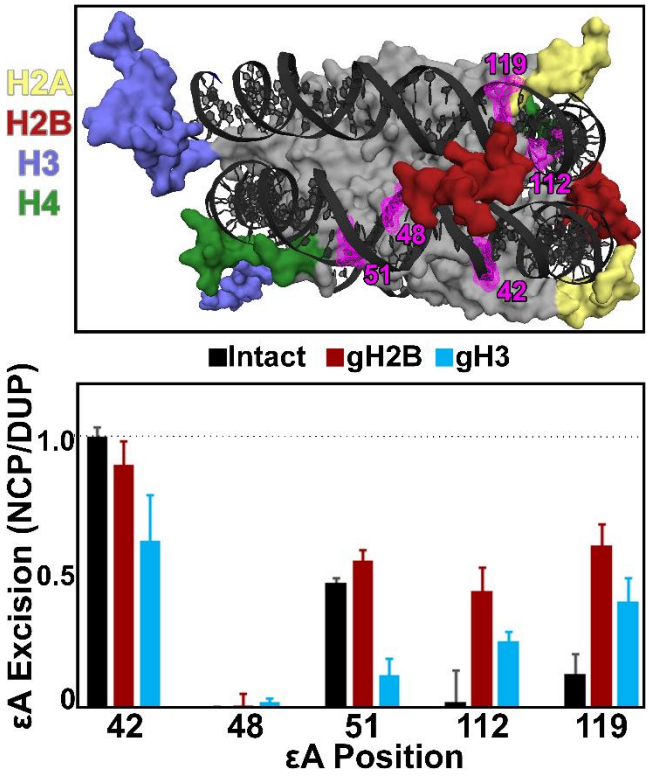

Figure 3.11. Location and excision of selected εA sites. (Top) The location of selected εA sites and histone tails are highlighted. (Bottom) The AAG excision activity for each NCP: native (black), gH2B (red), and gH3 (blue).

There have been limited studies of the effects of histone tails on BER. Digestion of histone tails by trypsin had a minimal effect on UDG activity.[47, 48] APE1 incision activity was also not affected.[48] When a portion of the H2B tail, known as the histone H2B repression (HBR) domain, is deleted, enhanced UDG and pol β activity are observed in the entry/exit regions.[49] This enhanced activity was attributed to DNA unwrapping in the absence of the HBR domain. Finally, DNA ligase 1 activity was reported to be enhanced in the dyad region following trypsin digestion of the histone tails.[50]

Examination of BER of alkylation damage in yeast with H2A or H3 tail deletions demonstrated the roles of the tails in the regulation of glycosylase expression, DNA damage signaling, and post replicative repair.[51] The removal of tails resulted in

diminished cell survival upon treatment with alkylating agents, even when the glycosylase responsible for excision of alkylation damage in yeast, Mag1 (the homolog of AAG), was overexpressed.

When interpreting the repair fingerprint of AAG activity on native, gH2B, and gH3 NCPs we considered that removal of the H2B or H3 could eliminate a steric block and lead to increased accessibility of nearby lesions. Sites 42, 48, 51, 102, 112, and 119 are located near the H2B tail (**Figure 3.11**) and distributed both in the central region of the DNA as well as the DNA entry/exit region. No significant enhancement in excision of lesions in the central region of the DNA was observed in the absence of the H2B or H3 tails. In fact, gH3 NCPs demonstrate inhibited εA excision relative to native NCPs at site 51. While the lesions near the DNA entry/exit region exhibit enhanced excision by AAG in gH2B NCPs, we do not ascribe this increase to removal of a steric block caused by the tail, but rather altered DNA structure and dynamics as discussed below.

Changes in the DNA periodicity in the absence of histone tails may affect εA excision. The excision at site 51 in the native NCP compared to the gH3 NCP demonstrates this potential effect. Despite being a MID site in both NCPs, there is significant inhibition of εA excision in the gH3 NCP. There are no tails in the crystal structure that interact with directly this position, so it is unlikely to be a steric effect from tail removal. The underwinding of the DNA helix in the gH3 NCP relative to the native NCP within this helical turn may help explain this result. The altered periodicity may be inhibitory to binding or substrate recognition by AAG. This effect of altered periodicity of the DNA in the central part of the NCP may, in part, explain more broadly the inhibitory effects of tail removal in this region.

While the DNA in the central part of the NCP does not unwrap, the DNA located in the entry/exit region of native NCPs is known to unwrap transiently and spontaneously to expose sites that would be otherwise occluded. For the Widom 601 "I" strand it has been shown that the 3'-end preferentially unwraps.[56] We have reported previously that glycosylase activity, including AAG, does not correlate with rotational orientation in certain translational locations prone to unwrapping.[29, 30, 41] Unwrapping has also been reported to be rate-limiting for the activity of endonuclease III-like protein 1 (NTH1) glycosylase [57, 58] and to be exploited by Nap1 during H2A/H2B dimer eviction.[59]

We find that lesions located near the DNA entry/exit region are better excised in NCPs lacking the H2B but not the H3 tail. Computational studies have predicted enhanced unwrapping when histone tail charges are neutralized, which is particularly pronounced for the H2B and H3 tails.[12, 60] This charge neutralization stabilizes unwrapped states out to 40 base pairs for H2B and 30 base pairs for H3 under salt conditions similar to those used in our study. For comparison, native NCPs demonstrate unwrapping of ~20 base pairs. Crystal structures have revealed that H2B and H3 tail deletion weakens histone interactions with DNA and undermines the stability of the NCP.[10] Similar observations were made by SAXS[61] and FRET[62, 63] which demonstrated enhanced dynamics and nucleosomal instability upon tail removal. Our results are consistent with the notion that removal of the H2B tail promotes greater DNA unwrapping from the histone proteins and this unwrapping allows for excision of otherwise occluded εA lesions by AAG. However, the removal of the H3 tail does not promote similar enhancement of εA excision, possibly due to a lesser degree of unwrapping than observed upon H2B tail removal.

While structural alterations and enhanced unwrapping of the DNA in the NCP explain the observations above, it is also important to consider interactions between the histone protein themselves. Interactions between the histone tails may explain some of the inhibition of AAG activity. Histone tails are essential for formation of nucleosomal arrays through extensive intra- and inter-nucleosomal contacts.[52] Even the presence of a bulky lesion in the DNA near the H2B tail has been simulated to change tail conformation.[53] Removal of εA at site 96, near the H2B and H4 tails (**Figure 3.10**), is significantly inhibited by H3 tail removal but not H2B tail removal. Surprisingly, the shift of the HRF maximum in this region to position 97, making it more OUT, for the gH3 NCP does not enhance εA excision. The H4 tail, important for inter-nucleosomal interactions,[54] in this region may undergo a conformational change in the absence of the H3 tail that inhibits AAG binding or excision activity. These potential synergistic tail-tail interactions are not unexpected as computational studies have shown that the acetylation of the H4 tail impacts the ability of the H3 tail to interaction with other proteins.[55] Similarly, the maximum shift from position 65 to position 64, making it a more OUT lesion, in the gH3 NCP does not confer enhanced εA excision. In contrast, the gH2B NCPs show a small enhancement of activity while retaining the same maximum at position 65 seen in native NCPs. The enhancement of excision at site 64 in the gH2B without a change in DNA periodicity and absent any steric interactions with the H2B tail indicate other modulating protein-protein interactions. Taken together these results indicate that it is not only DNA-protein contacts that affect εA excision in NCPs, but also protein-protein interactions. Only by taking all these factors cumulatively can the repair fingerprint of AAG in these varied NCPs be understood.

Biological observations of mutational hotspots and accumulation of alkylation damage can also be considered in light the results obtained here. In yeast, it has been reported that alkylation damage accumulates at IN lesions.[64] Such sites were also observed to be mutational hotspots in the analysis of human tumors.[65] These data suggests the need for alternate mechanisms to access these IN sites for repair, such enhanced unwrapping of DNA from histones. Indeed, H2B[60] and H3[6] acetylation has been shown to enhance DNA unwrapping and acetylation has been observed to occur as part of the DNA damage response.[66] More intriguingly, it has been recently reported that a complex is formed between AAG and RNA polymerase II that may access occluded lesions by utilization of chromatin decondensation.[67] This complex, along with the observation that the H3 tail protease JMJD5 relieves RNA polymerase II pausing[18] and the protease is active under DNA damaging conditions,[20] implicates tail clipping as a mechanism to repair DNA damage during transcription. Together with these findings, our results indicate a potential mechanism to access DNA damage by the BER pathway: utilizing tail clipping to promote DNA accessibility through unwrapping from the histone octamer.

3.6 References

1. Luger, K., Mäder, A. W., Richmond, R. K., Sargent, D. F., Richmond, T. J. (**1997)** Crystal structure of the nucleosome core particle at 2.8 Å resolution. *Nature 389* (6648), 251-260. DOI: 10.1038/38444

2. Eickbush, T. H. and Moudrianakis, E. N. (**1978**) The histone core complex: an octamer assembled by two sets of protein-protein interactions. *Biochemistry 17* (23), 4955-4964. DOI: 10.1021/bi00616a016

3. Lee, J. Y., Lee, J., Yue, H., Lee, T. H. (**2015**) Dynamics of nucleosome assembly and effects of DNA methylation. *J. Biol. Chem. 290* (7), 4291-303. DOI: 10.1074/jbc.M114.619213

4. Zhou, K., Gaullier, G., Luger, K. (**2019**) Nucleosome structure and dynamics are coming of age. *Nat. Struct. Mol. Biol. 26* (1), 3-13. DOI: 10.1038/s41594-018-0166-x

5. Venkatesh, S. and Workman, J. L. (**2015**) Histone exchange, chromatin structure and the regulation of transcription. *Nat. Rev. Mol. 16* (3), 178-189. DOI: 10.1038/nrm3941

6. Gansen, A., Tóth, K., Schwarz, N., Langowski, J. (**2015**) Opposing roles of H3- and H4-acetylation in the regulation of nucleosome structure - A FRET study. *Nucleic Acids Res. 43(3) 1433-43*. DOI: 10.1093/nar/gku1354

7. Kim, J., Lee, J., Lee, T.-H. (**2015**) Lysine Acetylation Facilitates Spontaneous DNA Dynamics in the Nucleosome. *J. Phys. Chem. B 119* (48), 15001-15005. DOI: 10.1021/acs.jpcb.5b09734

8. Campos, E. I. and Reinberg, D. (**2009**) Histones: Annotating Chromatin. *Annu. Rev. Genet. 43* (1), 559-599. DOI: 10.1146/annurev.genet.032608.103928

9. Azad, G. K., Swagatika, S., Kumawat, M., Kumawat, R., Tomar, R. S. (**2018**) Modifying Chromatin by Histone Tail Clipping. *J. Mol. Biol. 430* (18, Part B), 3051-3067. DOI: 10.1016/j.jmb.2018.07.013

10. Iwasaki, W., Miya, Y., Horikoshi, N., Osakabe, A., Taguchi, H., Tachiwana, H.; Shibata, T., Kagawa, W., Kurumizaka, H. (**2013**) Contribution of histone N-terminal tails to the structure and stability of nucleosomes. *FEBS Open Bio 3*, 363-9. DOI: 10.1016/j.fob.2013.08.007

11. Ferreira, H., Somers, J., Webster, R., Flaus, A., Owen-Hughes, T. (**2007**) Histone Tails and the H3 αN Helix Regulate Nucleosome Mobility and Stability. *Mol. Cell. Biol. 27* (11), 4037-4048. DOI: 10.1128/MCB.02229-06

12. Kenzaki, H. and Takada, S. (**2015**) Partial Unwrapping and Histone Tail Dynamics in Nucleosome Revealed by Coarse-Grained Molecular Simulations. *PLoS Comput. Biol. 11* (8), e1004443-e1004443. DOI: 10.1371/journal.pcbi.1004443

13. Polach, K. J., Lowary, P. T., Widom, J. (**2000**) Effects of core histone tail domains on the equilibrium constants for dynamic DNA site accessibility in nucleosomes. *J. Mol. Biol. 298* (2), 211-223. DOI: 10.1006/jmbi.2000.3644

14. Yang, Z., Zheng, C., Hayes, J. J. (**2007**) The core histone tail domains contribute to sequence-dependent nucleosome positioning. *J. Biol. Chem. 282* (11), 7930-8. DOI: 10.1074/jbc.M610584200

15. Santos-Rosa, H., Kirmizis, A., Nelson, C., Bartke, T., Saksouk, N., Cote, J., Kouzarides, T. (**2009**) Histone H3 tail clipping regulates gene expression. *Nat. Struct. Mol. Biol. 16* (1), 17-22. DOI: 10.1038/nsmb.1534

16. Kim, K., Punj, V., Kim, J.-M., Lee, S., Ulmer, T. S., Lu, W., Rice, J. C., An, W. (**2016**) MMP-9 facilitates selective proteolysis of the histone H3 tail at genes necessary for proficient osteoclastogenesis. *Genes Dev. 30* (2), 208-219. DOI: 10.1101/gad.268714.115

17. Protacio, R. U., Li, G., Lowary, P. T., Widom, J. (**2000**) Effects of histone tail domains on the rate of transcriptional elongation through a nucleosome. *Mol. Cell. Biol. 20* (23), 8866-8878. DOI: 10.1128/mcb.20.23.8866-8878.2000

18. Liu, H., Ramachandran, S., Fong, N., Phang, T., Lee, S., Parsa, P., Liu, X., Harmacek, L., Danhorn, T., Song, T., Oh, S., Zhang, Q., Chen, Z., Zhang, Q., Tu, T.-H., Happoldt, C., O'Conner, B., Janknecht, R., Li, C.-Y., Marrack, P., Kappler, J., Leach, S., Zhang, G. (**2020**) JMJD5 couples with CDK9 to release the paused RNA polymerase II. *Proc. Natl. Acad. Sci. U.S.A 117* (33), 19888. DOI: 10.1073/pnas.2005745117

19. Melo, F. R., Wallerman, O., Paivandy, A., Calounova, G., Gustafson, A.-M., Sabari, B. R., Zabucchi, G., Allis, C. D., Pejler, G. (**2017**) Tryptase-catalyzed core histone truncation: A novel epigenetic regulatory mechanism in mast cells. *J. Allergy Clin. Immunol. 140* (2), 474-485. DOI: 10.1016/j.jaci.2016.11.044

20. Shen, J., Xiang, X., Chen, L., Wang, H., Wu, L., Sun, Y., Ma, L., Gu, X., Liu, H., Wang, L., Yu, Y.-n., Shao, J., Huang, C., Chin, Y. E. (**2017**) JMJD5 cleaves monomethylated histone H3 N-tail under DNA damaging stress. *EMBO rep. 18* (12), 2131-2143. DOI: 10.15252/embr.201743892

21. Schermerhorn, K. M. and Delaney, S. (**2014**) A chemical and kinetic perspective on base excision repair of DNA. *Acc. Chem. Res. 47* (4), 1238-1246. DOI: 10.1021/ar400275a

22. Levine, R. L., Yang, I.-Y., Hossain, M., Pandya, G. A., Grollman, A. P., Moriya, M. (**2000**) Mutagenesis induced by a single 1,N-6-ethenodeoxyadenosine adduct in human hells. *Cancer Res. 60* (15), 4098-4104.

23. Riazuddin, S. and Lindahl, T. (**1978**) Properties of 3-methyladenine-DNA glycosylase from Escherichia coli. *Biochemistry 17* (11), 2110-2118. DOI: 10.1021/bi00604a014

24. El Ghissassi, F., Barbin, A., Nair, J., Bartsch, H. (**1995**) Formation of 1,N6-ethenoadenine and 3,N4-ethenocytosine by lipid peroxidation products and nucleic acid bases. *Chem. Res. Toxicol. 8* (2), 278-283. DOI: 10.1021/tx00044a013

25. Guengerich, F. P., Crawford, W. M., Watanabe, P. G. (**1979**) Activation of vinyl chloride to covalently bound metabolites: roles of 2-chloroethylene oxide and 2-chloroacetaldehyde. *Biochemistry 18* (23), 5177-5182. DOI: 10.1021/bi00590a023

26. Nair, U., Bartsch, H., Nair, J. (**2007**) Lipid peroxidation-induced DNA damage in cancer-prone inflammatory diseases: A review of published adduct types and levels in humans. *Free Radic. Biol. Med. 43* (8), 1109-1120. DOI: 10.1016/j.freeradbiomed.2007.07.012

27. O'Brien, P. J. and Ellenberger, T. (**2004**) Dissecting the broad substrate specificity of human 3-methyladenine-DNA glycosylase. *J. Biol. Chem. 279* (11), 9750-9757. DOI: 10.1074/jbc.M312232200

28. Kennedy, E. E., Li, C., Delaney, S. (**2019**) Global repair profile of human alkyladenine DNA glycosylase on nucleosomes reveals DNA packaging effects. *ACS Chem. Biol. 14* (8), 1687-1692. DOI: 10.1021/acschembio.9b00263

29. Li, C. and Delaney, S. (**2019**) Histone H2A variants enhance the initiation of base excision repair in nucleosomes. *ACS Chem. Biol. 14* (5), 1041-1050. DOI: 10.1021/acschembio.9b00229

30. Bilotti, K., Tarantino, M. E., Delaney, S. (**2018**) Human oxoguanine glycosylase 1 removes solution accessible 8-oxo-7,8-dihydroguanine lesions from globally substituted nucleosomes except in the dyad region. *Biochemistry 57* (9), 1436-1439. DOI: 10.1021/acs.biochem.7b01125

31. Luger, K., Rechsteiner, T. J., Richmond, T. J. (**1999**) Expression and purification of recombinant histones and nucleosome reconstitution. *Methods Mol. Biol. 119*, 1-16. DOI: 10.1385/1-59259-681-9:1

32. Luger, K., Rechsteiner, T. J., Richmond, T. J. (**1999**) Preparation of nucleosome core particle from recombinant histones. *Methods Enzymol. 304*, 3-19. DOI: 10.1016/S0076-6879(99)04003-3

33. Hayes, J. J., Tullius, T. D., Wolffe, A. P. (**1990**) The structure of DNA in a nucleosome. *Proc. Natl. Acad. Sci. U.S.A 87* (19), 7405-7409. DOI: 10.1073/pnas.87.19.7405.

34. Jain, S. S. and Tullius, T. D. (**2008**) Footprinting protein–DNA complexes using the hydroxyl radical. *Nat. Protoc. 3* (6), 1092-1100. DOI: 10.1038/nprot.2008.72

35. Das, R., Laederach, A., Pearlman, S. M., Herschlag, D., Altman, R. B. (**2005**) SAFA: semi-automated footprinting analysis software for high-throughput quantification of nucleic acid footprinting experiments. *RNA 11* (3), 344-54. DOI: 10.1261/rna.7214405

36. Vasudevan, D., Chua, E. Y. D., Davey, C. A. (**2010**) Crystal structures of nucleosome core particles containing the '601' strong positioning sequence. *J. Mol. Biol. 403* (1), 1-10. DOI: 10.1016/j.jmb.2010.08.039

37. Caffrey, P. J., Kher, R., Bian, K., Li, D., Delaney, S. (**2020**) Comparison of the base excision and direct reversal repair pathways for correcting 1,N6-ethenoadenine in strongly positioned nucleosome core particles. *Chem. Res. Toxicol. 33* (7), 1888-1896. DOI: 10.1021/acs.chemrestox.0c00089

38. Balasubramanian, B., Pogozelski, W. K., Tullius, T. D. (**1998**) DNA strand breaking by the hydroxyl radical is governed by the accessible surface areas of the

hydrogen atoms of the DNA backbone. *Proc. Natl. Acad. Sci. U.S.A 95* (17), 9738. DOI: 10.1073/pnas.95.17.9738

39. Samson, L., Derfler, B., Boosalis, M., Call, K. (**1991**) Cloning and characterization of a 3-methyladenine DNA glycosylase cDNA from human cells whose gene maps to chromosome 16. *Proc. Natl. Acad. Sci. U.S.A 88* (20), 9127-9131. DOI: 10.1073/pnas.88.20.9127

40. Chakravarti, D., Ibeanu, G. C., Tano, K., Mitra, S. (**1991**) Cloning and expression in Escherichia coli of a human cDNA encoding the DNA repair protein N-methylpurine-DNA glycosylase. *J. Biol. Chem. 266* (24), 15710-15715.

41. Olmon, E. D. and Delaney, S. (**2017**) Differential ability of five DNA glycosylases to recognize and repair damage on nucleosomal DNA. *ACS Chem. Biol. 12* (3), 692-701. DOI: 10.1021/acschembio.6b00921

42. Tarantino, M. E., Dow, B. J., Drohat, A. C., Delaney, S. (**2018**) Nucleosomes and the three glycosylases: High, medium, and low levels of excision by the uracil DNA glycosylase superfamily. *DNA Repair 72*, 56-63. DOI: 10.1016/j.dnarep.2018.09.008

43. Beard, B. C., Wilson, S. H., Smerdon, M. J. (**2003**) Suppressed catalytic activity of base excision repair enzymes on rotationally positioned uracil in nucleosomes. *Proc. Natl. Acad. Sci. U.S.A 100* (13), 7465-70. DOI: 10.1073/pnas.1330328100

44. Cole, H. A., Tabor-Godwin, J. M., Hayes, J. J. (**2010**) Uracil DNA glycosylase activity on nucleosomal DNA depends on rotational orientation of targets. *J. Biol. Chem. 285* (4), 2876-85. DOI: 10.1074/jbc.M109.073544

45. Hinz, J. M., Rodriguez, Y., Smerdon, M. J. (**2010**) Rotational dynamics of DNA on the nucleosome surface markedly impact accessibility to a DNA repair enzyme. *Proc. Natl. Acad. Sci. U.S.A 107* (10), 4646-4651. DOI: 10.1073/pnas.0914443107

46. Prasad, A., Wallace, S. S., Pederson, D. S. (**2007**) Initiation of base excision repair of oxidative lesions in nucleosomes by the human, bifunctional DNA glycosylase NTH1. *Mol. Cell. Biol. 27* (24), 8442-8453. DOI: 10.1128/MCB.00791-07

47. Beard, B. C., Stevenson, J. J., Wilson, S. H., Smerdon, M. J. (**2005**) Base excision repair in nucleosomes lacking histone tails. *DNA Repair 4* (2), 203-209. DOI: 10.1016/j.dnarep.2004.09.011

48. Beard, B. C., Wilson, S. H., Smerdon, M. J. (**2003**) Suppressed catalytic activity of base excision repair enzymes on rotationally positioned uracil in nucleosomes. *Proc. Natl. Acad. Sci. U.S.A 100* (13), 7465-7470. DOI: 10.1073/pnas.1330328100

49. Rodriguez, Y., Duan, M., Wyrick, J. J., Smerdon, M. J. (**2018**) A cassette of basic amino acids in histone H2B regulates nucleosome dynamics and access to DNA damage. *J. Biol. Chem. 293* (19), 7376-7386. DOI: 10.1074/jbc.RA117.000358

50. Chafin, D. R., Vitolo, J. M., Henricksen, L. A., Bambara, R. A., Hayes, J. J. **(2000)** Human DNA ligase I efficiently seals nicks in nucleosomes. *EMBO J 19* (20), 5492-501. DOI: 10.1093/emboj/19.20.5492

51. Meas, R., Smerdon, M. J., Wyrick, J. J. (**2015**) The amino-terminal tails of histones H2A and H3 coordinate efficient base excision repair, DNA damage signaling and postreplication repair in Saccharomyces cerevisiae. *Nucleic Acids Res. 43* (10), 4990-5001. DOI: 10.1093/nar/gkv372

52. Pepenella, S., Murphy, K. J., Hayes, J. J. (**2014**) Intra- and inter-nucleosome interactions of the core histone tail domains in higher-order chromatin structure. *Chromosoma 123* (1-2), 3-13. DOI: 10.1007/s00412-013-0435-8

53. Fu, I., Cai, Y., Zhang, Y., Geacintov, N. E., Broyde, S. (**2016**) Entrapment of a histone tail by a DNA lesion in a nucleosome suggests the lesion impacts epigenetic marking: a molecular dynamics study. *Biochemistry 55* (2), 239-242. DOI: 10.1021/acs.biochem.5b01166

54. Kan, P. Y., Caterino, T. L., Hayes, J. J. (**2009**) The H4 tail domain participates in intra- and internucleosome interactions with protein and DNA during folding and oligomerization of nucleosome arrays. *Mol Cell Biol 29* (2), 538-46. DOI: 10.1128/MCB.01343-08

55. Cai, Y., Fu, I., Geacintov, N. E., Zhang, Y., Broyde, S. (2018) Synergistic effects of H3 and H4 nucleosome tails on structure and dynamics of a lesion-containing DNA: Binding of a displaced lesion partner base to the H3 tail for GG-NER recognition. *DNA Repair 65*, 73-78. DOI: 10.1016/j.dnarep.2018.02.009

56. Ngo, T. T. M., Zhang, Q., Zhou, R., Yodh, J. G., Ha, T. (**2015**) Asymmetric unwrapping of nucleosomes under tension directed by DNA local flexibility. *Cell 160* (6), 1135-1144. DOI: 10.1016/j.cell.2015.02.001

57. Odell, I. D., Newick, K., Heintz, N. H., Wallace, S. S., Pederson, D. S. (**2010**) Non-specific DNA binding interferes with the efficient excision of oxidative lesions from chromatin by the human DNA glycosylase, NEIL1. *DNA Repair 9* (2), 134-143. DOI: 10.1016/j.dnarep.2009.11.005

58. Maher, R. L., Prasad, A., Rizvanova, O., Wallace, S. S., Pederson, D. S. (**2013**) Contribution of DNA unwrapping from histone octamers to the repair of oxidatively damaged DNA in nucleosomes. *DNA Repair 12* (11), 964-971. DOI: 10.1016/j.dnarep.2013.08.010

59. Lee, J. and Lee, T.-H. (**2017**) Single-molecule investigations on histone H2A-H2B dynamics in the nucleosome. *Biochemistry 56* (7), 977-985. DOI: 10.1021/acs.biochem.6b01252

60. Fu, I., Cai, Y., Geacintov, N. E., Zhang, Y., Broyde, S. (**2017**) Nucleosome histone tail conformation and dynamics: impacts of lysine acetylation and a nearby minor groove benzo[a]pyrene-derived Lesion. *Biochemistry 56* (14), 1963-1973. DOI: 10.1021/acs.biochem.6b01208

61. Bertin, A., Durand, D., Renouard, M., Livolant, F., Mangenot, S. (**2017**) H2A and H2B tails are essential to properly reconstitute nucleosome core particles. *Eur. Biophys. J. 36* (8), 1083-1094. DOI: 10.1007/s00249-007-0212-9

62. Andresen, K., Jimenez-Useche, I., Howell, S. C., Yuan, C., Qiu, X. (**2013**) Solution scattering and FRET studies on nucleosomes reveal DNA unwrapping effects of H3 and H4 Tail removal. *PLOS ONE 8* (11), e78587. DOI: 10.1371/journal.pone.0078587

63. Bertin, A., Renouard, M., Pedersen, J. S., Livolant, F., Durand, D. (**2007**) H3 and H4 histone tails play a central role in the interactions of recombinant NCPs. *Biophys. J. 92* (7), 2633-2645. DOI: 10.1529/biophysj.106.093815

64. Mao, P., Brown, A. J., Malc, E. P., Mieczkowski, P. A., Smerdon, M. J., Roberts, S. A., Wyrick, J. J. (**2017**) Genome-wide maps of alkylation damage, repair, and

mutagenesis in yeast reveal mechanisms of mutational heterogeneity. *Genome Res. 27* (10), 1674-1684. DOI: 10.1101/gr.225771.117

65. Pich, O., Muinos, F., Sabarinathan, R., Reyes-Salazar, I., Gonzalez-Perez, A., Lopez-Bigas, N. (**2018**) Somatic and germline mutation periodicity follow the orientation of the DNA minor groove around nucleosomes. *Cell 175* (4), 1074-1087.e18. DOI: 10.1016/j.cell.2018.10.004

66. van Attikum, H. and Gasser, S. M. (**2009**) Crosstalk between histone modifications during the DNA damage response. *Trends Cell Biol. 19* (5), 207-217. DOI: 10.1016/j.tcb.2009.03.001

67. Montaldo, N. P., Bordin, D. L., Brambilla, A., Rösinger, M., Fordyce Martin, S. L., Bjørås, K. Ø., Bradamante, S., Aas, P. A., Furrer, A., Olsen, L. C., Kunath, N., Otterlei, M., Sætrom, P., Bjørås, M., Samson, L. D., van Loon, B. (**2019**) Alkyladenine DNA glycosylase associates with transcription elongation to coordinate DNA repair with gene expression. *Nat. Commun. 10* (1), 5460. DOI: 10.1038/s41467-019-13394-w

Chapter 4: Preliminary Investigations of UV-DDB and Base Excision Repair in Packaged DNA

4.1 Abstract

UV-DNA damage binding protein (UV-DDB) binds tightly to the intermediate apurinic/apyrimidinic (AP) site generated during base excision repair (BER). While previous studies have found UV-DDB promotes BER in short oligonucleotides, little is known about the relationship between UV-DDB and BER in the packaged environment in which most cellular DNA exists. The basic unit of DNA packaging is the nucleosome core particle (NCP) which consists of 145-147 bp of DNA wrapped 1.7 times around a histone octamer core. Cryo-EM structures and DNaseI footprinting demonstrate UV-DDB binds occluded AP sites in NCPs and induces a register shift to generate a more accessible position. In this study, we investigated whether UV-DDB can stimulate the repair of the mutagenic 1,*N6*- ethenoadenine (εA) lesion by the BER enzyme alkyladenine glycosylase (AAG). We first conducted a global screening of εA excision in the presence of UV-DDB that evaluated 21 unique locations within the NCP. After identifying several sites of interest, we conducted further in-depth single site evaluations. Our preliminary data suggest that while UV-DDB did not stimulate activity at sites facing outwards away from the histone proteins, it may stimulate activity at sites facing inwards, as well as sites that experience dynamic unwrapping of the DNA from the histone core. Taken together, our results suggest that UV-DDB acts as a first responder that locates inaccessible εA damage and alters its location to allow for easier repair by AAG.

4.2 Introduction

If left unrepaired, DNA damage can result in genomic alterations and disease development. Modified bases, termed here as lesions, are repaired by the base excision repair (BER) pathway. As previously discussed in this work, one mutagenic lesion repaired by the BER pathway is 1,N^6-ethenoadenine (εA)[1, 2] generated both as a byproduct of endogenous lipid peroxidation and exogenous exposure to vinyl chloride.[3, 4] εA levels are elevated in tissues from individuals with chronic inflammatory diseases associated with carcinogenesis as well as cancerous tissues.[5] The BER pathway is comprised of several enzymes that catalyze the excision of a lesion and subsequent insertion of an unmodified nucleotide. Alkyladenine glycosylase (AAG) is responsible for excision of alkylated bases, including εA.[6] AAG mediated εA excision results in an apurinic/apyrimidinic (AP) site. This AP site is then incised by AP endonuclease 1 (APE1), creating a nick with 3'-OH and 5'-deoxyribose phosphate (5'-dRP) termini. Polymerase β (pol β) removes the 5'-dRP and incorporates the correct nucleotide at the 3'-OH. Finally, a DNA ligase completes the repair by sealing the nick in the backbone.[7]

The packaging of a lesion into chromatin serves as a hinderance to εA excision. The nucleosome core particle (NCP) is the basic unit of packaging in chromatin. The NCP is comprised of 145-147 base pairs of DNA wrapped approximately 1.7 times around an octamer core of histone proteins[8] and contains a 2-fold axis of pseudosymmetry known as the dyad axis. The octamer core is comprised of two copies of each histone protein: H2A, H2B, H3, and H4,[9] each containing a globular core region and a disordered tail.[8] Within an NCP, any given nucleobase is located in a unique geometric positioning. The two types of positioning are (1) rotational position, which defines the orientation of the base relative to the histone protein and (2) translational position, which

characterizes the location relative to the dyad axis. Rotational position is further defined as one of three orientations: outwards towards the solution (OUT), inwards towards the histone core (IN), or a position somewhere in between (MID). For translational positioning it is notable that the NCP is not a static structure but rather a dynamic one where DNA is transiently exposed through unwrapping at the entry/exit points located far from the dyad.[10, 11] Understanding the geometric positioning of lesions aids in understanding the factors that impact glycosylase activity.

The study of εA removal by AAG in NCPs has demonstrated the effects of geometric lesion positioning on excision activity. Specifically, εA removal by AAG is highly correlated with rotational position, with OUT positions excised more efficiently than IN, and MID positions lying somewhere in between these two.[12-14] These results are consistent with the general trends that have been observed previously for other glycosylases acting on NCPs such as OGG1,[12, 15] UDG,[12, 16] and TDG,[17] which exhibit activity at sites facing OUT from the histone core. Still, excision activity does not correlate as strongly with glycosylase activity in certain translational regions.[13, 18] This exception has been observed for AAG[13, 14] as well as UDG[16] and OGG1,[15] where enhanced activity at the DNA entry/exit regions is observed and attributed to the unwrapping of the DNA. However, this observation is not universal and is dependent upon the specific glycosylase. For example, NEIL1 has been reported to be unable to exploit this unwrapping due to its high affinity for undamaged bases.[19] We have earlier discussed how alterations to the histone tail domains can also promote this unwrapping and allow greater AAG excision activity. While opportunistic exploitation of unwrapped DNA can allow for the repair of otherwise occluded lesions, the limited amount of DNA

subject to this unwrapping necessitates an alternative mechanism of repair for occluded sites.

Newer investigations of nucleotide excision repair (NER) proteins, responsible for the repair of larger, helical distorting lesions, have revealed their roles in BER and overcoming the problems of DNA packaging. NER utilizes a multistep process to identify and remove damage. Damage recognition is the rate limiting step of NER[20] and is the key difference between the two NER pathways: global genomic (GG) and transcription coupled (TC). While TC-NER utilizes a stalled polymerase to detect damage, GG-NER utilizes specific DNA damage binding proteins to identify damage.[21] It has been demonstrated that NER lesions packaged into chromatin result in differential repair by the NER pathway.[22] UV-DNA damage binding protein (UV-DDB) is a heterodimeric protein consisting of DDB1 and DDB2 that has been shown to act as a damage sensor for lesions in the context of chromatin-packaged lesions.[23] Intriguingly, more recent work has shown the involvement of UV-DDB with the BER pathway. In short duplexes, UV-DDB has been shown the stimulate the activity of OGG1 on 8-oxoG, APE1 incision of AP sites, and pol β nucleotide incorporation.[24] Furthermore, UV-DDB binding to AP sites has been observed in cryo-EM structures to induce a register shift of occluded lesions independent of ATP.[25] Briefly, this study investigated the binding to 6-4 photoproducts or a THF abasic site analog located in NCPs. When these lesions were oriented OUT, cryo-EM revealed UV-DDB binding with minimal disruption to the translational positioning of the DNA. However, when these lesions were oriented IN, a three bp shift to a MID position was observed in both cryo-EM structures and DNase I footprinting. This study demonstrated the ability of UV-DDB alone to change the

rotational orientation of a lesion packaged IN within the NCP. This may explain earlier work that identified a "factor" in human cellular extracts that promoted ATP dependent BER activity in nucleosomes.[26] These results implicate UV-DDB as another potential factor for promoting BER in chromatin.

Until now, there have been no studies investigating UV-DDB's stimulation of BER in NCPs. Our results indicate UV-DDB can stimulate activity of AAG excision of εA at sites located IN or in areas of the NCP that are prone to DNA unwrapping. However, UV-DDB did not stimulate activity at OUT facing sites where AAG excision is higher. Taken together, these observations indicate a role for UV-DDB as a first responder to εA damage that can make otherwise occluded lesions more accessible to repair machinery.

4.3 Materials and methods

4.3.1 Oligonucleotide Synthesis and Purification

All oligonucleotides used in this study were synthesized on a MerMade 4 DNA synthesizer (BioAutomation). We used the 145 bp Widom 601 nucleosome positioning sequence (**Table 4.1**) as the unincorporated duplex control and to assemble NCPs. Synthesis of the 145 mer oligonucleotide containing εA was conducted on 1,400 Å controlled pore glass beads (BioAutomation) using phosphoramidites with ultramild protecting groups (Glen Research). Deprotection was performed according to the manufacturer's specifications. For global εA substitution for A throughout the "I" strand, a Poisson distribution was utilized, as described in recent reports.[15, 16, 27] The molar ratio determined by the Poisson distribution ($\lambda = 0.355$) was used to determine the correct mixture of A and εA phosphoramidites. This synthetic strategy yields a DNA population

containing either 0 or 1 εA lesion per 145 mer oligonucleotide while minimizing strands containing two or more lesions to 5% of the population. For single site incorporation, εA phosphoramidite alone was used to incorporate at any given site. For both types of incorporation, the final trityl group was removed on the synthesizer, and the DNA was cleaved from the solid support by incubation in NH_4OH at room temperature for 2 h. The DNA was then purified via the crush and soak method utilizing 8% denaturing polyacrylamide gel electrophoresis (PAGE).

Table 4.1 DNA Sequences used in this study

Name	Length	Sequence (5′ to 3′)
"I" strand	145mer	ATCAGAATCCCGGTGCCGAGGCCGCTCAATTGGTCGTAGACAG CTCTAGCACCGCTTAAACGCACGTACGCGCTGTCCCCCGCGTTT TAACCGCCAAGGGGATTACTCCCTAGTCTCCAGGCACGTGTCA GATATATACATCGAT
"J" strand	145mer	ATCGATGTATATATCTGACACGTGCCTGGAGACTAGGGAGTAA TCCCCTTGGCGGTTAAAACGCGGGGGACAGCGCGTACGTGCGT TTAAGCGGTGCTAGAGCTGTCTACGACCAATTGAGCGGCCTCG GCACCGGGATTCTGAT
IS1	23mer	ATCAGAATCCCGGTGCCGAGGCC
IS2	92mer	ATCAGAATCCCGGTGCCGAGGCCGCTCAATTGGTCGTAGACAG CTCTAGCACCGCTTAAACGCACGTACGCGCTGTCCCCCGCGTTT TAACC
J1	45mer	ATCGATGTATATATCTGACACGTGCCTGGAGACTAGGGAGTAA TC
J2	65mer	CCCTTGGCGGTTAAAACGCGGGGGACAGCGCGTACGTGCGTTT AAGCGGTGCTAGAGCTGTCTAC
J3	35mer	GACCAATTGAGCGGCCTCGGCACCGGGATTCTGAT
JS12	30mer	TTTAACCGCCAAGGGGATTACTCCCTAGTC
JS23	32mer	GCCGCTCAATTGGTCGTAGACAGCTCTAGCAC

A ligation strategy was utilized to prepare the complementary "J" strand 145 mer (**Figure 4.1**). The component oligonucleotides for ligation were synthesized using standard phosphoramidite protecting groups with the final trityl group retained. Reverse-

phase HPLC purification at 90 °C was used to purify the oligonucleotides (Agilent PLRP-S column, 250 mm × 4.6 mm; A = 100 mM triethylammonium acetate [TEAA] in 5% aqueous MeCN, B = 100 mM TEAA in MeCN; 5:95 to 35:65 A:B over 30 min, 35:65 to 5:95 A:B over 5 min at 1 mL/min). Removal of the trityl group was accomplished by incubation in 20% v/v aqueous glacial acetic acid for 1 h at room temperature. Subsequently, a second HPLC purification at 90 °C was performed (Agilent PLRP-S column, 250 mm × 4.6 mm; A = 100 mM triethylammonium acetate [TEAA] in 5% aqueous MeCN, B = 100 mM TEAA in MeCN; 0:100 to 15:85 A:B over 35 min, 15:85 to 35:65 A:B over 5 min at 1 mL/min). Electrospray ionization mass spectrometry was used to verify the identity of the component oligonucleotides. Five nmol of each component oligonucleotide J2 and J3 were 5′-phosphorylated using 2 mM ATP and T4 kinase (New England Biolabs). These phosphorylated components were then combined in equal molar amounts with component J1 and 10% excess of two scaffolding oligonucleotides, JS12 and JS23, and annealed by heating to 95 °C for 5 min and cooling at 1°C per min in 50 mM NaCl and 20 mM Tris (pH 8.0). These annealed oligonucleotides were then ligated at room temperature overnight using 4,800 units T4 DNA ligase in buffer (50 mM Tris-HCl, 10 mM NaCl, 10 mM $MgCl_2$, 10 mM DTT, 1 mM ATP, pH: 7.5) The product of the ligation reaction was then purified using 8% denaturing PAGE.

Figure 4.1 Ligation scheme for complementary J strand sequence. Five nmol of phosphorylated J2 and J3 was mixed with 5 nmol J1 and 5.5 nmol JS12 and JS23 and annealed. The annealed sample was then treated with ligase to assemble 145 mer complementary DNA. The ligation reaction was purified by 8% denaturing PAGE.

For normalization of AAG glycosylase excision data (*vide infra*), a 23 mer and a 92 mer were designed as internal standards such that they would not co-migrate with any εA cleavage product. They were synthesized as described above and purified by 12% and 8% denaturing PAGE, respectively.

4.3.2 Reconstitution of Nucleosome Core Particles with Global εA or Single Site εA

Recombinant *Xenopus laevis* histones were expressed and purified individually before assembly into octamers.[28, 29] NCPs were reconstituted as described previously[28] via salt gradient dialysis of the radiolabeled εA-containing duplex population and histone octamer. Briefly, a 5-10% molar excess of histone octamer was added to εA containing 145 bp duplex with a ^{32}P radiolabel attached at the 5'-end in buffer (10 mM Tris-HCl [pH 7.5], 1 mM EDTA, 1 mM dithiothreitol [DTT], 2 M NaCl, 500 μg/mL BSA) in a Slide-a-Lyzer dialysis device (0.1 mL capacity, 3.5 kDa MWCO; Thermo Fisher Scientific). The dialysis device was started in a buffer of 10 mM Tris-HCl (pH 7.5), 1 mM EDTA, 1mM dithiothreitol (DTT), 2 M NaCl at 4 °C before transfer to buffers containing decreasing concentrations of NaCl (1.2 M, 1.0 M, 0.6 M, 0 M) at hourly intervals. The final dialysis in 0 M buffer was conducted for 3 h and then the NCPs were filtered with a 0.45 μm cellulose acetate centrifuge tube filter (Corning Costar) to remove insoluble particles. NCP formation and relative purity were analyzed using a 7% native PAGE (60:1 acrylamide: bisacrylamide; 0.25X TBE) run for 3 h at 160 V in 4 °C (**Figure 4.2**). Only NCPs containing < 15% duplex were used in these studies.

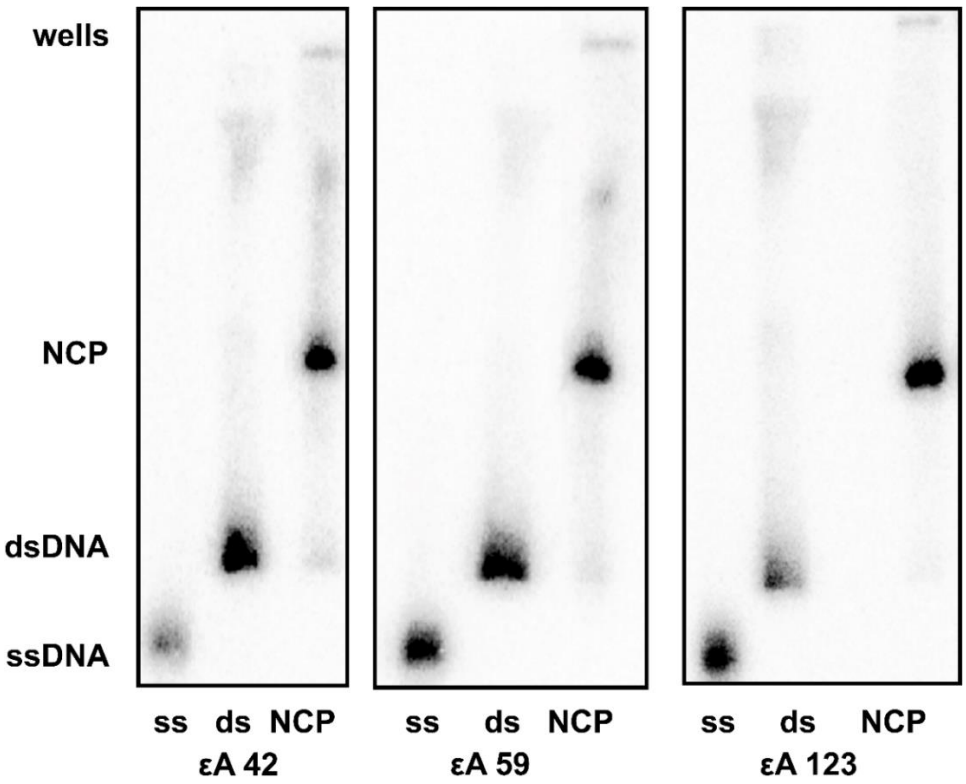

Figure 4.2 Native PAGE Analysis of εA Containing NCP. Representative native PAGE showing successful NCP formation as indicated by slower band migration in the NCP lane relative to the unincorporated duplex (dsDNA) lane. Only NCPs containing <15% dsDNA were used in these studies.

4.3.3 Enzymatic Reactions on Global εA Containing NCPs

Human AAG was purchased from New England Biolabs, and the total enzyme concentration determined by Bradford assay using γ-globulin standards (Bio-Rad Laboratories). Recombinant UV-DDB was provided by Bennett van Houten and prepared as previously described.[30] Baseline AAG excision was assessed by mixing 0.75 pmol NCP substrate with varying concentrations of AAG in a total volume of 15 μL of the reaction buffer (50 mM HEPES [pH: 7.5] 50 mM NaCl, 5 mM DTT, 1 mM EDTA, 100 μg/mL BSA) and incubated at 37 °C along with a negative control sample (no enzyme). For lower concentrations of AAG, dilutions were made by diluting AAG in the reaction buffer.

Duplex containing global εA were treated in the same manner but with a set amount of 40 pmol of AAG. After 1 or 3 h, samples were quenched with 15 μL of 1M NaOH which had been spiked with the radiolabeled internal standards and heated to at 90 ℃ for 3 min. 25:24:1 phenol:chloroform:isoamyl alcohol (PCI) extraction separated the DNA from protein and the aqueous layer was supplemented with 40 μL co-precipitation agent (0.5 mg/mL tRNA in 300 mM NaOAc [pH 8.0], 1 mM EDTA) and 600 μL of ethanol before being placed on dry ice for 30 min. The ethanol was then separated from the DNA via centrifugation, removed with a pipette, and all samples were resuspended in 50% v/v formamide:water, split in half, and loaded onto an 0.6 mm, 8% PAGE gel (Figure S3). One half of the samples were loaded to resolve bands 19-64, run 2 h at 80 W. The other half of the samples were loaded to resolve of bands 89-123, run 4 h at 80 W. For the UV-DDB titrations, the NCP reactions were conducted as above but with varying amounts of UV-DDB added before AAG. All samples were pre-incubated with UV-DDB for 2 min at 37°C before the addition of AAG.

After phosphorimaging of the gels, SAFA software was used to quantitate band intensity. The internal standards were used for band normalization. Sites 19-64 were normalized with the 23 mer standard and sites 89-123 with the 92 mer standard. The no enzyme control was used to subtract background from enzyme-treated samples. For each site, the ratio of corrected band intensity in the NCPs to the duplex was used to determine the NCP/Duplex (NCP/DUP) ratio for AAG activity. An NCP/DUP value of 1 indicates excision that is comparable to duplex, while a value below one indicates lower excision in NCPs relative to duplex. The standard error (SE) of NCP/DUP was calculated using

$SE = \sigma/\sqrt{(n)}$, where σ is the standard deviation of the population and n is the sample size. For global screening experiments, n=2.

4.3.4 Enzymatic Reactions on Single Site εA Containing NCPs

Baseline AAG excision was assessed by mixing 0.75 pmol NCP substrate with varying concentrations of AAG in a total volume of 15 μL of the reaction buffer (50 mM HEPES [pH: 7.5] 50 mM NaCl, 1 mM DTT, 5 mM EDTA, 100 μg/mL BSA) and incubated at 37 °C along with a negative control sample (no enzyme). For lower concentrations of AAG, dilutions were made by diluting AAG in the reaction buffer. After 1 or 3 h, samples were quenched with 20 μL of 1M NaOH. PCI extraction separated the DNA from protein and the aqueous layer was supplemented with 40 μL co-precipitation agent (0.5 mg/mL tRNA in 300 mM NaOAc [pH 8.0], 1 mM EDTA) and 600 μL of ethanol before being placed on dry ice for 30 min. The ethanol was then separated from the DNA via centrifugation, removed with a pipette, and all samples were resuspended in 50% v/v formamide:water. Products were resolved by 8% denaturing PAGE, imaged by phosphorimagery (BioRad PharosFX), and quantitated by densitometry (Bio-Rad Quantity One). The fraction product at each time, $F_p(t)$, was determined by the formula:

$$F_p = \frac{\delta_P(t)}{\delta_P(t) + \delta_S(t)}$$

where $\delta_P(t)$ and $\delta_s(t)$ are the densities of product and substrate bands, respectively, at time t. The time-dependent product yield, P(t), was corrected for incidental substrate damage using the formula:

$$P_t = \frac{F_P(t) - F_P(0)}{1 - F_P(0)}$$

Where $F_p(0)$ is the fraction product observed in the no enzyme control. P_t was then multiplied by 100% to give excision percentage. The standard error (SE) of NCP/DUP was calculated using $SE = \sigma/\sqrt{(n)}$, where σ is the standard deviation of the population and n is the sample size. For εA excision in the absence of UV-DDB at site 42, n=5. For εA excision in the presence of UV-DDB at sites 42, 59, and 123 n = 4, 3, and 2, respectively.

4.4 Results

4.4.1 Preparation of NCPs Containing Globally Substituted or single site εA Lesions

NCPs using the Widom 601 DNA sequence were prepared to examine the effects of UV-DDB on AAG excision activity.[31] The usage of the Widom 601 sequence creates a homogenous NCP population, as it is a strong positioning sequence that binds the histone octamer in a single translational and rotational position. Furthermore, crystal structures of the 601 NCP, are also available for reference.[31] For the global screening experiments, εA lesions were incorporated at A sites in the "I" strand of the 601 DNA to create εA:T base pairs throughout the sequence utilizing methods we have previously reported. [14-16, 27] Briefly, a Poisson distribution was used to determine the molar ratio of A to εA phosphoramidite building blocks such that 95% of the synthesized DNA sequences would incorporate no more than a single εA. For single site experiments, εA was used as an individual building block to incorporate at the site of interest (either site 42, 59, or 123) in the full population.

4.4.2 AAG Activity Titration on Global εA NCPs

To reveal stimulatory activity of AAG excision activity in global εA NCPs we titrated our AAG concentration to a level of 0.1-0.3 NCP/DUP. This level of εA excision

is detectable but also allows for improvement if UV-DDB can stimulate AAG. An initial broad titration was conducted from single turnover (STO) conditions (40:1 enzyme to total NCP) to multiple turnover (MTO) conditions (1:25 enzyme to total NCP). While there were some exceptions, lower excision activity was observed at sites with any baseline activity as AAG concentration was decreased (**Figure 4.3**).

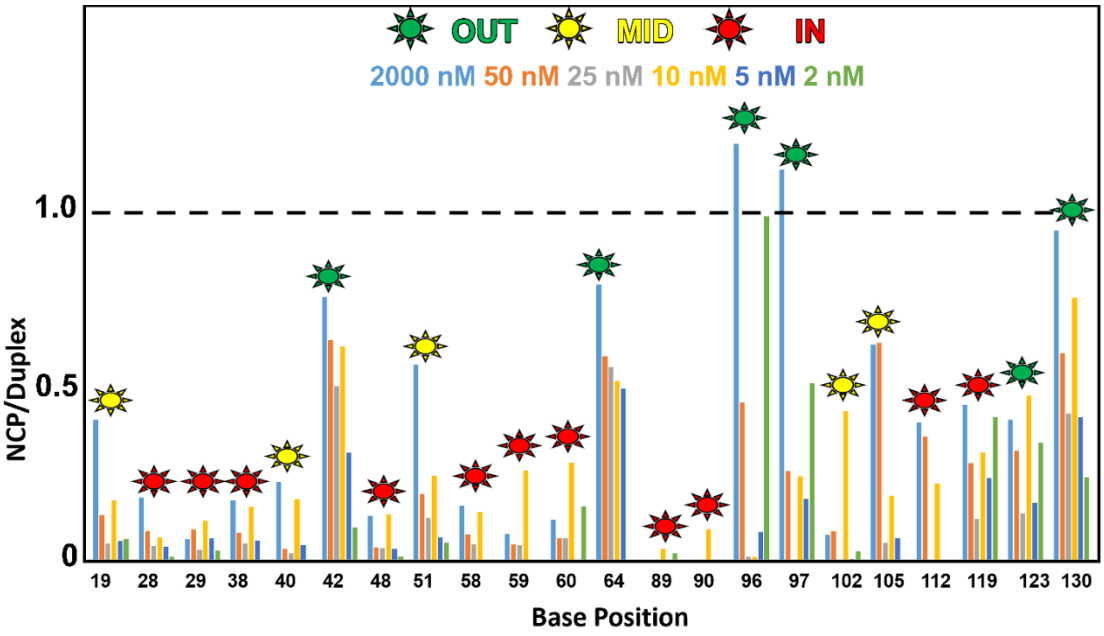

Figure 4.3 Titration of AAG concentration in global εA containing NCPs for 1h at 37°C. DUP was treated under STO conditions to ensure a full product yield. NCP was treated with decreasing amounts of AAG. The ratio of NCP/DUP was taken to determine the dose-response of εA excision. A value of 1 (dashed line) indicates comparable excision in NCPs relative to duplex. As expected, OUT sites (green stars) had generally higher levels of εA excision relative to MID (yellow stars) and IN (red stars) sites. For this experiment n=1.

OUT site 42 was chosen as the representative site for titration of AAG concentration in the global experiments. This site was chosen since OUT sites demonstrates high activity under STO conditions that diminishes in a dose dependent manner going into MTO conditions (**Figure 4.3**). With this site chosen as a reference, 6

nM of AAG was then chosen as the concentration for subsequent experiments as it demonstrated consistently low, but not abolished, activity at OUT sites (**Figure 4.4**).

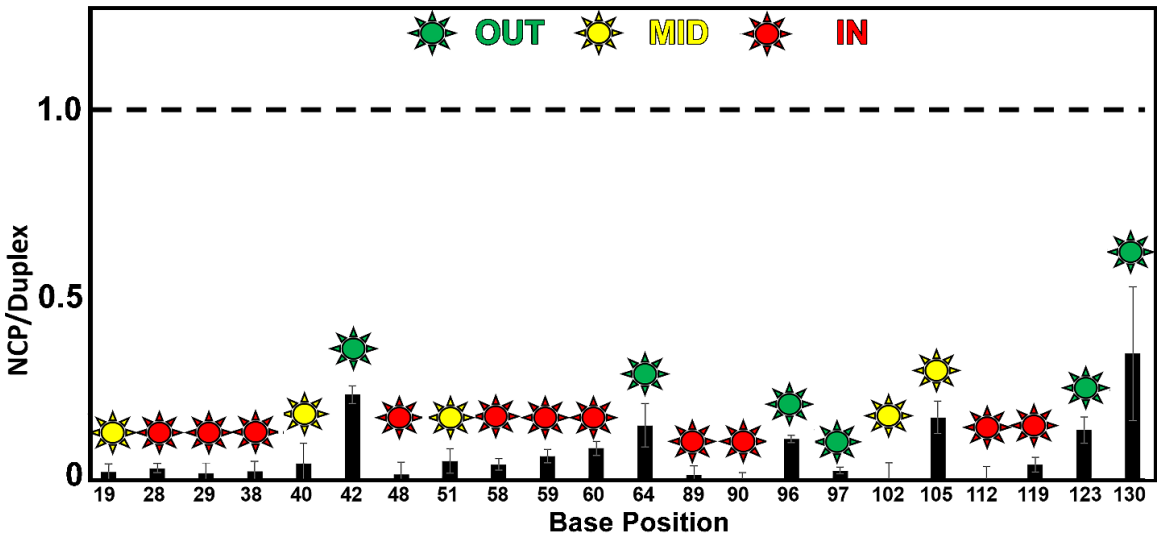

Figure 4.4 Baseline excision of εA by 6 nM AAG in global εA containing NCPs without UV-DDB for 1h at 37 °C. DUP was treated under STO conditions to ensure a full product yield. NCP was treated with 6 nM AAG. The ratio of NCP/DUP was taken to determine εA excision. A value of 1 (dashed line) represents maximal product yield in NCPs where excision is comparable to duplex. OUT sites (green stars) had generally higher levels of εA excision relative to MID (yellow stars) and IN (red stars) sites. For these experiments, n=5.

4.4.3 UV-DDB Titration on Global εA NCPs to Identify Sites of Interest

After establishment of baseline AAG excision activity, a titration with various concentrations of UV-DDB was conducted to determine the concentration of UV-DDB that may stimulate excision at lesion sites (**Figure 4.5**). In comparison to baseline AAG activity, the stimulatory effects of UV-DDB are generally more pronounced at IN sites (58, 59, 60, 89, 90), demonstrating up to five-fold enhancement. It is important to note that the low levels of baseline excision at these sites indicate that most lesions at these locations are not excised even with a five-fold stimulation. In contrast to other OUT sites, site 123 demonstrates a larger enhancement of excision activity. The unique translational

position of site 123 may play a larger factor than its rotational orientation as it is closer to the DNA entry/exit region.

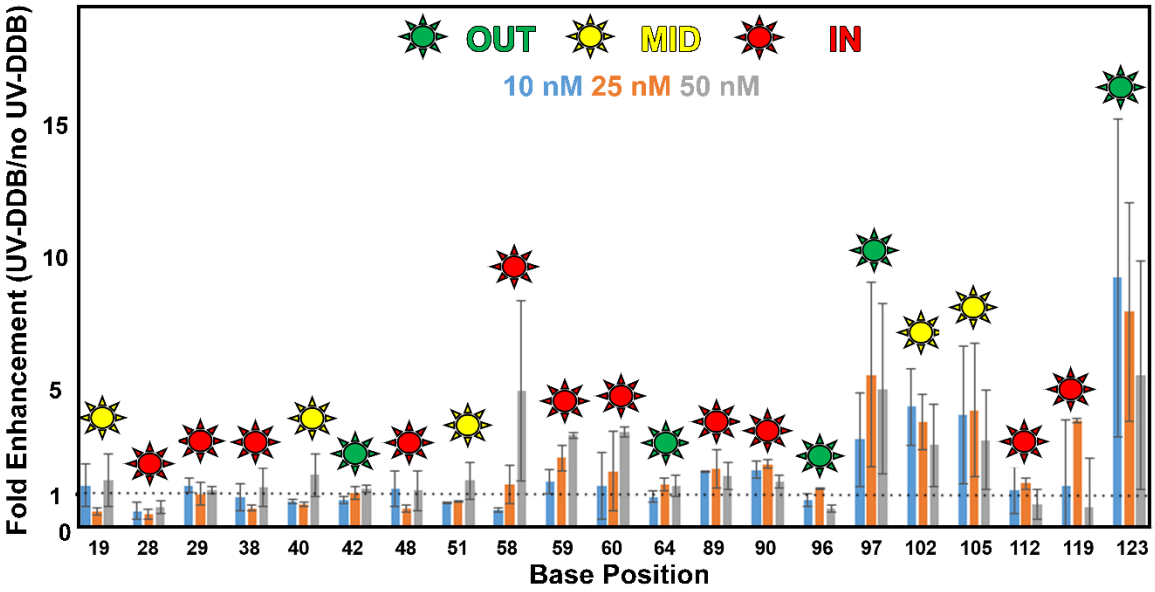

Figure 4.5 Titration with UV-DDB of global εA containing NCPs treated with 6 nM AAG. NCPs were pre-incubated with varying concentrations of UV-DDB before the addition of 6 nM AAG. Samples were then incubated for 3h at 37 °C. The ratio of NCP/DUP was divided by the NCP/DUP for NCPs treated with just AAG. A value of 1 (dashed line) represents the baseline activity of 6 nM AAG without UV-DDB. Values greater than one indicate higher excision at that specified UV-DDB concentration. NCPs were treated with AAG and either 10 nM (blue bars), 25 nM (orange bars), or 50 nM (gray bars) of UV-DDB. Stimulatory effects tended to be lesser for OUT sites (green stars) relative to MID (yellow stars) and particularly IN (red stars) sites. For these experiments, n=2.

4.4.4 Single Site AAG Titration

Due to the low prevalence (<1%) of any particular lesion site in the global system, we chose to evaluate a few sites of interest individually to better characterize and understand UV-DDB stimulation. Furthermore, single sites would allow for future structural studies using DNA-protein footprinting techniques that would aid in elucidating the mechanism of any observed stimulation. The sites chosen (42, 59, and 123) represent sites located in different translational and rotational positions that had

demonstrated varying levels of UV-DDB stimulation in our global screening. As we previously described, we titrated the concentration of AAG such that we could observe a stimulatory effect upon addition of UV-DDB. As site 59 demonstrated no significant baseline εA excision titrating the AAG concentration as described above was not possible. Therefore, titrations were conducted using OUT site 42 (**Figure 4.6**). The optimal AAG concentration from these titrations was determined to be 100 nM of AAG for 50 nM of NCP substrate, as this concentration demonstrates low, but not abolished εA excision. In contrast to the global experiments, a total and absolute product yield could be determined without reference to a duplex standard. This concentration was used for all single site UV-DDB experiments described below.

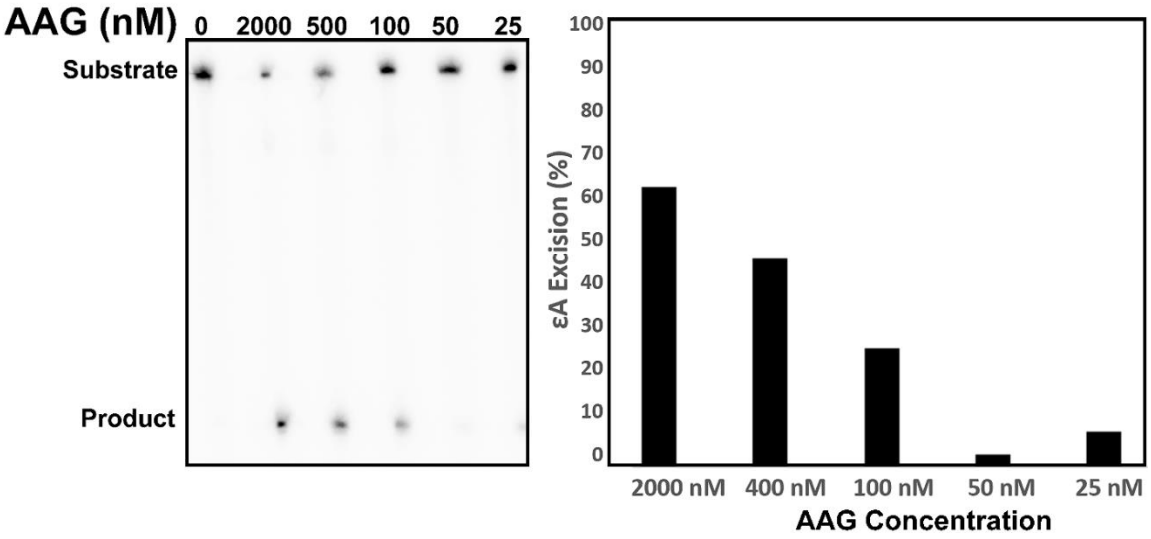

Figure 4.6 Titration of AAG concentration for NCPs with εA at site 42 for 1h at 37°C. NCP was treated with decreasing amounts of AAG. On the left is a representative gel showing conversion of 145 mer substrate to 42 mer product. From left to right is a no enzyme control followed by decreasing amounts of AAG. On the right is the quantitation of the gel. For this experiment, n=1.

4.4.5 Single Site UV-DDB Titration for εA 42

After determination of baseline excision activity at site 42, a titration with various concentrations of UV-DDB was conducted to determine any stimulatory activity. The reactions were conducted by utilizing a two-minute pre-incubation with UV-DDB and subsequent 1h incubation with AAG (**Figure 4.7**). Like the global screening (**Figure 4.5**), there is no apparent stimulation of εA excision by AAG in the single site experiments for site 42.

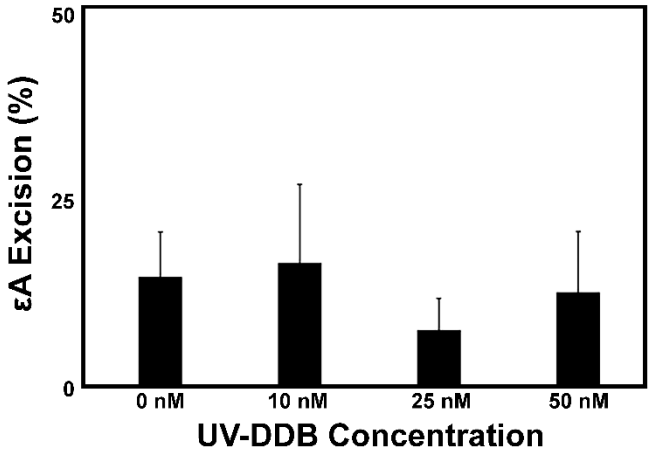

Figure 4.7 Titration of UV-DDB concentration with 100 nM AAG for NCPs with εA at site 42 for 1h at 37°C. NCPs was treated with a 100 nM AAG and varied amount of DDB. From left to right are the no DDB added sample and then increasing amounts of UV-DDB. There is no apparent difference in εA excision between the samples. For this experiment, n=3.

4.4.6 Single Site UV-DDB Titration for εA 59

Unlike the lack of stimulation observed at site 42, the IN site 59 demonstrates enhancement of εA excision by AAG upon addition of UV-DDB (**Figure 4.8**). As the baseline activity of AAG at this site is minimal, the appropriate experimental concentration of AAG was determined by the titration at site 42. However, in contrast to the site 42 experiments, the NCPs were pre-incubated for 1h with UV-DDB and subsequently incubated for 3h with AAG at 37°C to allow for any potential register shift

to occur. A previous study had demonstrated that incubation for 30 minutes on ice allowed for the register shift to occur.[25] The data demonstrate a dosage dependent response, with greater εA excision as the concentration of UV-DDB is increased. However, the overall excision remained quite low, below 10% for all samples.

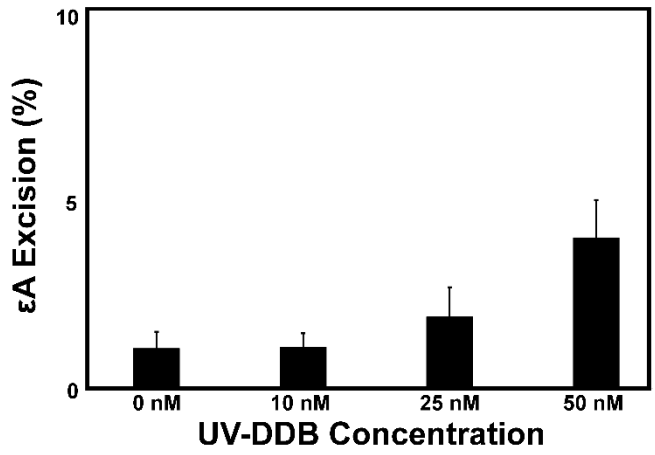

Figure 4.8 Titration of UV-DDB concentration with 100 nM AAG for NCPs with εA at site 59 for 3h at 37°C and 1h pre-incubation with UV-DDB. NCPs were treated with 100 nMAAG and varied amount of UV-DDB. From left to right are the no UV-DDB added sample and then increasing amounts of UV-DDB. There is no apparent difference in εA excision between the samples. For these experiments, n=3.

4.4.7 Single Site UV-DDB Titration for εA 123

Site 123 lies in an area of the NCP that is prone to spontaneous unwrapping of the DNA away from the histone octamer core. 100 nM of AAG was used to investigate if the addition of UV-DDB would increase εA excision. The addition of 25 nM of UV-DDB increases the excision by approximately three-fold relative to the no UV-DDB sample (**Figure 4.9**). In contrast to the minimal overall enhancement seen at site 59, the 25 nM sample displays increased excision from 8% in the no UV-DDB sample to 22% in the 25 nM sample. The 14% absolute increase observed is much greater than the 4% increase

observed at site 59. A smaller 1.5-fold enhancement was observed for 50 nM of UV-DDB while 10 nM of UV-DDB showed no stimulation.

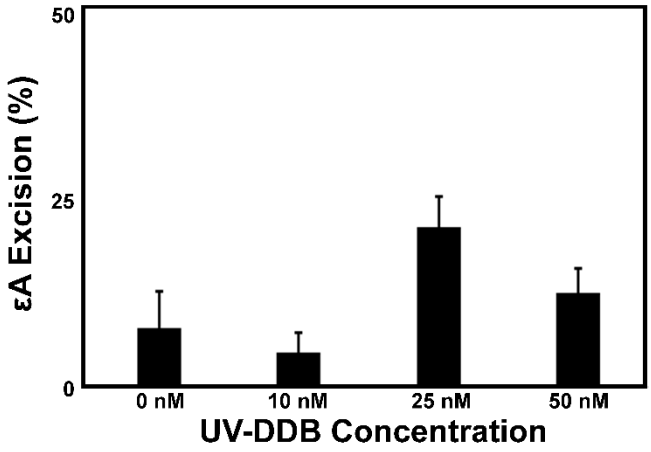

Figure 4.9 Titration of UV-DDB concentration with 100 nM AAG for NCPs with εA at site 123 for 1h at 37°C. NCPs was treated with 100 nM AAG and varied amount of UV-DDB. From left to right are the no UV-DDB added sample and then increasing amounts of UV-DDB. The 25 nM UV-DDB sample shows a marked three-fold increase in excision activity relative to the no UV-DDB sample. For these experiments, n=2.

4.5 Discussion

In this study, we report the role of UV-DDB in the BER of εA in the context of the NCP. Through our global screening system we identified several sites of interest where UV-DDB may stimulate the glycosylase activity of AAG. We then conducted single site experiments to further characterize the stimulatory potential of UV-DDB at these sites. While we observed little impact on sites oriented OUT in both global and single site investigations, we did observe enhancement at IN sites that increased as UV-DDB concentration was increased from 10 to 50 nM. Despite exhibiting up to a five-fold increase in excision at IN sites, the vast majority of lesions were left unrepaired. We also investigated stimulation at a location prone to DNA unwrapping and found enhanced excision activity in the presence of 25 and 50 nM UV-DDB. Together these results

implicate UV-DDB as a potential aid in exposing εA lesions to BER machinery at more occluded in the NCP.

One proposed mechanism of UV-DDB stimulation of BER activity is through stimulating turnover via displacement of glycosylases from AP sites.[24] Another related possibility is the relief of end product inhibition induced by AP sites. UV-DDB has been demonstrated to have a high affinity for AP sites[32] that are the product of successful excision by monofunctional glycosylases. Due to the generation of such toxic intermediates, the BER pathway has been described as a tightly coordinated pathway akin to the "passing of the baton." [33] Indeed, exposed AP sites have been shown to react with histone lysines leading to even more deleterious strand breaks.[34] In short oligos, APE1 has been demonstrated to stimulate AAG turnover through both the promotion of dissociation from AP sites as well as end product inhibition relief.[35] It is unknown how DNA packaging may disrupt the binding of AP sites by AAG. Our data suggests that the lack of stimulation at site 42 (OUT) suggests that if there is a similar AP site bound by AAG in the NCP it may be unable to be displaced by UV-DDB.

While we did not observe stimulation at OUT sites in the NCP, we did observe enhanced activity at occluded IN sites. We have reported that OGG1,[12, 15] UDG,[12, 16] TDG,[17] and AAG[12, 27] exhibit minimal activity at sites facing IN towards the histone core. These findings are also consistent with results reported by other groups.[36-39] These results reinforce a potential explanation for the accumulation of alkylation damage in yeast at IN sites in genomic DNA.[40] A further analysis of human tumors also revealed mutational hotspots at IN sites.[41] While BER enzymes have demonstrated a poor ability to access these IN lesions, UV-DDB has demonstrated an ability to bind 6-4 photoproducts and AP

site analogs facing the histone core.[25] The binding of these lesions led to a three bp register shift, termed "slide-assisted site exposure", that effectively turned the IN lesion to a MID. For AAG, we have reported a wide range of activity at MID sites[13, 14, 42] but generally they tend to exhibit excision no greater than 60% and sometimes as little as 10%. It is therefore not surprising that even though we see enhanced excision upon addition of UV-DDB, we do not see full repair at occluded sites. However, the enhancement observed does suggest that there could be a register shift induced by UV-DDB binding to occluded εA that allows for easier access by AAG. Despite this register shift, it remains possible that there is a higher affinity of UV-DDB to εA in the NCP that only allows for minimal displacement by AAG. Future experiments should be conducted to see if varying the concentration of AAG may promote the displacement of UV-DDB and promote greater excision of εA.

A final mechanism of UV-DDB enhancement of activity is exploiting the dynamic unwrapping of DNA located near the entry/exit region of the NCP. In particular, the 3′-end of the Widom 601 "I" strand has been shown to unwrap preferentially.[43] It has been demonstrated that unwrapping is rate-limiting for endonuclease III-like protein 1 (NTH1).[19, 44] We have previously reported excision εA by AAG[42] was enhanced at the DNA entry/exit regions and was attributed to the unwrapping of the DNA. Furthermore, the deletion of the H2B tail, postulated to promote DNA unwrapping,[45, 46] results in enhanced εA excision in this area of the NCP.[42] We have reported similar enhancements of excision of uracil by UDG[16] and excision of 8-oxo-7,8-dihydroguanine by OGG1[15] in these areas prone to unwrapping. We hypothesize that UV-DDB could potentially capture εA exposed in this unwrapped state and allow for easier removal by AAG. Our results

indicate that with 25 or 50 nM of UV-DDB we do indeed see enhancement of εA excision in lesions located in the area of the NCP prone to unwrapping. The overall absolute increase of εA excision in this area was the largest observed for any of the single sites studied. Furthermore, the observed increase at 25 nM of UV-DDB at site 119 in the global screening experiments further reinforces this possibility.

Taken together our results suggest a mechanism of UV-DDB acting as a first responder to εA damage in NCPs (**Figure 4.10**). The lack of stimulation observed at εA oriented OUT suggests that turnover stimulation is unlikely to be the mechanism of action of UV-DDB in the NCP. This discrepancy between UV-DDB in free duplex and NCPs may be explained by the altered binding and/or dissociation of UV-DDB to AP sites in these two unique substrates. For example, an increased K_D of UV-DDB to AP sites packaged in the NCP relative to AAG could prevent the displacement of AAG after successful εA excision. These altered mechanisms in NCPs relative to duplex could be beneficial to prevent reaction of AP sites with the histone lysines.[34] While UV-DDB may not enhance AAG turnover, it does promote excision at εA oriented IN and at locations prone to DNA unwrapping. These data suggest a mechanism whereby UV-DDB first locates εA and then is displaced by AAG to allow for excision to occur (**Figure 4.10**). The likely mechanism for the removal of εA oriented IN would first be binding by UV-DDB, followed by a register shift to a more accessible location that allows for AAG to displace UV-DDB and excise the lesion. A somewhat similar mechanism may be occurring in the unwrapped area whereby a transiently exposed εA is bound by UV-DDB and traps the lesion in the unwrapped state and is subsequently displaced by AAG.

However, it is important to note that our experiments do not rule out the potential for turnover stimulation occurring in this unwrapped state.

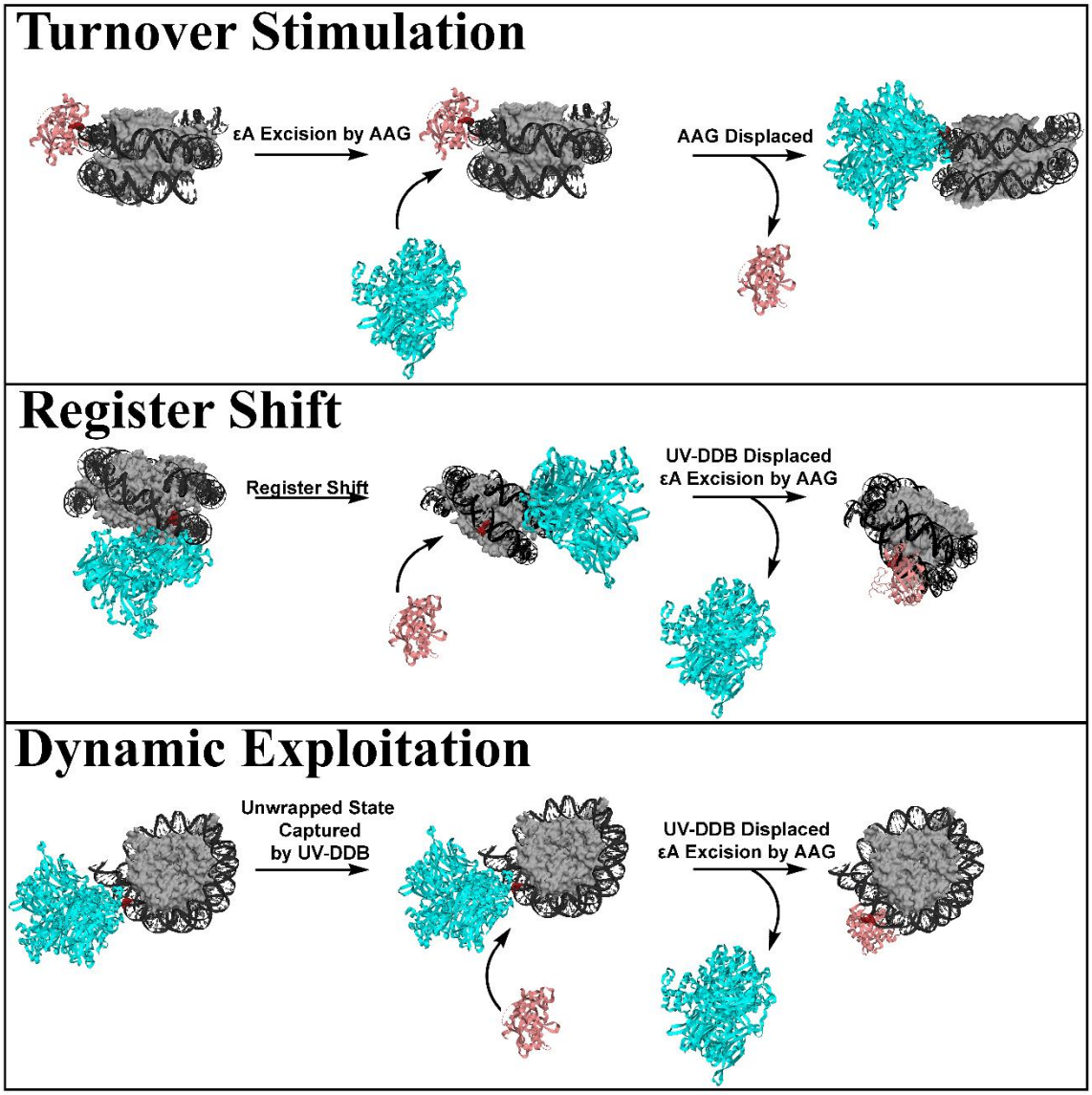

Figure 4.10 Potential mechanisms of UV-DDB stimulation of AAG excision activity. The top shows AAG excision of an OUT εA followed by turnover stimulation via UV-DDB displacement and subsequent binding of UV-DDB to the AP site generated. The middle shows UV-DDB binding an IN εA and shifting it to a MID position that allows for AAG binding and excision. The bottom shows UV-DDB capturing the unwrapped state of an εA lesion and subsequent displacement by AAG.

Understanding the mechanisms of εA recognition and repair on a molecular level is essential to insight and treatment of disease caused by alkylation damage to DNA. The loss of just one allele of DDB2 has been shown to promote tumors in mice,[47-49] which suggests an important role in carcinogenesis. Combined with the observed mutational hotspots of alkylation damage accumulating at IN sites and in areas not prone to unwrapping[40, 41] this suggests the absence of UV-DDB may exacerbate the accumulation of damage at these locations. Understanding the molecular mechanisms of DNA repair in the context of packaged DNA is essential to informing future therapies and understanding the paradox of DNA packaging that may prevent some damage but also repair. The addition of more complexity to our global modeling system will aid in future experiments to identify the key cellular factors that underlie DNA damage and repair.

4.6 References

1. Levine, R. L.; Yang, I.-Y.; Hossain, M.; Pandya, G. A.; Grollman, A. P.; Moriya, M., Mutagenesis Induced by a Single 1,*N6*-Ethenodeoxyadenosine Adduct in Human Cells. *Cancer Res.* **2000,** *60* (15), 4098-4104.

2. Riazuddin, S.; Lindahl, T., Properties of 3-methyladenine-DNA glycosylase from Escherichia coli. *Biochemistry* **1978,** *17* (11), 2110-2118.

3. El Ghissassi, F.; Barbin, A.; Nair, J.; Bartsch, H., Formation of 1,N6-Ethenoadenine and 3,N4-Ethenocytosine by Lipid Peroxidation Products and Nucleic Acid Bases. *Chem. Res. Toxicol.* **1995,** *8* (2), 278-283.

4. Guengerich, F. P.; Crawford, W. M.; Watanabe, P. G., Activation of vinyl chloride to covalently bound metabolites: roles of 2-chloroethylene oxide and 2-chloroacetaldehyde. *Biochemistry* **1979,** *18* (23), 5177-5182.

5. Nair, U.; Bartsch, H.; Nair, J., Lipid peroxidation-induced DNA damage in cancer-prone inflammatory diseases: A review of published adduct types and levels in humans. *Free Radic. Biol. Med.* **2007,** *43* (8), 1109-1120.

6. O'Brien, P. J.; Ellenberger, T., Dissecting the Broad Substrate Specificity of Human 3-Methyladenine-DNA Glycosylase. *J. Biol. Chem.* **2004,** *279* (11), 9750-9757.

7. Schermerhorn, K. M.; Delaney, S. A kinetic perspective on base excision repair of DNA. *Acc. Chem. Res.* **2014**, *47* (4) 1238–1246

8. Luger, K.; Mader, A. W.; Richmond, R. K.; Sargent, D. F.; Richmond, T. J., Crystal structure of the nucleosome core particle at 2.8 A resolution. *Nature* **1997,** *389* (6648), 251-60.

9. Eickbush, T. H.; Moudrianakis, E. N., The histone core complex: an octamer assembled by two sets of protein-protein interactions. *Biochemistry* **1978,** *17* (23), 4955-64.

10. Lee, J. Y.; Lee, J.; Yue, H.; Lee, T. H., Dynamics of nucleosome assembly and effects of DNA methylation. *J. Biol. Chem.* **2015,** *290* (7), 4291-303.

11. Zhou, K.; Gaullier, G.; Luger, K., Nucleosome structure and dynamics are coming of age. *Nat. Struct. Mol. Biol.* **2019,** *26* (1), 3-13.

12. Olmon, E. D.; Delaney, S., Differential Ability of Five DNA Glycosylases to Recognize and Repair Damage on Nucleosomal DNA. *ACS Chem. Biol.* **2017,** *12* (3), 692-701.

13. Kennedy, E. E.; Li, C.; Delaney, S., Global Repair Profile of Human Alkyladenine DNA Glycosylase on Nucleosomes Reveals DNA Packaging Effects. *ACS Chem. Biol.* **2019,** *14* (8), 1687-1692.

14. Caffrey, P. J.; Kher, R.; Bian, K.; Li, D.; Delaney, S., Comparison of the Base Excision and Direct Reversal Repair Pathways for Correcting 1,N6-Ethenoadenine in Strongly Positioned Nucleosome Core Particles. *Chem. Res. Toxicol.* **2020,** *33* (7), 1888-1896.

15. Bilotti, K.; Tarantino, M. E.; Delaney, S., Human Oxoguanine Glycosylase 1 Removes Solution Accessible 8-Oxo-7,8-dihydroguanine Lesions from Globally Substituted Nucleosomes Except in the Dyad Region. *Biochemistry* **2018,** *57* (9), 1436-1439.

16. Li, C.; Delaney, S., Histone H2A Variants Enhance the Initiation of Base Excision Repair in Nucleosomes. *ACS Chem. Biol.* **2019,** *14* (5), 1041-1050.

17. Tarantino, M. E.; Dow, B. J.; Drohat, A. C.; Delaney, S., Nucleosomes and the three glycosylases: High, medium, and low levels of excision by the uracil DNA glycosylase superfamily. *DNA Repair* **2018,** *72*, 56-63.

18. Bilotti, K.; Kennedy, E. E.; Li, C.; Delaney, S., Human OGG1 activity in nucleosomes is facilitated by transient unwrapping of DNA and is influenced by the local histone environment. *DNA Repair* **2017,** *59*, 1-8.

19. Odell, I. D.; Newick, K.; Heintz, N. H.; Wallace, S. S.; Pederson, D. S., Non-specific DNA binding interferes with the efficient excision of oxidative lesions from chromatin by the human DNA glycosylase, NEIL1. *DNA repair* **2010,** *9* (2), 134-143.

20. Gillet, L. C.; Schärer, O. D., Molecular mechanisms of mammalian global genome nucleotide excision repair. *Chem. Rev.* **2006,** *106* (2), 253-76.

21. Sugasawa, K., Regulation of damage recognition in mammalian global genomic nucleotide excision repair. *Mutat. Res.* **2010,** *685* (1-2), 29-37.

22. Erik Wellinger, R.; Thoma, F., Nucleosome structure and positioning modulate nucleotide excision repair in the non-transcribed strand of an active gene. *EMBO J.* **1997,** *16* (16), 5046-5056.

23. Sugasawa, K., UV-DDB: A molecular machine linking DNA repair with ubiquitination. *DNA Repair* **2009,** *8* (8), 969-972.

24. Jang, S.; Kumar, N.; Beckwitt, E. C.; Kong, M.; Fouquerel, E.; Rapić-Otrin, V.; Prasad, R.; Watkins, S. C.; Khuu, C.; Majumdar, C.; David, S. S.; Wilson, S. H.; Bruchez, M. P.; Opresko, P. L.; Van Houten, B., Damage sensor role of UV-DDB during base excision repair. *Nat. Struct. Mol. Biol.* **2019,** *26* (8), 695-703.

25. Matsumoto, S.; Cavadini, S.; Bunker, R. D.; Grand, R. S.; Potenza, A.; Rabl, J.; Yamamoto, J.; Schenk, A. D.; Schübeler, D.; Iwai, S.; Sugasawa, K.; Kurumizaka, H.; Thomä, N. H., DNA damage detection in nucleosomes involves DNA register shifting. *Nature* **2019,** *571* (7763), 79-84.

26. Maher, R. L.; Marsden, C. G.; Averill, A. M.; Wallace, S. S.; Sweasy, J. B.; Pederson, D. S., Human cells contain a factor that facilitates the DNA glycosylase-mediated excision of oxidized bases from occluded sites in nucleosomes. *DNA Repair* **2017,** *57*, 91-97.

27. Kennedy, E. E.; Li, C.; Delaney, S., Global Repair Profile of Human Alkyladenine DNA Glycosylase on Nucleosomes Reveals DNA Packaging Effects. *ACS Chem. Biol.* **2019,** *14* (8), 1687-1692.

28. Luger, K.; Rechsteiner, T. J.; Richmond, T. J., Expression and purification of recombinant histones and nucleosome reconstitution. *Methods Mol. Biol.* **1999,** *119*, 1-16.

29. Luger, K.; Rechsteiner, T. J.; Richmond, T. J., Preparation of nucleosome core particle from recombinant histones. *Methods Enzymol.* **1999,** *304*, 3-19.

30. Yeh, J. I.; Levine, A. S.; Du, S.; Chinte, U.; Ghodke, H.; Wang, H.; Shi, H.; Hsieh, C. L.; Conway, J. F.; Van Houten, B.; Rapić-Otrin, V., Damaged DNA induced UV-damaged DNA-binding protein (UV-DDB) dimerization and its roles in chromatinized DNA repair. *Proc. Natl. Acad. Sci. U.S.A.* **2012,** *109* (41), E2737-E2746.

31. Vasudevan, D.; Chua, E. Y. D.; Davey, C. A., Crystal Structures of Nucleosome Core Particles Containing the '601' Strong Positioning Sequence. *J. Mol. Biol.* **2010,** *403* (1), 1-10.

32. Wittschieben, B. Ø.; Iwai, S.; Wood, R. D., DDB1-DDB2 (Xeroderma Pigmentosum Group E) Protein Complex Recognizes a Cyclobutane Pyrimidine Dimer, Mismatches, Apurinic/Apyrimidinic Sites, and Compound Lesions in DNA*. *J. Biol. Chem.* **2005,** *280* (48), 39982-39989.

33. Prasad, R.; Shock, D. D.; Beard, W. A.; Wilson, S. H., Substrate channeling in mammalian base excision repair pathways: passing the baton. *J. Biol. Chem.* **2010,** *285* (52), 40479-88.

34. Sczepanski, J. T.; Wong, R. S.; McKnight, J. N.; Bowman, G. D.; Greenberg, M. M., Rapid DNA–protein cross-linking and strand scission by an abasic site in a nucleosome core particle. *Proc. Natl. Acad. Sci. U.S.A.* **2010,** *107* (52), 22475-22480.

35. Baldwin, M. R.; O'Brien, P. J., Human AP Endonuclease 1 Stimulates Multiple-Turnover Base Excision by Alkyladenine DNA Glycosylase. *Biochemistry* **2009,** *48* (25), 6022-6033.

36. Beard, B. C.; Wilson, S. H.; Smerdon, M. J., Suppressed catalytic activity of base excision repair enzymes on rotationally positioned uracil in nucleosomes. *Proc. Natl. Acad. Sci. U.S.A.* **2003,** *100* (13), 7465-70.

37. Cole, H. A.; Tabor-Godwin, J. M.; Hayes, J. J., Uracil DNA glycosylase activity on nucleosomal DNA depends on rotational orientation of targets. *J. Biol. Chem.* **2010,** *285* (4), 2876-85.

38. Hinz, J. M.; Rodriguez, Y.; Smerdon, M. J., Rotational dynamics of DNA on the nucleosome surface markedly impact accessibility to a DNA repair enzyme. *Proc. Natl. Acad. Sci. U.S.A.* **2010,** *107* (10), 4646-4651.

39. Prasad, A.; Wallace, S. S.; Pederson, D. S., Initiation of base excision repair of oxidative lesions in nucleosomes by the human, bifunctional DNA glycosylase NTH1. *Mol. Cell. Biol.***2007,** *27* (24), 8442-8453.

40. Mao, P.; Brown, A. J.; Malc, E. P.; Mieczkowski, P. A.; Smerdon, M. J.; Roberts, S. A.; Wyrick, J. J., Genome-wide maps of alkylation damage, repair, and mutagenesis in yeast reveal mechanisms of mutational heterogeneity. *Genome Res.***2017,** *27* (10), 1674-1684.

41. Pich, O.; Muinos, F.; Sabarinathan, R.; Reyes-Salazar, I.; Gonzalez-Perez, A.; Lopez-Bigas, N., Somatic and Germline Mutation Periodicity Follow the Orientation of the DNA Minor Groove around Nucleosomes. *Cell* **2018,** *175* (4), 1074-1087.e18.

42. Caffrey, P. J.; Delaney, S., Nucleosome Core Particles Lacking H2B or H3 Tails Are Altered Structurally and Have Differential Base Excision Repair Fingerprints. *Biochemistry* **2021,** *60* (3), 210-218.

43. Ngo, Thuy T. M.; Zhang, Q.; Zhou, R.; Yodh, Jaya G.; Ha, T., Asymmetric Unwrapping of Nucleosomes under Tension Directed by DNA Local Flexibility. *Cell* **2015,** *160* (6), 1135-1144.

44. Maher, R. L.; Prasad, A.; Rizvanova, O.; Wallace, S. S.; Pederson, D. S., Contribution of DNA unwrapping from histone octamers to the repair of oxidatively damaged DNA in nucleosomes. *DNA Repair* **2013,** *12* (11), 964-971.

45. Andresen, K.; Jimenez-Useche, I.; Howell, S. C.; Yuan, C.; Qiu, X., Solution Scattering and FRET Studies on Nucleosomes Reveal DNA Unwrapping Effects of H3 and H4 Tail Removal. *PLOS ONE* **2013,** *8* (11), e78587.

46. Bertin, A.; Renouard, M.; Pedersen, J. S.; Livolant, F.; Durand, D., H3 and H4 Histone Tails Play a Central Role in the Interactions of Recombinant NCPs. *Biophys. J.* **2007,** *92* (7), 2633-2645.

47. Yoon, T.; Chakrabortty, A.; Franks, R.; Valli, T.; Kiyokawa, H.; Raychaudhuri, P., Tumor-prone phenotype of the DDB2-deficient mice. *Oncogene* **2005,** *24* (3), 469-478.

48. Itoh, T.; Cado, D.; Kamide, R.; Linn, S., DDB2 gene disruption leads to skin tumors and resistance to apoptosis after exposure to ultraviolet light but not a chemical carcinogen. *Proc. Natl. Acad. Sci. U.S.A.* **2004,** *101* (7), 2052-2057.

49. Pines, A.; Backendorf, C.; Alekseev, S.; Jansen, J. G.; de Gruijl, F. R.; Vrieling, H.; Mullenders, L. H. F., Differential activity of UV-DDB in mouse keratinocytes and fibroblasts: Impact on DNA repair and UV-induced skin cancer. *DNA Repair* **2009,** *8* (2), 153-161.

Chapter 5: Conclusions and Future Work

5.1 Conclusions

In the preceding work, we investigated the impact of differential DNA packaging on the repair of 1,*N6*-ethenoadenine (εA) by the base excision repair (BER) and direct reversal repair (DRR) pathways and how the addition of nucleotide excision repair (NER) proteins may stimulate this repair. We studied a model system consisting of the basic unit of DNA packaging, the nucleosome core particle (NCP) to elucidate the effects of DNA packaging on DNA repair. We utilized the strongly position Widom 601 sequence to create a homogenous population of NCPs that occupy a single translational and rotational position.[1, 2] Through the usage of unique chemical synthetic approaches,[3-6] we have been able to study the repair of damage distributed throughout the NCP that capture the effects of unique architectural microenvironments that exist in the NCP. Through these experiments, we have begun to unravel the molecular mechanisms that underlie observed genomic mutational hotspots that may lead to elevated εA levels associated with cancerous tissues and chronic inflammatory diseases.[7]

Our work comparing the repair of εA BER and DRR pathways provided us with valuable insight in how two different repair mechanisms are affected by packaging of εA into NCPs. Our goal was to examine the possibility that previously identified impediments to BER caused by the packaging of lesions into NCPs[3, 4, 6, 8-10] would not be as detrimental to the DRR pathway. We hypothesized the impediment to alkyladenine glycosylase (AAG) activity may be due to generation of an apurinic/apyrimidic (AP) site upon successful εA excision[11] that has been shown to react with the histone lysines to create an even more deleterious strand break.[12] In contrast, the removal of εA lesions by DRR enzyme ALKBH2[13] utilizes molecular oxygen, Fe (II), and α-ketoglutarate to directly transform εA to canonical A[14-17] without the production of an AP site. A

combinatorial approach of hydroxyl radical footprinting (HRF) and enzymatic reactions allowed the evaluation of the repair profiles for both AAG and ALKBH2 in NCPs. We utilized our global incorporation system to evaluate 23 εA unique locations distributed across various translational and rotational positions within the NCP. For AAG, there was a strong correlation between rotational positioning and εA excision with OUT facing lesions repaired better than IN and MID facing lesions. This correlation was not observed for ALKBH2, with similar levels of repair regardless of rotational orientation. While ALKBH2 was more effective than AAG at repairing occluded lesions, only AAG could fully repair εA at any location in the NCP. There were notable exceptions to these trends that serve to highlight the complexity of the NCP as a substrate for these DNA repair enzymes. In particular, lesions located in the area close to the DNA entry/exit region known to preferentially unwrap in NCPs containing the 601 sequence[18] demonstrate higher repair regardless of rotational orientation. We also generated molecular models of enzyme binding which revealed steric interactions between ALKBH2 and the histones are particularly deleterious to DNA binding and results in diminished activity. These data aid in understanding *in vivo* observations of alkylation damage profiles that show mutational hotspots located at IN sites.[19, 20]

After determining that neither the BER nor DRR pathways could fully repair εA in NCPs, we turned our efforts to determine if alteration of the histone proteins could rescue AAG activity at occluded sites. The NCP is notably a dynamic structure where DNA can unwrap near the entry/exit points,[21, 22] canonical histones can be exchanged for variants,[23] and the histones themselves can undergo posttranslational modifications (PTMs).[24, 25] We had previously demonstrated the enhancement of U excision by two

glycosylases when canonical H2A was exchanged for variants.[26] While there are numerous PTMs that the canonical histones under go, we chose to focus our efforts on the new discovered and irreversible proteolytic clipping of the N-terminal histone tails.[27, 28] We focused our efforts on the H2B and H3 tails as these have been observed biologically and demonstrate the ability to promote DNA unwrapping[29, 30] that has been exploited by DNA repair enzymes in our previous experiments. Like above, we utilized a combination of chemical footprinting and enzymatic reactions to determine the repair profiles of AAG excising εA in native, tailless H2B, and tailless H3 NCPs. We found that the absence of H2B or H3 tails results in altered DNA periodicity in the NCP relative to NCPs with fully intact tails. Using our global approach, we were able to correlate these structural alterations to AAG activity. We found that in comparison to native NCPs, tailless H2B demonstrated greater εA excision in transiently unwrapped areas. In contrast, tailless H3 NCPs did not show this enhancement and in fact showed inhibition in more static areas of the NCP that do not undergo unwrapping. Again, however, IN sites that were not in areas subject to unwrapping demonstrated extremely low levels of repair for all NCPs. Together these results demonstrate a potential mechanism to access occluded lesions by utilizing histone tail clipping to promote unwrapping of DNA. However, the detrimental effects on repair in areas not subject to unwrapping demonstrate a need to carefully balance the effects of tail clipping. Further understanding of these mechanisms and how they are balanced in the cell may elucidate why certain disease states are associated with higher[31] and lower[32] levels of tail clipping.

Having investigated the effects of histone modification on BER, we next investigated if there was a mechanism to stimulate BER in NCPs by the addition of other

factors. While remodeling complexes like SWI/SNF[33] and Chd1[34] use ATP to drive octamer sliding and ejection of histone proteins, we were interested in investigating less disruptive and energetically costly ways of promoting BER in NCPs. Previous work had identified a "factor" from human cellular extracts that stimulated BER in an ATP independent manner.[35] We hypothesized that UV-DNA damage binding protein (UV-DDB) may have been the factor identified in this experiment. UV-DDB is has been shown to act as a damage sensor for NER lesions in the context of chromatin[36] and to stimulate BER in short oligonucleotides.[37] Furthermore, UV-DDB binding to AP sites has been observed in cryo-EM structures and DNase I footprinting experiments to induce a register shift of occluded lesions independent of ATP.[38] Having established a strong baseline of AAG excision of εA we wished to further investigate the potential for stimulation by the addition of UV-DDB. We first utilized our global screening system to identify sites of interest that could be studied more thoroughly. In both global and single site experiments we found that UV-DDB may not stimulate activity at OUT sites but may stimulate excision at IN and transiently unwrapped sites. Our preliminary studies investigate three potential mechanisms for DDB stimulation of AAG activity: (1) stimulation of AAG turnover by displacement from AP sites by UV-DDB, (2) slide assisted site exposure of occluded lesions via a UV-DDB induced register shift, and (3) a trapping of the transiently unwrapped state by UV-DDB. The lack of stimulation at OUT facing lesions seems to diminish the likelihood that turnover stimulation is a primary mechanism of UV-DDB stimulation in NCPs. An increased K_D of UV-DDB to AP sites packaged in the NCP relative to AAG could preclude the type of displacement that would promote enzymatic turnover. It is important to note that we cannot definitively rule out

this mechanism based on the experiments we conducted. However, it does appear that both a register shift and trapping of the unwrapped state may be occurring due to the stimulation observed for excision of εA at locations subject to these phenomena. Our data suggest a role for UV-DDB as a first responder to damage in the NCP where it finds the damage and presents it to repair enzymes in a more accessible orientation.

5.2 Future Work

5.2.1 DNA Repair Enzymes as Epigenetic Regulators

While there is a tendency to define an enzyme as having a particular role, biology often presents us with multifunctional enzymes that are involved in multiple processes. In this work, we have investigated enzymes from the BER and DRR pathways and their roles of DNA repair. These enzymes certainly have a fundamental role in DNA repair, but recent studies have suggested broader functionality than initially thought. Epigenetics is the study of regulation of gene expression without fundamentally altering the DNA sequence. If the DNA is the alphabet of genes, epigenetics can be thought of as the punctuation. There are a variety of epigenetic markers such as histone modifications (whether it be variants or PTMs), but the most widely known epigenetic marker is 5-methylcytosine (5-mC).[39] Greater than 4% of cytosines in the genome are methylated[40] and methylation acts to silence gene expression.[39] While the process of methylation by DNA methyltransferases has been well characterized, there is less known about demethylation.

To activate genes that have been silenced due to methylation, there must exist a demethylation pathway. There are two proposed demethylation mechanisms: passive and active. The passive mechanism utilizes replication to dilute 5-mC by incorporating an unmodified cytosine into the newly synthesized strands. In the active pathway it is

thought that a direct demethylation event occurs that allows for the replacement of 5-mC with an unmodified cytosine. An upregulation of BER elements has been observed and has been indicated to be concurrent with demethylation observed during embryonic development.[41] However, there is no known human glycosylase that directly removes 5-mC from DNA. 5-mC is a substrate for oxidation by the Ten-Eleven Translocation (TET) enzymes to iteratively produce 5-hydroxymethylcytosine (5-hmC), 5-formylcytosine (5-fC), and 5-carboxycytosine (5-caC) with the latter two being substrates for the BER enzyme thymine DNA glycosylase (TDG).[42] More recently, it has been discovered that ALKBH2 can also iteratively oxidize 5-mC in a similar manner.[43] While these have been characterized in unincorporated DNA, it has not been described in NCPs. Given the role of histones in epigenetic regulation, understanding the interaction between packaging and DNA demethylation could expand our understanding of gene regulation. Particularly interesting would be the production and excision of 5-fC in the NCP as it has been shown to form reversible crosslinks with histones that alter replication and transcription.[44-46] Understanding the demethylation process in the context of NCPs could broaden our understanding of what DNA "damage" and "repair" may entail.

5.2.2 The Interaction of Epigenetic Histone Variants and BER

A particularly important location in chromatin is the centromere, where kinetochore assembly occurs to allow for chromosome segregation during mitosis. Human centromeres consist of a sequence of highly repetitive alpha satellite DNA wrapped around a histone octamer.[47] This process has been shown to be driven by a histone H3 variant, centromere protein A (CENP-A).[48] The finding of CENP-A at neo-

centromeres lacking the alpha satellite DNA reinforces the pivotal role of CENP-A in centromere formation.

Significantly, CENP-A has been associated with a variety of DNA damage response and repair pathways, including interactions with poly(ADP-ribose) polymerase 2.[49] CENP-A has been found in nuclear foci following irradiation of cells and depletion of CENP-A leads to greater apoptosis in these cells after 24 hours.[50] Furthermore, it has been suggested that spindle assembly checkpoint mediated DNA repair occurs through interactions at the nuclear pore with CENP-A.[51] Additionally, induction of double strand breaks has been shown to recruit CENP-A in both human and mice in vivo.[52] While there is less exploration of the role of CENP-A in BER, evidence in literature does suggest a linkage between the two. CENP-A has been shown to co-localize with a cytidine deaminase and Uracil DNA Glycosylase (UDG) in both *Xenopus laevis*[53] and human cells.[54] Inhibition of deaminase activity was shown to prevent the formation of CENP-A loci, indicative that specific deamination rather than incorporation from the dNTP pool was the impetus for CENP-A localization.[53] The timing of the localization during G2 is interesting as UDG levels are significantly upregulated[55] during S phase, not the G2 phase, to alleviate the misincorporation of uracil during replication. This observation further reinforces the interplay between intentional deaminase activity, BER, and CENP-A deposition. Furthermore, reduction of UDG in human cells leads to a reduction in CENP-A assembly; conversely, overexpression increases CENP-A assembly.[54] Taken together these results demonstrate a clear relationship between the BER pathway and CENP-A deposition. Understanding the regulation of CENP-A deposition is essential as higher levels of CENP-A are observed in breast cancer,[56] colorectal cancer,[57] and

testicular cancer.[58] CENP-A overexpression has also been observed with ectopic localization to regions of high histone turnover.[57, 59] As the literature stands, it begs to wonder whether any potential uracil that is incorporated into a CENP-A NCP at this point can be excised by UDG before becoming a deleterious mutation or if there is another mechanism that may be driving the strong association of this histone variant and carcinogenesis.

CENP-A has been proposed as an epigenetic marker for centromere location, due to the reliance of centromere location on CENP-A and not DNA sequence.[60] An interesting observation between CENP-A and 5-mC has shown there is general hypomethylation associated with CENP-A in stem cells,[61] although there is hypermethylation in somatic cells, albeit with regions of hypomethylation.[62] While most histones undergo degradation to protamines during spermatogenesis, CENP-A is selectively retained.[63] This observation combined with the observed depletion of methylation of the paternal genome suggests the potential potentiation of both 5-mC oxidation and TDG excision of oxidized derivatives within a CENP-A containing NCP. As mentioned above, it is imperative to examine the repair fingerprint of TDG on 5-fC and 5-caC in NCPs, with a further importance for understanding this process in CENP-A containing NCPs. These future experiments may shed light on mechanisms of epigenetic regulation that underlie healthy and cancerous cells.

5.2.3 Post Translational Modifications of Histone Tails

As discussed previously, post translational modifications (PTMs) to the histone tails can modulate DNA accessibility and, consequently, accessibility to DNA repair enzymes. While we have characterized the effect of histone clipping of the H3 and H4

tails on the initiation of BER on alkylated substrates, these are not the only tails in which clipping has been observed. Furthermore, H2A tail deletion disrupts NCP stability,[64] and H2A makes internuclesomal contacts with H4 tails that drive compaction in chromatin.[29, 65] These H2A and H4 tails contacts also occur in mononucleosomes.[65] Investigation of these tail deletions both in mononucleosomes and broader nucleosome arrays may elucidate further regulation of DNA accessibility and a broader impact on DNA repair.

While proteolytic clipping of histone tails may be the largest, irreversible PTM to tails, other reversible PTMs may also regulate DNA repair. There are numerous PTMs that modulate the accessibility of DNA in the NCP including: acetylation, methylation, phosphorylation, sumolyation, and ubiquitination.[66, 67] It is known that certain modifications, such as acetylation, promote dynamic unwrapping of DNA in NCPs.[24, 25] Acetylation, in particular, has been observed as part of the DNA damage response[68] and even a single lysine acetylation promotes enhance DNA unwrapping.[25] The reversibility of these modifications allow for a precise regulation of DNA accessibility. This regulation may help balance the protection of genomic DNA from damaging agents and accessibility of DNA to repair machinery.

5.3 Final Thoughts

The packaging of DNA into chromatin presents our bodies with both beneficial and detrimental outcomes. The compaction of our genome and the protection from damage allowed by packaging into chromatin are extremely beneficial for regulation and fidelity of our genome. Paradoxically, however, we have shown this packaging can be extremely detrimental to the access and repair of DNA damage that can lead to deleterious mutations. Our studies have looked at different repair pathways, alterations to the histone proteins, and the addition of UV-DDB to try and overcome the impediment

imposed by DNA packaging. None of these studies revealed the ability to fully repair any occluded lesions packaged into the NCP. These results support the observed mutational hotspots that occur in tumors and underlie the essential need to understand how these repair processes occur not just in free floating DNA but in the packaged environment of our cells. Through greater understanding of these processes on a fundamental molecular level we can hope to prevent and treat diseases that result from the accumulation of unrepaired DNA damage.

5.4 References

1. Lowary, P. T.; Widom, J., New DNA sequence rules for high affinity binding to histone octamer and sequence-directed nucleosome positioning. *J. Mol. Biol.* **1998,** *276* (1), 19-42.

2. Vasudevan, D.; Chua, E. Y. D.; Davey, C. A., Crystal Structures of Nucleosome Core Particles Containing the '601' Strong Positioning Sequence. *J. Mol. Biol.* **2010,** *403* (1), 1-10.

3. Kennedy, E. E.; Li, C.; Delaney, S., Global Repair Profile of Human Alkyladenine DNA Glycosylase on Nucleosomes Reveals DNA Packaging Effects. *ACS Chem. Biol.* **2019,** *14* (8), 1687-1692.

4. Caffrey, P. J.; Kher, R.; Bian, K.; Li, D.; Delaney, S., Comparison of the Base Excision and Direct Reversal Repair Pathways for Correcting 1,N6-Ethenoadenine in Strongly Positioned Nucleosome Core Particles. *Chem. Res. Toxicol.* **2020,** *33* (7), 1888-1896.

5. Caffrey, P. J.; Delaney, S., Nucleosome Core Particles Lacking H2B or H3 Tails Are Altered Structurally and Have Differential Base Excision Repair Fingerprints. *Biochemistry* **2021,** *60* (3), 210-218.

6. Bilotti, K.; Tarantino, M. E.; Delaney, S., Human Oxoguanine Glycosylase 1 Removes Solution Accessible 8-Oxo-7,8-dihydroguanine Lesions from Globally Substituted Nucleosomes Except in the Dyad Region. *Biochemistry* **2018,** *57* (9), 1436-1439.

7. Nair, U.; Bartsch, H.; Nair, J., Lipid peroxidation-induced DNA damage in cancer-prone inflammatory diseases: A review of published adduct types and levels in humans. *Free Radic. Biol. Med.* **2007,** *43* (8), 1109-1120.

8. Olmon, E. D.; Delaney, S., Differential Ability of Five DNA Glycosylases to Recognize and Repair Damage on Nucleosomal DNA. *ACS Chem. Biol.* **2017,** *12* (3), 692-701.

9. Li, C.; Delaney, S., Histone H2A Variants Enhance the Initiation of Base Excision Repair in Nucleosomes. *ACS Chem. Biol.* **2019,** *14* (5), 1041-1050.

10. Tarantino, M. E.; Dow, B. J.; Drohat, A. C.; Delaney, S., Nucleosomes and the three glycosylases: High, medium, and low levels of excision by the uracil DNA glycosylase superfamily. *DNA repair* **2018,** *72*, 56-63.

11. Schermerhorn, K. M.; Delaney, S., A chemical and kinetic perspective on base excision repair of DNA. *Acc. Chem. Re.s* **2014,** *47* (4), 1238-1246.

12. Sczepanski, J. T.; Wong, R. S.; McKnight, J. N.; Bowman, G. D.; Greenberg, M. M., Rapid DNA–protein cross-linking and strand scission by an abasic site in a nucleosome core particle. *Proc. Natl. Acad. Sci. U.S.A.* **2010,** *107* (52), 22475-22480.

13. Ringvoll, J.; Nordstrand, L. M.; Vågbø, C. B.; Talstad, V.; Reite, K.; Aas, P. A.; Lauritzen, K. H.; Liabakk, N. B.; Bjørk, A.; Doughty, R. W.; Falnes, P. Ø.; Krokan, H. E.; Klungland, A., Repair deficient mice reveal mABH2 as the primary

oxidative demethylase for repairing 1meA and 3meC lesions in DNA. *EMBO J.* **2006,** *25* (10), 2189-2198.

14. Aravind, L.; Koonin, E. V., The DNA-repair protein AlkB, EGL-9, and leprecan define new families of 2-oxoglutarate- and iron-dependent dioxygenases. *Genome Biol.* **2001,** *2* (3), research0007.1.

15. Sedgwick, B., Repairing DNA-methylation damage. *Nat. Rev. Mol. Cell Biol.* **2004,** *5* (2), 148-157.

16. Delaney, J. C.; Smeester, L.; Wong, C.; Frick, L. E.; Taghizadeh, K.; Wishnok, J. S.; Drennan, C. L.; Samson, L. D.; Essigmann, J. M., AlkB reverses etheno DNA lesions caused by lipid oxidation in vitro and in vivo. *Nat. Struct. Mol. Biol.* **2005,** *12* (10), 855-860.

17. Mishina, Y.; Yang, C.-G.; He, C., Direct Repair of the Exocyclic DNA Adduct 1,N6-Ethenoadenine by the DNA Repair AlkB Proteins. *J. Am. Chem. Soc.* **2005,** *127* (42), 14594-14595.

18. Ngo, Thuy T. M.; Zhang, Q.; Zhou, R.; Yodh, Jaya G.; Ha, T., Asymmetric Unwrapping of Nucleosomes under Tension Directed by DNA Local Flexibility. *Cell* **2015,** *160* (6), 1135-1144.

19. Mao, P.; Brown, A. J.; Malc, E. P.; Mieczkowski, P. A.; Smerdon, M. J.; Roberts, S. A.; Wyrick, J. J., Genome-wide maps of alkylation damage, repair, and mutagenesis in yeast reveal mechanisms of mutational heterogeneity. *Genome Res.* **2017,** *27* (10), 1674-1684.

20. Pich, O.; Muinos, F.; Sabarinathan, R.; Reyes-Salazar, I.; Gonzalez-Perez, A.; Lopez-Bigas, N., Somatic and Germline Mutation Periodicity Follow the Orientation of the DNA Minor Groove around Nucleosomes. *Cell* **2018,** *175* (4), 1074-1087.e18.

21. Lee, J. Y.; Lee, J.; Yue, H.; Lee, T. H., Dynamics of nucleosome assembly and effects of DNA methylation. *J. Biol. Chem.* **2015,** *290* (7), 4291-303.

22. Zhou, K.; Gaullier, G.; Luger, K., Nucleosome structure and dynamics are coming of age. *Nat. Struct. Mol. Biol.* **2019,** *26* (1), 3-13.

23. Venkatesh, S.; Workman, J. L., Histone exchange, chromatin structure and the regulation of transcription. *Nat. Rev. Mol. Cell Biol.* **2015,** *16* (3), 178-189.

24. Gansen, A.; Tóth, K.; Schwarz, N.; Langowski, J., Opposing roles of H3- and H4-acetylation in the regulation of nucleosome structure - A FRET study. *Nucleic Acids Res.* **2015,** *43*.

25. Kim, J.; Lee, J.; Lee, T.-H., Lysine Acetylation Facilitates Spontaneous DNA Dynamics in the Nucleosome. *J. Phys. Chem. B* **2015,** *119* (48), 15001-15005.

26. Li, C.; Delaney, S., Histone H2A Variants Enhance the Initiation of Base Excision Repair in Nucleosomes. *ACS Chem. Biol.* **2019,** *14* (5), 1041-1050.

27. Campos, E. I.; Reinberg, D., Histones: Annotating Chromatin. *Annu. Rev. Genet.* **2009,** *43* (1), 559-599.

28. Azad, G. K.; Swagatika, S.; Kumawat, M.; Kumawat, R.; Tomar, R. S., Modifying Chromatin by Histone Tail Clipping. *J. Mol. Biol.* **2018,** *430* (18, Part B), 3051-3067.

29. Iwasaki, W.; Miya, Y.; Horikoshi, N.; Osakabe, A.; Taguchi, H.; Tachiwana, H.; Shibata, T.; Kagawa, W.; Kurumizaka, H., Contribution of histone N-terminal tails to the structure and stability of nucleosomes. *FEBS Open Bio* **2013,** *3*, 363-9.

30. Ferreira, H.; Somers, J.; Webster, R.; Flaus, A.; Owen-Hughes, T., Histone Tails and the H3 αN Helix Regulate Nucleosome Mobility and Stability. *Mol. Cell. Biol.* **2007,** *27* (11), 4037-4048.

31. Liu, H.; Wang, C.; Lee, S.; Deng, Y.; Wither, M.; Oh, S.; Ning, F.; Dege, C.; Zhang, Q.; Liu, X.; Johnson, A. M.; Zang, J.; Chen, Z.; Janknecht, R.; Hansen, K.; Marrack, P.; Li, C. Y.; Kappler, J. W.; Hagman, J.; Zhang, G., Clipping of arginine-methylated histone tails by JMJD5 and JMJD7. *Proc. Natl. Acad. Sci. U.S.A.* **2017,** *114* (37), E7717-e7726.

32. Sandoval-Basilio, J.; Serafín-Higuera, N.; Reyes-Hernandez, O. D.; Serafín-Higuera, I.; Leija-Montoya, G.; Blanco-Morales, M.; Sierra-Martínez, M.; Ramos-Mondragon, R.; García, S.; López-Hernández, L. B.; Yocupicio-Monroy, M.; Alcaraz-Estrada, S. L., Low Proteolytic Clipping of Histone H3 in Cervical Cancer. *J. Cancer* **2016,** *7* (13), 1856-1860.

33. Dechassa, M. L.; Sabri, A.; Pondugula, S.; Kassabov, S. R.; Chatterjee, N.; Kladde, M. P.; Bartholomew, B., SWI/SNF Has Intrinsic Nucleosome Disassembly Activity that Is Dependent on Adjacent Nucleosomes. *Mol. Cell* **2010,** *38* (4), 590-602.

34. Qiu, Y.; Levendosky, R. F.; Chakravarthy, S.; Patel, A.; Bowman, G. D.; Myong, S., The Chd1 Chromatin Remodeler Shifts Nucleosomal DNA Bidirectionally as a Monomer. *Mol. Cell* **2017,** *68* (1), 76-88.e6.

35. Maher, R. L.; Marsden, C. G.; Averill, A. M.; Wallace, S. S.; Sweasy, J. B.; Pederson, D. S., Human cells contain a factor that facilitates the DNA glycosylase-mediated excision of oxidized bases from occluded sites in nucleosomes. *DNA Repair* **2017,** *57*, 91-97.

36. Sugasawa, K., UV-DDB: A molecular machine linking DNA repair with ubiquitination. *DNA Repair* **2009,** *8* (8), 969-972.

37. Jang, S.; Kumar, N.; Beckwitt, E. C.; Kong, M.; Fouquerel, E.; Rapić-Otrin, V.; Prasad, R.; Watkins, S. C.; Khuu, C.; Majumdar, C.; David, S. S.; Wilson, S. H.; Bruchez, M. P.; Opresko, P. L.; Van Houten, B., Damage sensor role of UV-DDB during base excision repair. *Nat. Struct. Mol. Biol.* **2019,** *26* (8), 695-703.

38. Matsumoto, S.; Cavadini, S.; Bunker, R. D.; Grand, R. S.; Potenza, A.; Rabl, J.; Yamamoto, J.; Schenk, A. D.; Schübeler, D.; Iwai, S.; Sugasawa, K.; Kurumizaka, H.; Thomä, N. H., DNA damage detection in nucleosomes involves DNA register shifting. *Nature* **2019,** *571* (7763), 79-84.

39. Kumar, S.; Chinnusamy, V.; Mohapatra, T., Epigenetics of Modified DNA Bases: 5-Methylcytosine and Beyond. *Front. Genet.* **2018,** *9* (640).

40. Breiling, A.; Lyko, F., Epigenetic regulatory functions of DNA modifications: 5-methylcytosine and beyond. *Epigenetics Chromatin* **2015,** *8* (1), 24.

41. Hajkova, P., Epigenetic reprogramming in the germline: towards the ground state of the epigenome. *Philos. Trans. R. Soc. B* **2011,** *366* (1575), 2266-2273.

42. He, Y.-F.; Li, B.-Z.; Li, Z.; Liu, P.; Wang, Y.; Tang, Q.; Ding, J.; Jia, Y.; Chen, Z.; Li, L.; Sun, Y.; Li, X.; Dai, Q.; Song, C.-X.; Zhang, K.; He, C.; Xu, G.-L.,

Tet-Mediated Formation of 5-Carboxylcytosine and Its Excision by TDG in Mammalian DNA. *Science* **2011,** *333* (6047), 1303-1307.

43. Bian, K.; Lenz, S. A. P.; Tang, Q.; Chen, F.; Qi, R.; Jost, M.; Drennan, C. L.; Essigmann, J. M.; Wetmore, S. D.; Li, D., DNA repair enzymes ALKBH2, ALKBH3, and AlkB oxidize 5-methylcytosine to 5-hydroxymethylcytosine, 5-formylcytosine and 5-carboxylcytosine in vitro. *Nucleic Acids Res.* **2019,** *47* (11), 5522-5529.

44. Ji, S.; Park, D.; Kropachev, K.; Kolbanovskiy, M.; Fu, I.; Broyde, S.; Essawy, M.; Geacintov, N. E.; Tretyakova, N. Y., 5-Formylcytosine-induced DNA-peptide cross-links reduce transcription efficiency, but do not cause transcription errors in human cells. *J. Biol. Chem.* **2019,** *294* (48), 18387-18397.

45. Ji, S.; Shao, H.; Han, Q.; Seiler, C. L.; Tretyakova, N. Y., Reversible DNA-Protein Cross-Linking at Epigenetic DNA Marks. *Angew. Chem. Int. Ed. Eng.l* **2017,** *56* (45), 14130-14134.

46. Naldiga, S.; Ji, S.; Thomforde, J.; Nicolae, C. M.; Lee, M.; Zhang, Z.; Moldovan, G. L.; Tretyakova, N. Y.; Basu, A. K., Error-prone replication of a 5-formylcytosine-mediated DNA-peptide cross-link in human cells. *J. Biol. Chem.* **2019,** *294* (27), 10619-10627.

47. Waye, J. S.; Willard, H. F., Structure, organization, and sequence of alpha satellite DNA from human chromosome 17: evidence for evolution by unequal crossing-over and an ancestral pentamer repeat shared with the human X chromosome. *Mol. Cell. Biol.* **1986,** *6* (9), 3156-3165.

48. Carroll, C. W.; Silva, M. C. C.; Godek, K. M.; Jansen, L. E. T.; Straight, A. F., Centromere assembly requires the direct recognition of CENP-A nucleosomes by CENP-N. *Nat. Cell Biol.* **2009,** *11*, 896.

49. Saxena, A.; Wong, L. H.; Kalitsis, P.; Earle, E.; Shaffer, L. G.; Choo, K. H. A., Poly(ADP-ribose) polymerase 2 localizes to mammalian active centromeres and interacts with PARP-1, Cenpa, Cenpb and Bub3, but not Cenpc. *Hum. Mol. Genet.* **2002,** *11* (19), 2319-2329.

50. Ambartsumyan, G.; Gill, R. K.; Perez, S. D.; Conway, D.; Vincent, J.; Dalal, Y.; Clark, A. T., Centromere protein A dynamics in human pluripotent stem cell self-renewal, differentiation and DNA damage. *Hum. Mol. Genet.* **2010,** *19* (20), 3970-3982.

51. Lawrence, K. S.; Chau, T.; Engebrecht, J., DNA Damage Response and Spindle Assembly Checkpoint Function throughout the Cell Cycle to Ensure Genomic Integrity. *PLoS Genet.* **2015,** *11* (4), e1005150.

52. Zeitlin, S. G.; Baker, N. M.; Chapados, B. R.; Soutoglou, E.; Wang, J. Y. J.; Berns, M. W.; Cleveland, D. W., Double-strand DNA breaks recruit the centromeric histone CENP-A. *Proc. Natl. Acad. Sci. U.S.A.* **2009,** *106* (37), 15762-15767.

53. Zeitlin, S. G.; Patel, S.; Kavli, B.; Slupphaug, G., Xenopus CENP-A assembly into chromatin requires base excision repair proteins. *DNA Repair* **2005,** *4* (7), 760-772.

54. Zeitlin, S. G.; Chapados, B. R.; Baker, N. M.; Tai, C.; Slupphaug, G.; Wang, J. Y., Uracil DNA N-glycosylase promotes assembly of human centromere protein A. *PloS One* **2011,** *6* (3), e17151.

55. Cho, R. J.; Huang, M.; Campbell, M. J.; Dong, H.; Steinmetz, L.; Sapinoso, L.; Hampton, G.; Elledge, S. J.; Davis, R. W.; Lockhart, D. J., Transcriptional regulation and function during the human cell cycle. *Nat. Genet.* **2001,** *27* (1), 48-54.

56. McGovern, S. L.; Qi, Y.; Pusztai, L.; Symmans, W. F.; Buchholz, T. A., Centromere protein-A, an essential centromere protein, is a prognostic marker for relapse in estrogen receptor-positive breast cancer. *Breast Cancer Res.* **2012,** *14* (3), R72.

57. Tomonaga, T.; Matsushita, K.; Yamaguchi, S.; Oohashi, T.; Shimada, H.; Ochiai, T.; Yoda, K.; Nomura, F., Overexpression and Mistargeting of Centromere Protein-A in Human Primary Colorectal Cancer. *Cancer Res.* **2003,** *63* (13), 3511-3516.

58. Biermann, K.; Heukamp, L.C.; Steger, K.; Zhoi, H.; Franke, F.E.; Guetgemann, I.; Sonnack, V.; Brehm, R.; Berg, J.; Bastian, P.J.; Müller, S.C.; Wang-Eckert, L.; Schorle, H.; Büttner R., Gene Expression Profiling Identifies New Biological Markers of Neoplastic Germ Cells. *Anticancer Res.* **2007,** *27* (5A), 3091-3100.

59. Lacoste, N.; Woolfe, A.; Tachiwana, H.; Garea, Ana V.; Barth, T.; Cantaloube, S.; Kurumizaka, H.; Imhof, A.; Almouzni, G., Mislocalization of the Centromeric Histone Variant CenH3/CENP-A in Human Cells Depends on the Chaperone DAXX. *Mol. Cell* **2014,** *53* (4), 631-644.

60. Bernad, R.; Sánchez, P.; Losada, A., Epigenetic specification of centromeres by CENP-A. *Exp. Cell Res.* **2009,** *315* (19), 3233-3241.

61. Yamagata, K.; Yamazaki, T.; Miki, H.; Ogonuki, N.; Inoue, K.; Ogura, A.; Baba, T., Centromeric DNA hypomethylation as an epigenetic signature discriminates between germ and somatic cell lineages. *Dev. Biol.* **2007,** *312* (1), 419-426.

62. Ichikawa, K.; Tomioka, S.; Suzuki, Y.; Nakamura, R.; Doi, K.; Yoshimura, J.; Kumagai, M.; Inoue, Y.; Uchida, Y.; Irie, N.; Takeda, H.; Morishita, S., Centromere evolution and CpG methylation during vertebrate speciation. *Nat. Comm.* **2017,** *8* (1), 1833.

63. Palmer, D. K.; O'Day, K.; Margolis, R. L., The centromere specific histone CENP-A is selectively retained in discrete foci in mammalian sperm nuclei. *Chromosoma* **1990,** *100* (1), 32-6.

64. Biswas, M.; Voltz, K.; Smith, J. C.; Langowski, J., Role of histone tails in structural stability of the nucleosome. *PLoS Comput. Biol.* **2011,** *7* (12), e1002279.

65. Kan, P. Y.; Caterino, T. L.; Hayes, J. J., The H4 tail domain participates in intra- and internucleosome interactions with protein and DNA during folding and oligomerization of nucleosome arrays. *Mol. Cell. Biol.* **2009,** *29* (2), 538-46.

66. Allis, C. D.; Jenuwein, T., The molecular hallmarks of epigenetic control. *Nat. Rev. Genet.* **2016,** *17* (8), 487-500.

67. Klemm, S. L.; Shipony, Z.; Greenleaf, W. J., Chromatin accessibility and the regulatory epigenome. *Nat. Rev. Genet.* **2019,** *20* (4), 207-220.

68. Gong, F.; Miller, K. M., Mammalian DNA repair: HATs and HDACs make their mark through histone acetylation. *Mutat. Res.-Fund. Mol. M.* **2013,** *750* (1), 23-30.